



**Ernest Orlando Lawrence**  
**Berkeley National Laboratory**  
1 Cyclotron Road, 70R0108B  
Berkeley CA 94720-8168  
(510) 495-2679; fax: (510) 486-4260

November 18, 2013

Mr. Tien Q. Duong  
EE-2G/Forrestal Building  
Office of Vehicle Technologies  
U.S. Department of Energy  
1000 Independence Avenue, S.W.  
Washington D.C. 20585

Dear Tien,

Here is the fourth quarter FY 2013 report for the Batteries for Advanced Transportation Technologies (BATT) Program. This report and prior Program reports can be downloaded from <http://batt.lbl.gov/reports/quarterly-reports/>.

Sincerely,

Venkat Srinivasan  
Acting Head  
BATT Program

edited by: V. Battaglia  
M. Foure  
S. Lauer

cc: J. Barnes           DOE/OVT  
P. Davis           DOE/OVT  
D. Howell         DOE/OVT  
J. Muhlestein     DOE-BSO

## SIX FEATURED HIGHLIGHTS

### *Anodes*

- ✦ Both Kumta (Pitt) and Cui (Stanford) Groups developed templates for Si-nanotubes that demonstrate > 1500 mAh/g stable cycling capacity.

### *Cathodes*

- ✦ Looney and Wang Group (BNL) developed an *in situ* reactor for studying the phase transitions of an ion-exchange reaction.

### *Diagnostics*

- ✦ Grey's Group (Cambridge) developed an NMR methodology that is highly sensitive to changes in Li dynamics and cation ordering and to two-phase reactions vs. solid solutions as a cathode is cycled.
- ✦ Through a combination of Molecular Dynamics Simulations and X-ray Adsorption Spectroscopy, the Balsara Group (UCB) demonstrated that lithium polysulfides form nanoagglomerates in tetraglyme solutions.

### *Modeling*

- ✦ Using first-principles methods, Persson's Group (LBNL) identified a path for Mn migration in delithiated  $\text{Li}_2\text{MnO}_3$ .
- ✦ Wheeler and Mazzeo (BYU) completed the development and analysis of a micro four-line probe for measuring the electronic conductivity and surface contact resistance of an electrode.

## BATT TASK 1

### ELECTRODE ARCHITECTURE

**Task 1.1-PI, INSTITUTION:** Vincent Battaglia, Lawrence Berkeley National Laboratory

**TASK TITLE:** Electrode Architecture — Cell failure: electrochemical diagnostics

**BASELINE SYSTEM:** Conoco Philips CPG-8 Graphite/1 M LiPF<sub>6</sub>+EC:DEC (1:2)/Toda High-energy layered (NMC)

**BARRIERS:** Energy density of today's batteries is not high enough; cyclability is not high enough; calendar life is not long enough.

**OBJECTIVE:** To accurately assign the primary sources of energy and power fade of prominent chemistries and electrode designs that lead to advanced Li-ion technologies.

**GENERAL APPROACH:** Identify critical technology pathway to meet the USABC performance, life, and cost targets; and then identify cross-cutting failure modes of battery materials and electrodes that prevent the attainment of those goals. Design experiments and hardware that will provide fundamental insight into the problems. Materials from credible battery suppliers of a chemistry of particular interest to the BATT Program are procured. Electrochemical experiments are designed to draw out the identified problem. Additional hardware capable of extracting critical data is also designed, developed, and implemented.

**STATUS OCT. 1, 2012:** New project initiated October 1, 2012. The presently accepted mechanism, based on an acidic, aqueous solution is suspect in the aprotic solvents found in Li-ion cells. Preliminary experiments suggested that the loss of Mn may be driven by the oxidation of electrolyte decomposition products and not by reduction reactions driven by the presence of protons.

The three-electrode cell hardware can be modified such that the third electrode can be substituted with a tube. The present hardware is not showing satisfactory sensitivity. The source of an inductance loop in the ac-impedance is presently unknown.

**STATUS SEP. 30, 2013:** The loss of Mn from a commercial Mn-spinel cathode material, as a function of voltage, temperature, and time, will be measured. The loss of Mn in the presence of a LiPF<sub>6</sub>-based electrolyte will be compared to the loss of a LiTFSI-based electrolyte. The gas-sensing hardware for a coin cell will be verified while cycling. The source of the inductance loop in a 3-electrode coin cell, as identified by the Modeling Group, will be validated.

**RELEVANT USABC GOALS:** 200 to 300 Wh/kg; 1000 to 5000 full cycles; 10- to 15-year calendar life

#### MILESTONES:

- (a) Make a modification to the three-electrode cell hardware based on guidance from Modeling Group and measure difference in response. (May 13) **Complete**
- (b) Demonstrate gas-sensing apparatus for a coin cell on full cell. (Jun. 13) **Complete**
- (c) Measure potential dependence of Mn loss from Mn-spinel. (Jun. 13) **Delayed until Jan. 14**

## PROGRESS TOWARDS MILESTONES

- (a) Make a modification to the three electrode cell hardware based on guidance from Modeling Group and measure difference in response, May 2013. **Completed.** Reported on in the 3<sup>rd</sup> Quarter Report.
- (b) Gas sensing apparatus for a coin cell demonstrated on full cell, June 2013. **Completed**  
Please see the first two quarterly reports of 2013 for details.
- (c) Potential dependence of Mn loss from Mn-spinel measured, June 2013. **Delayed.**  
Student recently returned, results will be reported early in next fiscal year.

As part of the BATT Program, our group contributes to Focus Groups, specifically, our group will investigate the performance of a Si-based anode in a full cell. The Liu Group will supply the Si anodes and our group will develop the cathodes. Since many of the oxide cathodes are known to lose transition metals during cell cycling, the decision was made to use LiFePO<sub>4</sub> for the active material in the cathode. This material is considered to perform well with regard to cycling. Our group has little experience in making a cycleable electrode from this material. An SEM of the material is provided in Fig. 1. The sample is a distribution of particles from 100 to 700 nm. A 7.5 wt% PVDF and an equal amount of Super-PLi was added to the active material and mixed in

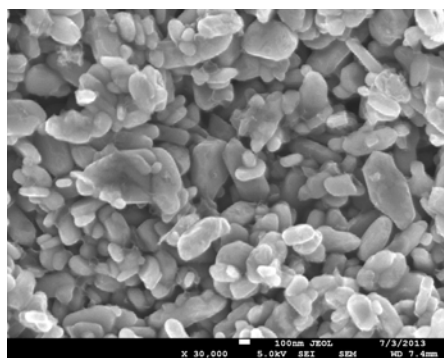


**Figure 1.** SEM of LiFePO<sub>4</sub> powder.

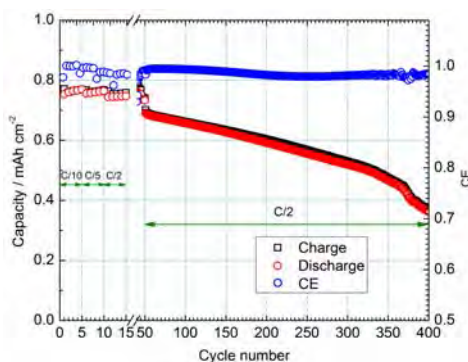


**Figure 2.** Rate and cycling behavior of LiFePO<sub>4</sub> in a half-cell with 1 M LiPF<sub>6</sub> in EC:DEC 1: 2.

NMP. Half cells of the electrodes were tested at different discharge rates and for cyclability. The results of the cyclability are provided in Fig. 2.

The cycling results are not acceptable at this point. A more in-depth analysis shows that there is

side reactions and impedance rise with cycling. There are several possible reasons for the sub-optimum performance. First, this is our first experience with this material and thus the typical electrode formulation was applied. Since this is a sub-micron material, it is possible that the typical formulation does not contain enough carbon conductive additive to ensure particle-to-particle connectivity amongst all of the particles. It is also possible that with the large number of particles per gram for this material that the time of mixing as recommended in the typical formulation protocol is not long enough to lead to complete mixing among the components. Also, the cells with these electrodes were cycled between 2.8 and 4.1 V. Shifting the cycling regime to 2.1 to 3.8 V may reduce the side reactions. Together with Hydro-Québec, the hope is to achieve low capacity-loss electrodes within the next couple of months.

**Task 1.2-PI, INSTITUTION:** Karim Zaghbi, Hydro-Québec (IREQ)

**TASK TITLE:** Electrode Architecture — Assembly of Battery Materials and Electrodes

**BASELINE SYSTEM:** Conoco Philips CPG-8 Graphite/1 M LiPF<sub>6</sub>+EC:DEC (1:2)/Toda High-energy layered (NMC).

**BARRIERS:** Low energy and poor cycle/calendar life

**OBJECTIVE:** To develop high-capacity, low-cost electrodes with good cycle stability and rate capability to replace graphite in Li-ion batteries.

**GENERAL APPROACH:** To address and overcome the electrochemical capacity limitations (both gravimetric and volumetric) of conventional carbon anodes, proposal is to develop low-cost electrode architectures based on silicon that can tolerate its volumetric expansion and provide an acceptable cycle life with low capacity fade. Volume expansion, which is a common problem with Si-based electrode materials, will be addressed by: i) tortuosity/porosity optimization, and ii) improved current collector technology.

**STATUS OCT. 1, 2012:** This is a new project initiated April 1, 2013. In our recent study on the *in situ* analyses of SiO<sub>x</sub> electrodes, HQ showed that the bigger particles (*ca.* 13 μm) start to crack at around 0.1 V. During the charging process, all of the major cracks remained, while some fissures collapsed and others expanded. In general, it appeared that the smaller particles (<2 μm) did not crack. Furthermore, the *in situ* study revealed that delamination occurred at the particle/binder interface and the Cu current collector/electrode interface. These experiments provided a better understanding of the anode cycling mechanism and the failure mode associated with capacity fade. These results will help us to redesign the anode architecture.

**STATUS SEP. 30, 2013:** Complete the fabrication and testing of high-density Si-based electrodes with optimized tortuosity/porosity obtained by a dry-blended process. New current collector architecture will be used to coat the Si-based anode. *In-situ* SEM and TEM analyses will be utilized to monitor the real-time change to the structure undergoing volume expansion. These analyses will help to understand the failure mode and to guide further improvements.

**RELEVANT USABC GOALS:** High energy and low cost: 96 Wh/kg (PHEV, 40 miles). Cycle life, calendar life: 15 year life (at 40°C).

**MILESTONES:**

- (a) Identify an optimized dry-blended silicon-carbon powder composition. (Jun. 13) **Complete**
- (b) Optimize the architecture of the Si-anode and LiMn<sub>1.5</sub>Ni<sub>0.5</sub>O<sub>4</sub> cathode. (Sep. 13) **Complete**
- (c) Complete *in situ* SEM and TEM analyses of the optimized anodes. (Sep. 13) **Complete**

## PROGRESS TOWARD MILESTONES

In this quarter, the focus was on finalizing the Si-anode formulation and electrode architecture for the reference Si (Umicore) material. Studies identified that the optimal range of the anode composition (Si:binder:carbon) is between (50:25:25) and (60:20:20). When the Si content was increased to 70%, the specific capacity faded faster. The porosity and tortuosity of the electrode, strongly influenced by the electrode composition, are major parameters dictating electrode performance. The porosity varies from 0.5 to 0.4 for cells having a Si content from 50 to 70% (Fig.1), respectively. The capacity fade was more pronounced when the Si content was higher and the porosity lower. This implies that the current mixing technique and composition will allow only up to 60% of Si material to be active in the electrode. On another issue, a Cu current collector with rougher surface showed lower impedance compared to a standard one; but this does not appear to improve the cycling stability.

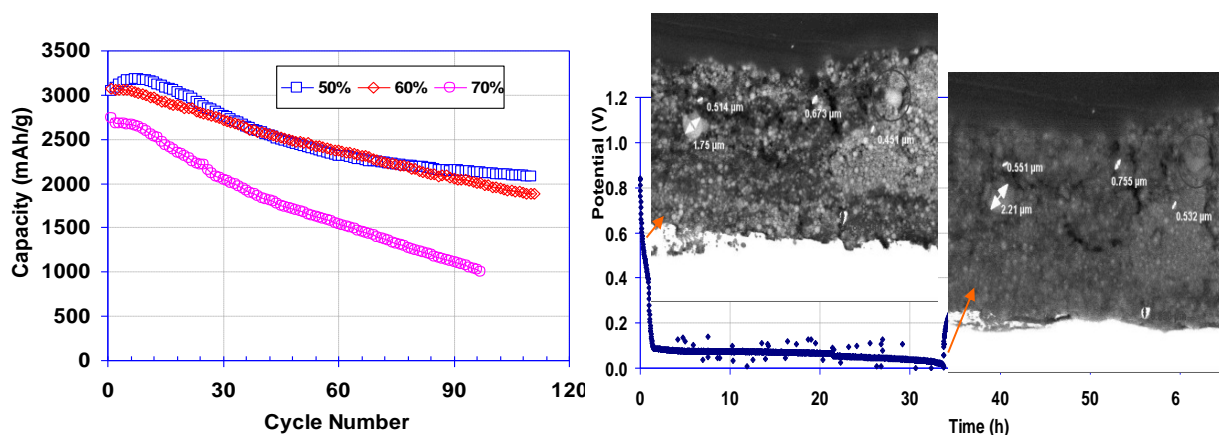


**Figure 1:** Cycle life of Li/EC-DEC-LiPF<sub>6</sub>/Si cells at C/6 with anodes having different Si contents.

**Figure 2:** *In-situ* analysis of Li/polymer/Si cell in a polymer matrix.

The stress on the Si particles during charge and discharge spread throughout the electrode, and thus destroyed the integrity of the anode, as observed by *in situ* SEM. The *in situ* study was performed on an electrode containing Si from Umicore (as recommended by BATT) with the composition (50%:25%:25%). The results of the *in situ* analysis revealed an increase in the electrode thickness during discharge to 5 mV, resulting from Li insertion in the host structure of the Si particles. The average electrode expansion was about 58%. The volume expansion also depends on the electrode composition; a different value could be obtained with different electrode compositions. An increase in the primary particle size was noted, with a significant morphology change in the electrode (Fig. 2). Less cracks in the particles were observed with this material and only a few larger particles broke down during Li de-insertion and insertion. Several fractures in the electrode were observed during the first charge. These fractures could be a consequence of electrode densification.

HQ continues collaboration with LBNL researchers V. Battaglia and G. Liu in the BATT Program.

**Task 1.3-PI, INSTITUTION:** Yet-Ming Chiang, Massachusetts Institute of Technology

**TASK TITLE - PROJECT:** Electrode Architecture – Design and Scalable Assembly of High Density Low Tortuosity Electrodes

**SYSTEMS:** Conoco Philips CPG-8 Graphite/1 M LiPF<sub>6</sub>+EC: DEC (1:2)/Toda High-energy layered (NMC)

**BARRIERS:** Achieving sufficient electronic conductivity, achieving mechanical failure upon cycling, meeting automotive duty cycles, lowering cost.

**OBJECTIVES:** Develop scalable high density binder-free low-tortuosity electrode designs and fabrication processes to enable increased cell-level energy density compared to conventional Li-ion technology. Characterize electronic and ionic transport as a function of state-of-charge in relevant systems including Li(Ni,Co,Al)O<sub>2</sub> (NCA), Li<sub>2</sub>MnO<sub>3</sub>-LiMO<sub>2</sub> alloys and high-voltage spinels LiM<sub>x</sub>Mn<sub>2-x</sub>O<sub>4</sub> and LiM<sub>x</sub>Mn<sub>2-x</sub>O<sub>4-y</sub>F<sub>y</sub>.

**GENERAL APPROACH:** Fabricate high-density sintered cathodes with controlled pore volume fraction and pore topology. Test electrodes in laboratory half-cells and small Li-ion cells. Increase cell-level specific energy and energy density, and lower inactive materials cost, by maximizing area capacity (mAh/cm<sup>2</sup>) at C-rates or current densities commensurate with operating conditions for PHEV and EV. Measure electronic and ionic transport in pure single-phase sintered porous electrodes while electrochemically titrating the Li concentration.

**STATUS OCT 1, 2012:** This is a new project initiated April 1, 2013. Directional freeze-casting and sintering methodology were demonstrated for LiCoO<sub>2</sub>, LiNi<sub>0.5</sub>Mn<sub>1.5</sub>O<sub>4</sub>, and NMC. Measurement of electronic conductivity and ionic conductivity vs. Li concentration are substantially complete for LiNi<sub>0.5</sub>Mn<sub>1.5</sub>O<sub>4</sub> and Li<sub>4</sub>Ti<sub>5</sub>O<sub>12</sub> as a model “zero strain” system.

**STATUS SEP. 30, 2013:** Complete directional freeze-casting and sintering process development for NCA electrodes. Complete measurement of electronic conductivity and Li diffusivity vs. *x* in sintered NCA. Complete pulse-power characterization tests on sintered LCO electrodes as a model material.

**RELEVANT USABC GOALS:** EV: 200 Wh/kg; 1000 cycles (80% DOD).

**MILESTONES:**

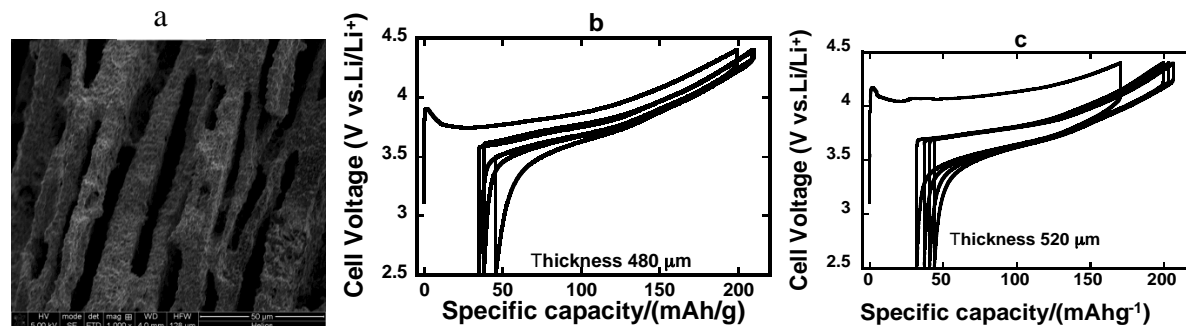
- (a) Fabricate at least five NCA cathodes by directional freeze casting and sintering. (Apr. 13) **Complete**
- (b) Complete electrochemical testing of cathodes in (a), and complete measurement of electronic conductivity and diffusivity vs. *x* in sintered NCA. (Jun. 13) **Complete**
- (c) Complete measurement of electronic conductivity vs. *x* in sintered doped LiM<sub>x</sub>Mn<sub>2-x</sub>O<sub>4-y</sub>F<sub>y</sub>. (Sep. 13) **Complete; composition was previously revised to LiMn<sub>1.5</sub>Ni<sub>0.5-x5</sub>Fe<sub>x</sub>O<sub>4</sub> based on preliminary results.**

## PROGRESS TOWARD MILESTONES

**Collaborator:** Antoni P. Tomsia (LBNL)

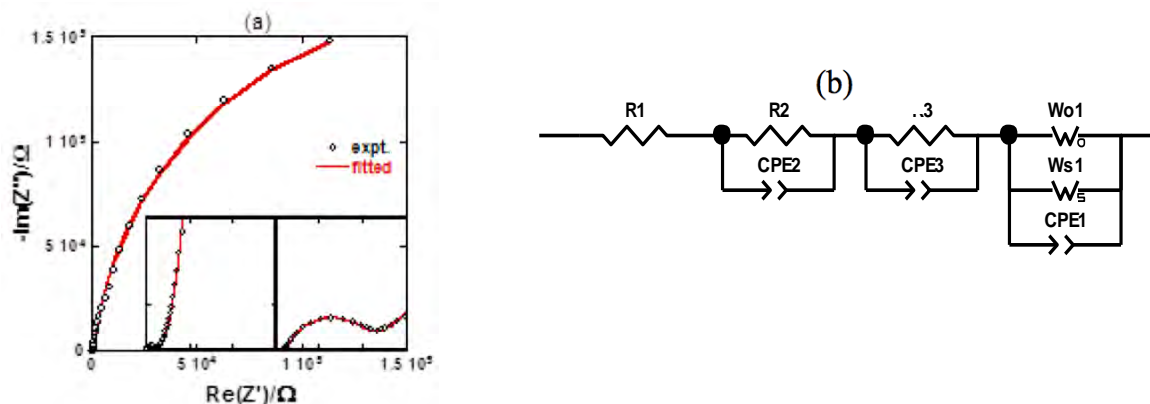
### Electrochemical characterization of freeze-cast and sintered $\text{LiNi}_{0.8}\text{Co}_{0.15}\text{Al}_{0.05}\text{O}_2$ (NCA).

Figure 1a shows the microstructure of a representative directionally-freeze-cast and sintered NCA electrode, showing low-tortuosity aligned-pores separating sintered, polycrystalline regions. Figures 1b and 1c show charge-discharge behavior of electrodes of 480  $\mu\text{m}$  and 520  $\mu\text{m}$  thickness, at C/50 rate measured in half-cells of Swagelok™ configuration (1M  $\text{LiPF}_6$  in 1:1 EC/DEC). Although near-theoretical capacity is obtained at C/50, polarization increases and capacity drops off rapidly with increasing C-rate, unlike previous  $\text{LiCoO}_2$  electrodes that showed 2C capability.



**Figure 1.** (a) Freeze-cast microstructure parallel to the growth direction (a) charge-discharge curves for 480  $\mu\text{m}$  (b) and 520  $\mu\text{m}$  (c) thick samples at C/50 rate.

Similar resistive processes were found in all samples, *e.g.*, Fig. 2a, with all resistances being of similar value except for the low-frequency element,  $W_{s1-R}$ , representing mass transport in the sintered electrode phase. Results suggest that too dense a sintered matrix of *ca.* 10  $\mu\text{m}$  dimension becomes rate limiting, and, hence, efforts to increase porosity in this phase *via* sintering control are underway. Results for the high voltage spinel,  $\text{LiMn}_{1.5}\text{Ni}_{0.5-x}\text{Fe}_x\text{O}_4$ , will be reported next quarter.



**Figure 2.** (a) EIS spectra for additive-free, freeze-cast NCA cathode in a half-cell, and (b) equivalent circuit used to separate the individual electrochemical processes.

**Task 1.4-PI, INSTITUTION:** Gao Liu, Lawrence Berkeley National Laboratory

**TASK TITLE – PROJECT:** Electrode Architecture – Hierarchical Assembly of Inorganic/Organic Hybrid Si Negative Electrodes

**SYSTEMS:** High-voltage, high-energy: Conoco Philips CPG-8 Graphite/1 M LiPF<sub>6</sub>+EC:DEC (1:2)/Toda High-energy layered (NMC).

**BARRIERS:** High-energy system: poor cycle life, high first-cycle irreversible capacity, low coulomb efficiency.

**OBJECTIVES:** Enable Si as a high capacity and long cycle-life material for negative electrode to address two of the barriers of lithium-ion chemistry for EV/PHEV application - insufficient energy density and poor cycle life performance.

**GENERAL APPROACH:** The volume change of Si during lithiation and delithiation disrupts the integrity of electrode and induces excessive side reactions, leading to fast capacity fade. This work will combine material synthesis and composite particle formation with electrode design and engineering to develop high capacity, long-life, and low-cost hierarchical Si-based electrode. The research and development activity will provide an in-depth understanding of the challenges associated with assembling large volume change materials into electrodes, and will develop a practical hierarchical assembly approach to enable Si materials as negative electrodes in Li-ion batteries.

**STATUS OCT. 1, 2012:** New project initiated October 1, 2012.

**STATUS SEP. 30, 2013:** Understand the function of polarity in the binder performance using the triethyleneoxide (TEO) side-chain conductive binders; design and synthesize a series of alkyl-substituted vinylene-carbonate (VC) additives. These additives form a compliance coating on Si surface during cycling. Study the impact of the compliance polymer coating on the coulombic efficiency of Si materials.

**RELEVANT USABC GOALS:** PHEV-40: 144 Wh/l, 4000 deep-discharge cycles.

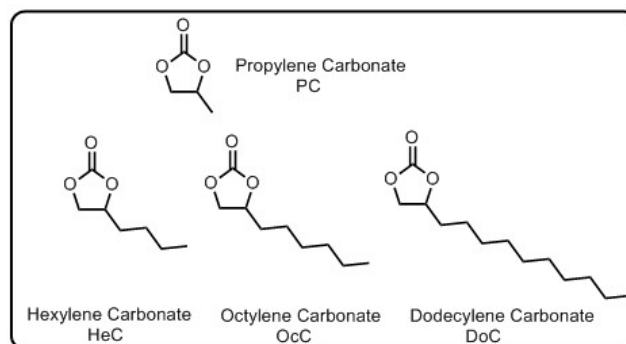
**MILESTONES:**

- (a) Measure the adhesion of the triethyleneoxide (TEO)-containing conductive polymer binder, and characterize the electrode performance. (Mar. 13) **Complete**
- (b) Design and synthesize the alkyls-substituted VC additives. (Sep. 13) **Complete**
- (c) Investigate the performance of Si electrode using the substituted VC additive electrolyte vs. baseline electrolyte. (Sep. 13) **Complete**

## PROGRESS TOWARD MILESTONES

Ethylene carbonate (EC) forms a stable solid-electrolyte-interphase (SEI) at *ca.* 0.8 V, way before Li intercalation occurs. Li<sup>+</sup> permeable and electronically non-conductive, the SEI prevents further electrolyte decomposition and allows reversible lithiation and delithiation of the anode. The major disadvantage of EC is its high melting point of around 37°C that limits the use of Li-ion batteries at low temperatures. Propylene carbonate (PC) has a wide liquid temperature range (-48.8 to 242.0°C) and very good low-temperature performance compared to EC. However, with only a small structural difference from EC, PC undergoes a detrimental solvent decomposition on graphite. This decomposition is accompanied by disintegration of the graphite electrode, delamination of the active material from the current collector, and cell failure.

A homologous series of PC analogue solvents (Scheme 1) with increasing length of the linear alkyl constituent were synthesized and tested as co-solvents with PC for graphite-based Li-ion half-cells. Graphite anodes reach a capacity of around 310 mAh/g in PC and its analogue co-solvents, with 99.95% coulombic efficiency, similar to the values obtained with EC-based electrolytes. Figure 1 shows cycling performance of graphite half-cells using co-solvents of hexylene carbonate



**Scheme 1.** The structure of hexylene carbonate (HeC), octylene carbonate (OcC) and dodecylene carbonate (DoC).

of hexylene carbonate (HeC)/PC=4, octylene carbonate (OcC)/PC=2, and dodecylene carbonate (DoC)/PC=1 with 1 M LiPF<sub>6</sub>. Cell capacities reached *ca.* 310 mAh/g in the first 10 cycles in all of the electrolytes. This data indicates the formation of a stable SEI on graphite surfaces that prevents PC exfoliation and allows reversible cycling of the graphitic anodes. The PC co-solvents with different batches of HeC, OcC, and DoC gave the same cell performance, which is reflected in the consistency of the data shown in Fig. 1.

After proving to be effective with graphite electrodes, the derivatives of the PC additives were also applied to Si electrodes. Significantly improved Si cycling performance is observed.

**Collaborations:** LBNL: V. Battaglia, P. Ross.

### Publication:

Hui Zhao, Sang-Jae Park, Feifei Shi, Yanbao Fu, Vince Battaglia, Phillip N. Ross Jr. and Gao Liu, “New Propylene Carbonate (PC)-Based Electrolytes with High Coulombic Efficiency for Lithium-ion Batteries,” Submitted to *Journal of The Electrochemical Society*, Revision.

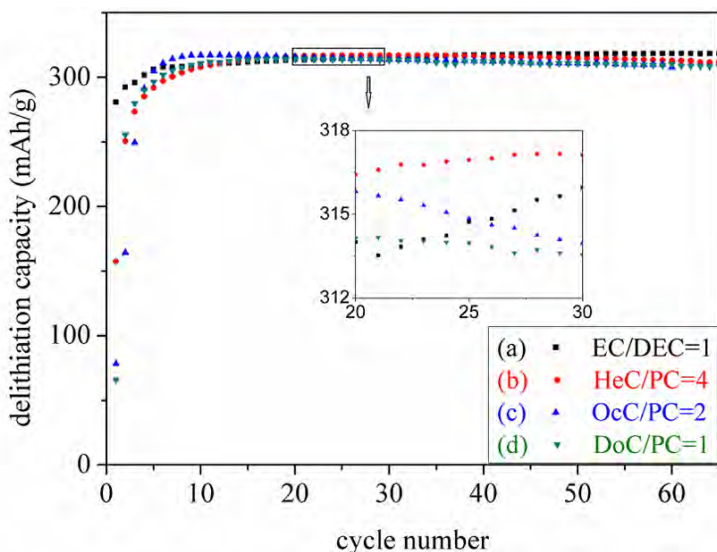


**Figure 1.** Cycling performances of a graphite half-cell in a 1 M LiPF<sub>6</sub> solution of (a) EC/DEC=1, (b) HeC/PC=4, (c) OcC/PC=2, and (d) DoC/PC=1 (v/v) at a C/10 rate.

**Task 1.5-PI, INSTITUTION:** Vincent Battaglia, Lawrence Berkeley National Laboratory

**TASK TITLE:** Electrode Architecture – Electrode fabrication and materials benchmarking

**BASELINE SYSTEM:** Conoco Philips CPG-8 Graphite/1 M LiPF<sub>6</sub>+EC:DEC (1:2)/Toda High-energy layered (NMC)

**BARRIERS:** Energy density of today's batteries is not high enough; cyclability is not high enough; calendar life is not long enough.

**OBJECTIVE:** To develop a robust set of processes for fabricating electrodes and to understand the fundamental properties that underlie electrode performance. Then to use the set of processes to evaluate small quantities of BATT Program developed materials.

**GENERAL APPROACH:** Materials are identified through our own testing or testing performed in the Applied Battery Research Program to make up a baseline chemistry. Ultimately a set of processes for each electrode is developed that is robust enough so that when a small quantity of comparable BATT Program material arrives, the same processes will result in an equally good electrode. The Program material is then evaluated in a series of rate and cycling tests and the results are compared to the baseline material. Sources of cell failure are identified and communicated back to the originator of the material. Materials that look promising are considered for further scale-up and testing or as a possible focus area.

**STATUS OCT. 1, 2012:** New project initiated October 1, 2012. The group developed a fabrication manual over 5 years ago. The manual has been generally followed over the past two years. Many of the processes involved were developed based on a trial-and-error basis; although a methodical analysis of mixing order indicated that mixing the solids together before adding the polymer led to longer cycle life, and an analysis of carbon to polymer ratio indicated that this ratio should be kept between 1:5 and 4:5. It was recently determined that long mixing times can lead to a decline in viscosity.

**STATUS SEP. 30, 2013:** With regard to mixing, there are two steps: 1) mixing the solids together, 2) mixing the binder with the solids. By the end of the year the expectation is to know the most important of three variables: first, mixing time, speed of mixer; second, mixing time and optimum value of each of the three. Expectation is also to understand to what extent the drop in viscosity with mixing is a good thing or a bad result.

**RELEVANT USABC GOALS:** 200 to 300 Wh/kg; 1000 to 5000 full cycles; 10- to 15-year calendar life

**MILESTONES:**

- (a) Measure the effect of mixing variables on electrode performance. (May 13) **Delayed until Jan. 14**
- (b) Measure the viscosity with mixing time and the effect on performance. (Jun. 13) **Complete**
- (c) Determine the optimum composition of an anode with high MW polymer. (Sep. 13) **Delayed until Jan. 14**
- (d) Test three materials developed in the BATT Program. (Sep. 13) **Complete**

## PROGRESS TOWARD MILESTONES

1. Measure the effect of mixing variables on electrode performance, May 2013. **Delayed.** Post-doc took a position with a company; cycling data delayed to next year.
2. Measure the viscosity with mixing time and the effect on performance, June 2013. **Complete.** Reported last quarter.
3. Determine the optimum composition of an anode with High MW polymer, September 2013. **Delayed.** Work initiated but not completed. Results should be reported next quarter.
4. Test three materials developed in the BATT Program, September 2013. **Completed.**

Two LNMO materials were received from Prof. Manthiram (Univ. Texas Austin). These materials were synthesized specifically to take into account the findings of the High-voltage Focus Group. However, as shown in previous reports, the biggest problems identified for this class of materials is the high first-cycle capacity loss, capacity loss as a result of impedance rise in the cell, and rapid capacity fade at 55°C which only occurs in full-cells. These problems are believed to be a result of interactions with the graphite anode, which were not considered by the Focus Group. As it turns out, the materials from Manthiram did not improve upon these limitations in cells when cycled against graphite.

Prof. Scherson (CWRU) sent our lab a second FRION for testing. The results of full-cell testing

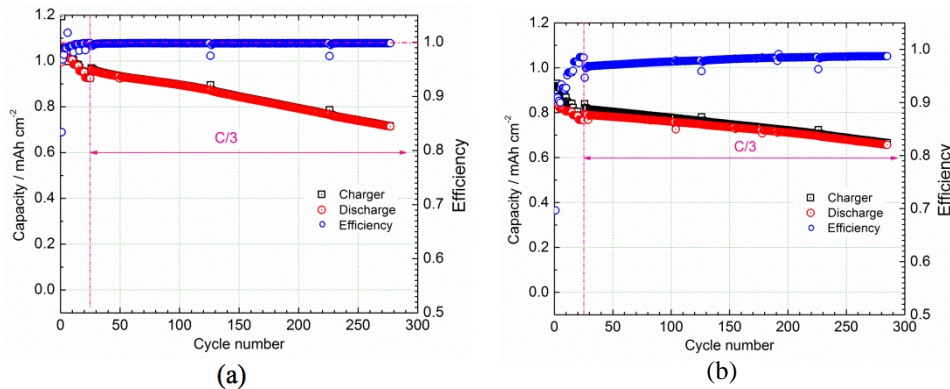


**Figure 1.** Cycle life of Graphite/NCM cells with 1 M LiPF<sub>6</sub> in EC:DEC 1:2, (a) no additives and (b) with 1% additive in the electrolyte.

are provided in Fig. 1. Figure 1a shows the cycling of a Graphite/NCM cell with baseline electrolyte 1M LiPF<sub>6</sub> in EC:DEC 1:2, and in Fig. 1b, the same chemistry plus 1 wt% FRION.

These graphs demonstrate that the cyclability of the cell is not adversely affected by the presence of the salt and actually shows less capacity fade than the cell without the FRION. Rate performance, not shown, was not affected to a C-rate of 1C. However, there are some differences between the two cells. For one, the first-cycle loss is worse for the cell with the FRION; second, the cell with the FRION shows less coulombic efficiency. In fact, the coulombic inefficiency is 15 times worse with the FRION than without it, yet shows better cyclability. At this stage it is not evident that this coulombic inefficiency will lead to a faster loss of electrolyte and therefore fewer overall cycles before catastrophic cell failure. If the FRION does not adversely affect long-term cycle life, it is possible that addition of more FRION may lead to a protective shuttle.

## BATT TASK 2

### ANODES

**Task 2.1-PI, INSTITUTION:** Jack Vaughey, Argonne National Laboratory

**TASK TITLE:** Anodes — Novel Anode Materials

**BASELINE SYSTEMS:** Conoco Philips CPG-8 Graphite/1 M LiPF<sub>6</sub>+EC:DEC (1:2)/Toda High-energy layered (NMC)

**BARRIERS:** Low energy, poor low-temperature operation, and abuse tolerance limitations

**OBJECTIVES:** To overcome the electrochemical capacity limitations (both gravimetric and volumetric) of conventional carbon anodes by designing electrode architectures containing main group metal, metalloid or intermetallic components that can tolerate the volumetric expansion of the materials and provide an acceptable cycle life.

**GENERAL APPROACH:** To search for anode materials or formulations that provide an electrochemical potential a few hundred mV above the potential of metallic Li. Effort will be predominantly on Sn- and Si-based systems. A major thrust will be to design new electrode architectures in which an electrochemically active species is attached to the surface of a porous current collector providing a strong connection from the active species to the substrate. Such an approach minimizes the need for conductive additives and increases the power capabilities of these high energy anodes.

**STATUS OCT. 1, 2012:** Studies on the interfacial structure of Si-based electrodes bound to the substrate using metallic binders have been completed. Techniques have been determined and optimized to deposit electrochemically-active Si and Sn into porous substrates. Development of appropriate characterization tools to study active material/current collector interactions and their effect on cycle life and fade rate were optimized.

**STATUS SEP. 30, 2013:** A series of porous electrode structures with high loadings of active materials will be designed, created, and evaluated. Building on methodologies established earlier, diagnostic studies and *in situ* techniques will be employed to help refine required particle morphologies and other related issues associated with limited active material loadings and cycling.

**RELEVANT USABC GOALS:** 200 Wh/kg (EV requirement); 96 Wh/kg, 316 W/kg, 3000 cycles (PHEV 40 mile requirement). Calendar life: 15 years. Improved abuse tolerance.

#### MILESTONES:

- (a) Identify the thickness limits of Si film-based electrodes utilizing tools including tomography in a working electrode structure. (Mar. 13) **Complete**
- (b) Identify and demonstrate methodologies to incorporate higher levels. (>2 mAh/cm<sup>2</sup>) of active Si into three-dimensional electrode structures. (Sep. 13) **Complete**
- (c) Demonstrate an *in situ* probe that can be used to correlate performance with sample preparation of an electrodeposited electrode. (Sep. 13) **Complete**
- (d) Synthesize, characterize, and evaluate the role of polymeric film coatings in increasing the cycle life of Si-based electrodes. (Sep. 13) **Delayed to Mar. 14**

## PROGRESS TOWARD MILESTONES

**Team:** Fulya Dogan, Lynn Trahey, Fik Brushett (MIT)

One of the biggest issues for Si-based electrodes when incorporated into Li-ion batteries is the effect the volume expansion of Si has on the surrounding electrode structure. This expansion has dramatic effects on both the ability of the binder to maintain good contact with the particles and the ability to maintain good electrical contact throughout the electrode. Previous efforts (*e.g.* Liu, et al., *ACS Nano*, **2012**, 6(2) 1522–1531) have shown that there exists a critical particle size for Si particles: above approximately 150 nm, the particles are unable to withstand the stress of lithiation and degrade; below this number they are stable. In this report, the team has continued the X-Ray tomographic studies of Si electrodes to evaluate the role of cycling on Si particles greater than 150 nm. Because most binders require the secondary particles to be on the micron scale, the team evaluated a standard 70% active Si/PVdF/AB to establish how the particle breakdown is absorbed by the electrode. The electrode was evaluated before cycling and again after 20 cycles (*vs.* Li and with Gen2 electrolyte).

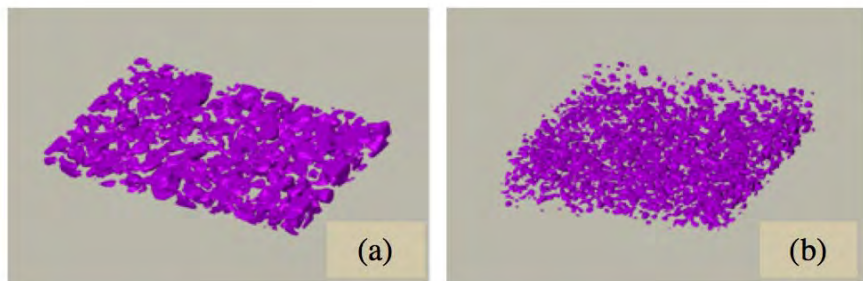


**Figure 1.** (a) a Si electrode of average particle size of 20  $\mu\text{m}$  before cycling, (b) the same electrode after 20 cycles (*vs.* Li).

In Fig. 1, the element sensitive X-Ray tomography data is shown. In Fig. 1a, the Si within the electrode is shown before cycling with a typical particle size (primary) of *ca.* 20  $\mu\text{m}$ .

In Fig. 1b, the pulverization due to repeated cycling is evident with the largest particle size now in the 300-500 nm range. Additionally, an overall expansion of the entire electrode from 60 to 160  $\mu\text{m}$  occurred. In Fig. 2a, the initial pre-cycled electrode is shown, with the void volume highlighted. In Fig. 2b, the compactness and even distribution of pores has been altered, in part to take into account the formation (and continuous growth) of SEI within the sample. In these electrodes it

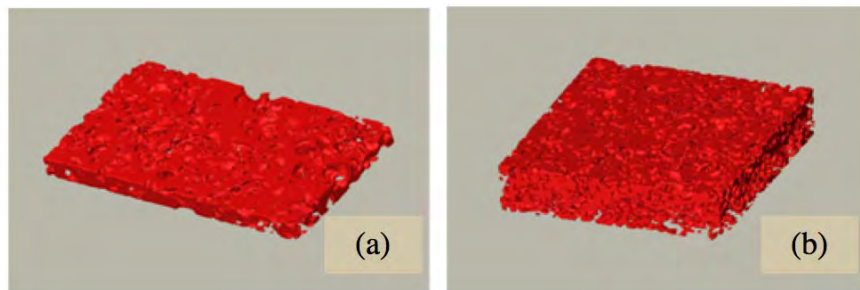


**Figure 2.** (a) the void volume within a Si electrode of average particle size of 20  $\mu\text{m}$  before cycling, (b) the same electrode after 20 cycles (*vs.* Li).

can be seen that the volume expansion of the Si has multiple effects on its surroundings, including pulverization leading to poor connectivity to the current collector, and gross changes in volume from SEI formation and inclusion within the voids

of the electrodes. The effect of the void filling on performance over time is under investigation as it is probably tied to electrolyte starvation effects and capacity fade.

**TASK 2.2 - PI, INSTITUTION:** Stanley Whittingham, Binghamton University

**TASK TITLE - PROJECT:** Anodes – Metal-based High Capacity Li-ion Anodes

**BASELINE SYSTEMS:** Conoco Philips CPG-8 Graphite/1 M LiPF<sub>6</sub>+EC:DEC (1:2)/Toda High-energy layered (NMC)

**BARRIERS:** Cost, safety and volumetric capacity limitations of lithium-ion batteries

**OBJECTIVES:** To replace the presently used carbon anodes with safer materials that have double the volumetric energy density, and will be compatible with low-cost layered oxide and phosphate cathodes and the associated electrolyte.

**GENERAL APPROACH:** Our anode approach is to synthesize, characterize and develop inexpensive materials that have a potential around 500 mV above that of pure Li (to minimize risk of Li plating and thus enhance safety), and to have higher volumetric energy densities than carbon. Emphasis will be placed on simple metal alloys/composites at the nano-size. Initially, Sn will be emphasized, building on what has been learned from our studies of the tin-cobalt anode, the only commercial anode besides carbon. All materials will be evaluated electrochemically in a variety of cell configurations, and for thermal, kinetic and structural stability to gain an understanding of their behavior.

**STATUS OCT. 1, 2012:** It has been shown that amorphous nano-size Sn alloys have a high capacity and maintain it on deep or shallow cycling, when stabilized with elements like Co. In contrast, bulk crystalline metals have a high capacity, but their capacity fades rapidly after several deep cycles in carbonate-based electrolytes due to resistive continuous SEI formation. A nano-Sn material which shows electrochemical behavior comparable to that of the Sn-Co alloy, but where all the Co has been replaced by low-cost Fe, has been successfully formed by mechanical synthesis. This material has a higher volumetric capacity than Conoco Philips CPG-8 Graphite and has been formed by two different synthesis methods.

**STATUS SEP. 30, 2013:** The proposed work will result in the development of durable metal-based Li-ion battery anodes with volumetric energy densities that approach double those of the state-of-the art carbons. The reaction mechanism of the nano-Sn materials and the role of the carbon in their electrochemical activity will be understood. The major cause of the first-cycle excess charge capacity will be determined, and approaches to mitigate it will be proposed. Some clues as to how to control the SEI on such materials to optimize lifetime will be obtained.

**RELEVANT USABC GOALS:** 5000 deep and 300,000 shallow discharge cycles, abuse tolerance to cell overcharge and short circuit, and maximum system volume.

**MILESTONES:**

- (a) Determine the reaction mechanism of the nano-Sn-Fe-C system. (May 13) **Complete**
- (b) Identify the cause of the first-cycle excess charge capacity; propose approaches to mitigate it. (Sep 13) **Complete**
- (c) Identify an anode candidate having an energy density of 2 Ah/cc for at least 100 cycles. (Sep. 13) **Ongoing, complete up to 50 cycles**
- (d) Determine the electrochemistry of the leached nano-Si material, and compare to the standard Si. (Sep. 13) **Complete**

## PROGRESS TOWARD MILESTONES

The goal of this project is to synthesize new tin- and Si-based anodes that have double the volumetric capacity of the present carbons, without diminishing the gravimetric capacity.

**Milestones:** (a) The reaction mechanism of nano-sized Sn-Fe-C anode materials has been studied by X-ray absorption spectroscopy (XAS), which reveals it is a conversion reaction that converts Sn and Sn<sub>2</sub>Fe to Li-Sn alloys. An obvious absorption edge energy shift can be found for the tin K-edge, which confirms that the oxidation state of Sn undergoes a substantial change during the lithiation/delithiation process. More studies are underway to achieve a fuller understanding of the reaction mechanism. (b) The first-cycle excess capacity of this material is mainly due to the formation of LiC<sub>2</sub> from the carbon; this carbon contributes significantly to the overall capacity. In addition, the existence of titanium oxides may also contribute to the first cycle excess capacity, since the lithium titanium oxide formed in the first discharge is not reversible at the charging potentials used. Further investigation is in progress to mitigate this excess capacity (such as decreasing the graphite amount). (c) The electrochemical performance of nano-sized Sn-Fe-C is detrimentally impacted by the presence of pure Sn, and a capacity approaching 1.6 Ah/cm<sup>3</sup> has been achieved for up to 50 cycles.

**Milestone (d):** The electrochemistry of leached nano-Si has been determined; the initial results are promising and have now been published (see below). A comparative study has been carried out on the leached nano-Si, standard Si, and another company's Si sample. The testing protocol is set as follows: 0.12 mA (~C/40) for the first cycle, followed by 0.5 mA (~C/10) for the remaining cycles over the potential range 0.01 to 2 V. Among these Si materials, the leached nano-Si possesses a good capacity stability, which attains 1350 mAh/g after 18 cycles and is still growing. The standard Si has a high capacity up to 2300 mAh/g but it fades gradually. The company provided Si behaves similarly, with a capacity of 1250 mAh/g after 17 cycles.

**Further plans to meet or exceed milestones:** None  
**Reason for changes from original milestones:**  
 Milestone (a) was delayed from May 2013 until September 2013 to obtain synchrotron time at BNL.

### Publication and Presentation:

Wenchao Zhou, Tianchan Jiang, Hui Zhou, Yuxuan Wang, Jiye Fang and M. Stanley Whittingham, "The nanostructure of the Si-Al eutectic and its use in lithium batteries", *MRS Communications*, **3**, 119-121, (2013).

M. Stanley Whittingham, "What are the Materials Limitations to Intercalation Batteries", September 25, 2013, King Abdullah University of Science and Technology, Saudi Arabia.

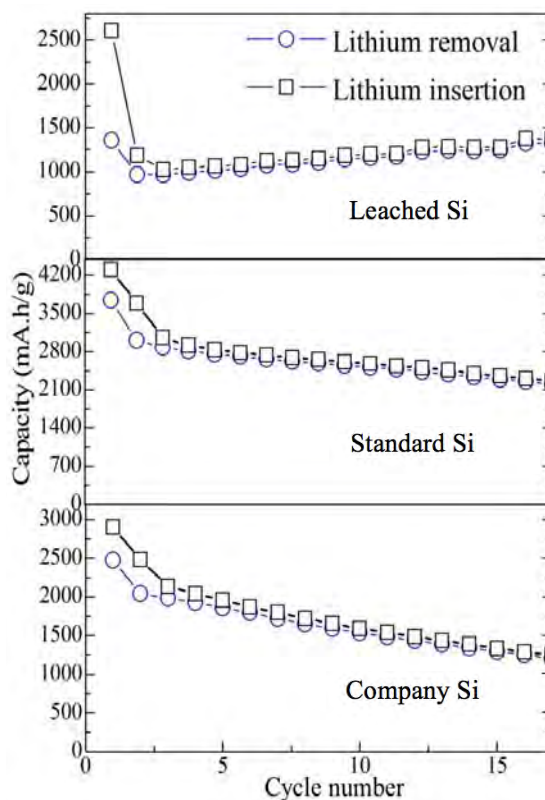


**Figure 1.** Electrochemical performance of (top) leached nano-Si (middle), standard Si, and (bottom) another company Si.

**Task 2.3 – PI, INSTITUTION:** Prashant Kumta, University of Pittsburgh

**TASK TITLE:** Anodes – Nanoscale Heterostructures and Thermoplastic Resin Binders: Novel Li-ion Anode Systems

**BASELINE SYSTEMS:** Conoco Philips CPG-8 Graphite/1 M LiPF<sub>6</sub>+EC:DEC (1:2)/Toda High-energy layered (NMC)

**BARRIERS:** Low specific energy and energy density, poor cycle life and coulombic efficiency, large irreversible loss, poor rate capability, and calendar life.

**OBJECTIVES:** To identify new alternative nanostructured anode materials to replace graphite that will provide higher gravimetric and volumetric energy density. The goal is to replace carbon with an inexpensive nanostructured composite exhibiting higher capacity (1200 mAh/g) than carbon while exhibiting similar irreversible loss (<15%), coulombic efficiency (>99.9%), and cyclability. The project addresses the need to improve the capacity, specific energy, energy density, rate capability, cycle life, coulombic efficiency, and irreversible loss issues of Si anode.

**GENERAL APPROACH:** Our approach is to search for inexpensive silicon, carbon, and other inactive matrix-based composites (powders rather than thin films) that provide 1) an electrochemical potential a few hundred mV above the potential of Li, and 2) a capacity of 1200 mAh/g or greater (>2600 mAh/ml). The focus will be on exploring novel economical methods to generate nanoscale heterostructures of various Si nanostructures and different forms of C derived from graphitic carbon nanotubes (CNT) and new binders. Other electrochemically inactive matrices will also be explored. Promising electrodes will be tested in half cells against Li and compared to graphite as well as in full cells. Electrode structure, microstructure, rate capability, long- and short-term cyclability, coulombic efficiency, SEI origin and nature will also be studied.

**STATUS OCT. 1, 2012:** Nano-scale electrodes comprising Si-graphitic carbon-polymer derived C, and CNT related systems have been successfully synthesized and analyzed in half cells. The nano-composite Li-Si-C hetero-structures exhibit stable capacities of 700-3000 mAh/g with first cycle irreversible loss less than 15% and coulombic efficiency in the ~99.5-99.9% range.

**STATUS SEP. 30, 2013:** Efforts will continue to generate nano-composite ‘core-shell’, random, and aligned nanoscale Si, boron (B), and C exhibiting 1500 mAh/g and higher capacities. Research will be conducted to generate novel binders, explore novel synthesis and nano-scale microstructure affecting energy density, rate capability, first-cycle irreversible loss (FIR) and coulombic efficiency, characterize the SEI layer, and outline steps to yield stable capacity, reduce FIR, increase the coulombic efficiency and also improve the rate capability.

**RELEVANT USABC GOALS:** Available energy - CD Mode, 10 kW Rate: 3.4 kWh (10 mile) and 11.6 kWh (40 mile); Available Energy - CS Mode: 0.5 kWh (10 mile) and 0.3 kWh (40 mile); 10s peak pulse discharge power: 45 kW (10 mile) and 38 kW (40 mile); Peak Regen Pulse Power (10 sec): 30 kW (10 mile) and 25 kW (40 mile); Cold cranking power at -30°C, 2sec-3 Pulses: 7kW; Calendar life: 15 years (at 40°C); CS HEV Cycle Life, 50 Wh Profile: 300,000 Cycles

**MILESTONES:**

- (a) Identify binders and approaches to reach stable reversible capacity  $\geq 1500$  mAh/g (Sep. 13) **Complete**
- (b) Identify strategies to achieve first cycle irreversible loss ( $\leq 15\%$ ), efficiency ( $\geq 99.95\%$ ), and rate capability matching carbon (Sep. 13) **Complete**

## PROGRESS TOWARD MILESTONES

Large scale synthesis of hollow Si nanotubes (SiNTs) with high capacity (1000 to 1500 mAh/g) and cycle life were demonstrated in previous reports. In Q4, the SiNT electrodes were cycled according to DOE-BATT recommended test conditions and the rate capability characteristics are reported (Fig. 1). According to the DOE-BATT test protocol, the SiNTs were cycled at a current density of 0.02 mA/cm<sup>2</sup> between the voltage range 0.005 to 1 V vs. Li<sup>+</sup>/Li for the first 3 cycles (for stable SEI layer formation). A first discharge and charge capacity of 2810 mAh/g and 2035 mAh/g were observed resulting in a first cycle irreversible loss of 27%. Current densities of 0.5 and 0.75 mA/cm<sup>2</sup> were applied for lithiation and de-lithiation processes respectively. A stable and reversible capacity around 1500 mAh/g was obtained for 100 cycles and a coulombic efficiency close to 99.5% was achieved when cycled with current densities of 0.5 and 0.75 mA/cm<sup>2</sup> for lithiation and de-lithiation, respectively. This translates to a capacity retention of 93.2% for 100 cycles and a fade rate of 0.07% loss per cycle. The SiNTs also showed good rate capability when cycled from a current density of 0.5 to 4 A/g (Fig. 2). Capacities close to 1200 to 1500 mAh/g were obtained at high current densities of 4 A/g. The excellent electrochemical characteristics of SiNTs and the low-cost, scalable-production approach makes it an excellent candidate to replace graphite for the next generation of Li ion batteries. The electrodes comprising SiNTs as anodes contain 50 wt% active material (SiNTs), 40 wt% binder (sodium alginate), and 10 wt% Super-P. The loadings of the electrode (active+inactive) are 0.7 to 0.8 mg/cm<sup>2</sup>. It should be noted that the specific capacities reported here are based on the active material loading.

The electrochemical data of GG and MGG elastomeric binders for Si/C based anodes, reported in Q2, shows an improvement in long term cyclability when compared to PVDF. Recently, a modified amine based binder (MAB) has been identified that shows excellent cyclability even when tested with high specific capacity Si/C based anodes (*ca.* 1000 mAh/g) synthesized by high energy mechanical milling (Fig. 3). Si/C composite with MAB shows 21% first-cycle irreversible loss and excellent capacity retention of specific capacity of *ca.* 800 mAh/g when cycled at a rate of 300 mA/g. The Si/C electrodes comprise 85 wt% active material (Si/C), 5 wt% binder, and 10 wt% Super-P. The loadings of the electrode (active+inactive) are 3 mg/cm<sup>2</sup>.

**STATUS SEPT. 30, 2013:** Hollow Si nanotubes (SiNTs) synthesized using a novel, cost-effective approach exhibit stable and reversible capacities *ca.* 1500 mAh/g at 2 A/g current density. Interface control agents (ICA) developed for Si/C composites exhibit low first-cycle irreversible loss (<15%) and good capacity retention. Novel high strength and elastomeric polymer binders were identified and engineered to control the volumetric expansion in Si based anodes. These binders out performed the commercial and currently used binders for Li-ion anodes, PVDF.

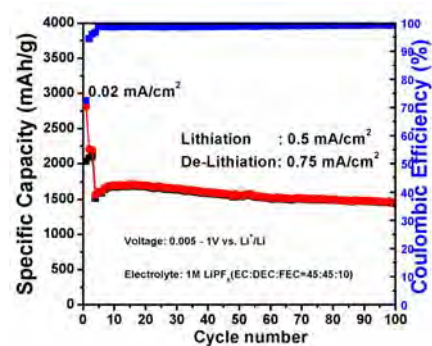


**Figure 1:** Charge-discharge characteristics obtained on hollow SiNTs using DOE recommended test conditions.

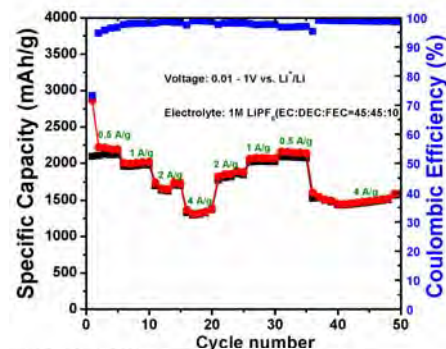


**Figure 2:** Rate capability of hollow SiNTs

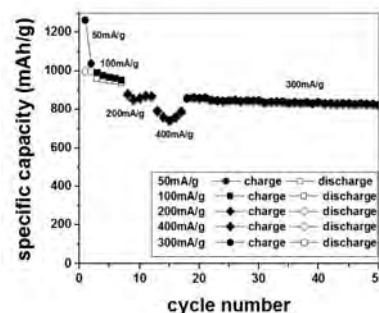


**Figure 3:** Charge-discharge characteristics of Si/C composite with MAB binder.

**TASK 2.4 – PI, INSTITUTION:** Ji-Guang (Jason) Zhang and Jun Liu, Pacific Northwest National Laboratory

**TASK TITLE – PROJECT:** Anodes – Development of Silicon-based High Capacity Anodes

**BASELINE SYSTEMS:** Conoco Philips CPG-8 Graphite/1 M LiPF<sub>6</sub>+EC:DEC (1:2)/Toda High-energy layered (NMC)

**BARRIERS:** Low energy density, high cost, limited cycle life

**OBJECTIVES:** To develop high-capacity, low-cost electrodes with good cycle stability and rate capability to replace graphite in Li-ion batteries

**GENERAL APPROACH:** The main failure mechanism in Si-based anodes will be addressed using three approaches: improve the mechanical stability of Si-based anodes by manipulating the nano-structure of Si; improve electrical stability and conductivity of Si-based anodes by using conductive coating and binder; improve interface stability of Si-based anodes by choosing a stable electrolyte/binder with selective additives.

**STATUS OCT. 1, 2012:** Hollow core-shell structured porous Si-C nanocomposites with void space up to 30 nm between the Si core and the carbon shell have been designed and synthesized, and their electrochemical performance has been investigated. The porous core-shell structure of the Si-C composite helps to accommodate the large volume variations that occur during Li-insertion/extraction processes. In another effort, a conductive rigid skeleton-supported Si, such as B<sub>4</sub>C/Si/C core-shell composite, was developed using the scalable ball-milling method. A high capacity of ~822 mAh/g (based on the full electrode) and capacity retention of ~94% over 100 cycles were obtained at a current density of ~0.63 A/g.

**STATUS SEP. 30, 2013:** The porous Si and the skeleton-supported core-shell structured composite (*e.g.*, B<sub>4</sub>C/Si/C) will be further optimized. The optimized B<sub>4</sub>C/Si/C material will be used as the baseline material for fundamental understanding of the failure mechanism. New binders, electrolyte, and electrolyte additives will be investigated to further improve the performance of Si-based anodes. New approaches will be developed to increase the capacity of thick Si-based anodes. An initial capacity of >800 mAh/g (based on the whole electrode) and ~80% capacity retention over 300 cycles will be obtained. Fundamental understanding of the formation and evolution of SEI layer, electrolyte additives, and the effect of electrode thickness will be investigated by *in situ* microscopic analysis.

**RELEVANT USABC GOALS:** >96 Wh/kg (for plug-in hybrid electric vehicles [PHEVs]), 5000 deep-discharge cycles, 15-year calendar life, improved abuse tolerance, and less than 20% capacity fade over a 10-year period.

**MILESTONES:**

- (a) Optimize the hollow core-shell structured porous Si and the rigid skeleton-supported Si composite for high capacity and stable cycling. (Mar. 13) **Complete**
- (b) Improve the performance of Si-based anodes with a capacity retention of >700 mAh/g over 250 cycles using new binders/electrolyte additives. (Sep. 13) **Complete**
- (c) Develop new approaches to improve the cyclability of thick electrodes (>3 mAh/cm<sup>2</sup>). (Sep. 13) **Complete**

## PROGRESS TOWARD MILESTONES

All the milestones for FY13 were met. Porous Si-based anodes using new binders/electrolyte additives can retain a capacity retention of >700 mAh/g over more than 300 cycles. High loading Si composite (initial capacity *ca.* 1.5 mAh/cm<sup>2</sup>) with CMC-SBR binder can retain more than 1.31 mAh/cm<sup>2</sup> capacity over 100 cycles.

The fundamental mechanism behind the effectiveness of fluoroethylene carbonate (FEC) as an electrolyte additive that can significantly improve the cycleability of Si was investigated. Based on the results obtained from <sup>6</sup>Li NMR (Fig. 1), XPS (Table 1), and calculated Mulliken charges of atoms in FEC (Fig. 2(a)), a molecular-level mechanism (Fig. 2(b)) was established to understand how FEC affects the formation of a SEI: 1) FEC is reduced through the opening of the five-member ring leading to the formation of lithium poly(vinyl carbonate), LiF, and some dimers; 2) FEC-derived lithium poly(vinyl carbonate) enhances the stability of the SEI film. The proposed reduction mechanism opens a new path to explore new electrolyte additives that can improve the cycling stability of Si-based electrodes.

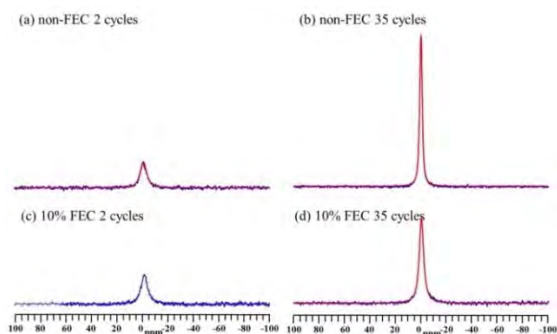


**Figure 1.** <sup>6</sup>Li NMR of the SEI of SBG electrodes with and without FEC additive.

Samples	Elements	Li	C	O	F	Li/F ratio
Electrolyte (a), 2 cycles		27.7	23.3	24.1	24.9	1.11
Electrolyte (a), 35 cycles		22.7	31.3	37.6	8.4	2.70
Electrolyte (b), 2 cycles		22.9	32.5	32.1	12.5	1.83
Electrolyte (b), 100 cycles		21	33.8	31.9	13.3	1.58
Electrolyte (c), 2 cycles		211	34.7	32.2	12	1.76

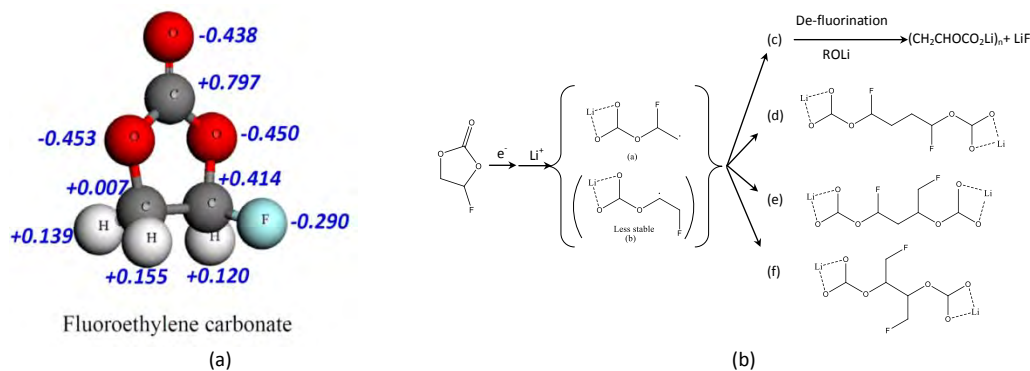


**Figure 2.** (a) Calculated Mulliken Charges of atoms in FEC. (b) A proposed decomposition mechanism of FEC.

### Publication:

Xilin Chen, Xiaolin Li, Donghai Mei, Ju Feng, Mary Y Hu, Jianzhi Hu, Mark Engelhard, Jianming Zheng, Wu Xu, Jie Xiao, Jun Liu, Ji-Guang Zhang, “Reduction and polymerization of fluoroethylene carbonate for stable SEI *via* alternative ring opening mechanism,” accepted for publication in *ChemSusChem* (2013).

**TASK 2.5 - PI, INSTITUTION:** Chunmei Ban, National Renewable Energy Laboratory; Co-PIs Steven M. George and Se-Hee Lee, University of Colorado (CU), Boulder

**TASK TITLE - PROJECT:** Anodes – Atomic Layer Deposition for Stabilization of Amorphous Silicon Anodes

**BASELINE SYSTEMS:** Conoco Philips CPG-8 Graphite/1 M LiPF<sub>6</sub>+EC:DEC (1:2)/Toda High-energy layered (NMC)

**BARRIERS:** Cost, low gravimetric and volumetric capacities, safety, rate capability, calendar and cycle life.

**OBJECTIVES:** To develop a low-cost, thick, and high-capacity Si anode with sustainable cycling performance. In FY13, our specific objectives are to develop a novel conductive and elastic scaffold by using Atomic Layer Deposition (ALD) and Molecular Layer Deposition (MLD), demonstrate the durable cycling by using our coating and electrode design, and investigate the effect of the atomic surface modification on the irreversible capacity loss.

**GENERAL APPROACH:** Chemical vapor deposition *via* silane decomposition on a hot filament has been used to synthesis the a-Si or nano-Si powders. Recently, a Nanocrystal RF Plasma Reactor was also utilized to synthesis Si/alloy nanocrystals with uniform size and shape. Size may be tuned from <10 to ~100 nm by varying the plasma conditions that will allow the study of how Si nanocrystal size affects the electrochemical performance. The conventional electrodes containing active material, conductive additive, and binder have been fabricated to evaluate the cycling properties. ALD is employed to coat both Si particles and Si electrodes in order to enhance the surface stability and electrode integrity.

**STATUS OCT. 1, 2012:** A Si anode coated with a unique copper/carbon composite was demonstrated to have a highly durable capacity at C/20 and C/10 with a coulombic efficiency of ~98%. ALD was employed on the thick Si anode to achieve the sustainable cycling performance. Recently, more durable cycling at higher rates (C/5 and C/3) has been achieved by using ALD-coated nano-Si anode. The thick Si electrodes (>15 μm) were recently sent to Dr. Vince Battaglia at LBNL for electrochemical testing.

**STATUS SEP. 30, 2013:** The optimal composition and structure of the ALD/MLD surface coatings will be established to improve the surface stability of Si particles as well as increase the integrity of Si electrodes. A thick Si anode with the appropriate ALD/MLD coatings will be demonstrated to have a high durable capacity as well as high rate capability. *In situ* characterization will be completed to better understand the structural evolution of the coated Si anodes during cycling.

**RELEVANT USABC GOALS:** 200 Wh/kg (EV requirement); 96 Wh/kg, 316 W/kg, 3000 cycles (PHEV 40 mile requirement). Calendar life: 15 years. Improved abuse tolerance.

#### **MILESTONES**

- (a) Identify and characterize the MLD hybrid metal-organic coating on Si anode. (Dec. 12) **Complete**
- (b) Demonstrate durable cycling (>100 cycles) of the surface-engineered thick Si anodes (>15μm) at C/3. (Mar. 13) **Complete**
- (c) Characterize the effect of MLD metal alkoxide coatings on the cyclability of Si anodes, and demonstrate an MLD-coated Si anode with an irreversible capacity loss at 1<sup>st</sup> cycle less than 10%. (Jun. 13) **Complete**
- (d) Supply the optimized thick electrodes (>20um) fabricated in the MLD flexible network to LBNL for verification. (Sep. 13) **Ongoing evaluation, due Dec. 13**

## PROGRESS TOWARD MILESTONES

All the tasks planned in the FY 13 AOP were completed. The optimal composition and structure of the MLD surface coatings were established to improve the surface stability of Si particles as well as increase the integrity of Si electrodes. The MLD-coated, thick, Si anodes have shown greatly improved cycling performance. Using advanced microscopy and electrochemical analysis further confirmed the conformity and uniformity of MLD coatings on nano-Si composite electrodes.

**The conformal MLD coating greatly improved Coulombic Efficiency of the coated Si anodes.** The optimization of the MLD coating parameters was performed over the past months, in order to obtain a thin and conformal coating for the laminated electrodes. A conformal thin coating on the nano-Si particles was observed through the use of high-resolution microscopy. High-angle, annular, dark-field (HAADF), scanning-transmission-electron microscopy (STEM), which is highly sensitive to atomic number contrast (Z-contrast imaging), was used to further clarify the conformity of the aluminum alkoxide (Alucone) coating on the nano-Si particles. An HAADF-STEM image (Fig. 1) shows that the Alucone layer is a thin (~5 nm), dense, and conformal coating adherent to the nano-Si particles.

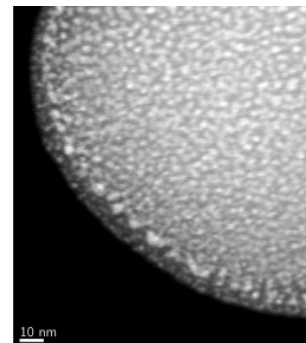


**Figure 1.** HAADF-STEM of an uncycled nano-Si particle coated with MLD Alucone.

The significantly improved cycling performance was demonstrated by the Alucone-coated Si anodes, as shown in Fig. 2. Furthermore, the coated Si anode exhibits highly reversible capacity for the first cycle, resulting in much higher coulombic efficiency (CE), as emphasized in Fig. 2. The Alucone-coated Si anode has a CE of 84%, compared to the CE of 68% for an uncoated Si anode. The high CE is evidence of an improved interface between the electrode and liquid-electrolyte, suggesting that the MLD coating layer limits the irreversible charge loss due to side reactions. To confirm the possible passivating properties of the MLD coating, the voltage profiles of the initial lithiation cycle are plotted as a function of normalized capacity for both uncoated and coated electrodes and displayed in Fig. 3. The bare electrode shows a plateau between the potentials 0.8 to 0.5 V (vs.  $\text{Li}^+$ ), whereas the coated electrode only shows a smooth slope. Figure 3 confirms the coating helps mitigate the secondary reactions that happen between the liquid electrolyte and the electrode surface during the first lithiation process. By this mechanism, the employment of an Alucone coating on conventional nano-Si composite electrodes provides significant improvement in cycling stability.

### Publication:

Chunmei Ban, et al., “Atomic layer deposition of amorphous  $\text{TiO}_2$  on graphene as an anode for Li-ion batteries,” *Nanotechnology*, **24** 424002, (2013). DOI:10.1088/0957 4484/24/42/424002.

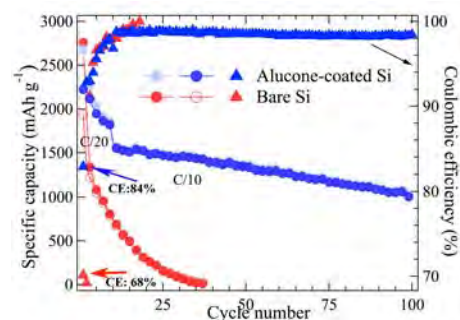


**Figure 2.** Sustainable cycling performance observed in the MLD Alucone coated Si anodes; higher coulombic efficiency obtained in the coated Si anodes.

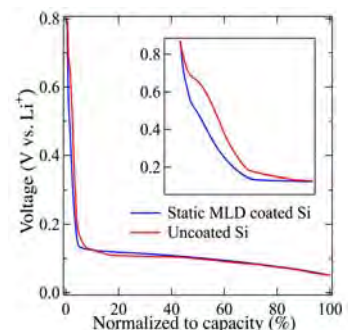


**Figure 3.** Voltage profile of the initial lithiation cycles of both uncoated and coated electrodes normalized to capacity. The inset plot focuses only from 0 to 8% for a clearer view of the passivating effect the AIGL coating has on the electrode.

**TASK 2.6 - PI, INSTITUTION:** Yury Gogotsi and Michel Barsoum, Drexel University

**TASK TITLE - PROJECT:** Anodes – New Layered Nanolaminates for Use in Lithium Battery Anodes

**BASELINE SYSTEMS:** Conoco Philips CPG-8 Graphite/1 M LiPF<sub>6</sub>+EC:DEC (1:2)/Toda High-energy layered (NMC)

**BARRIERS:** Needs increased life, capacity and improved safety.

**OBJECTIVES:** Replace graphite with new solids: the layered binary carbides and nitrides known as MXenes, where the A-group element is selectively etched from the MAX phases – the latter ternary layered carbides and nitrides, may offer combined advantages of graphite and Si anodes with a higher capacity than graphite, less expansion, longer cycle life, and a lower cost than Si nanoparticles.

**GENERAL APPROACH:** Since, at this time the relationship between capacity and MXene phase chemistry is unknown, a rapid screening of as many MXene phases as possible is being carried out to determine the most promising chemistry by testing their performance in Li ion batteries. This work will also be guided by *ab initio* calculations.

**STATUS OCT. 1, 2012:** Fully exfoliate select MAX phases into two-dimensional layers of transition metal carbides or carbonitrides (MXenes) and test the different MXenes as anode materials in LIBs.

**STATUS SEP. 30, 2013:** Complete a study of the effect of different exfoliated MXenes chemistries and structures on SEI formation. Optimize the performance of MXenes anode materials in LIBs, by selecting the best carbon and binder additives for the MXenes.

**RELEVANT USABC GOALS:** 200 Wh/kg (EV requirement); 96 Wh/kg, 316 W/kg, 3000 cycles (PHEV 40 mile requirement). Calendar life: 15 years. Improved abuse tolerance.

**MILESTONES:**

- (a) Select the best carbon additive and binder that results in the highest Li uptake for select MXenes. (Dec. 12) **Complete**
- (b) Develop higher volumetric capacity anodes for LIBs than the commercial anodes. (Jun. 13) **Complete**
- (c) Produce MXenes of new chemistries (such as Nb<sub>2</sub>C, V<sub>2</sub>C) that can achieve anode capacities of 400 mAhg<sup>-1</sup> at cycling rates of 1C or faster. (Sep. 13) **Complete**
- (d) Produce MXene anodes with capability of delivering a stable performance at 10 C cycling rates. (Sep. 13) **Ongoing, delayed to Dec. 13**

## PROGRESS TOWARD MILESTONES

In the preceding quarter, synthesis of two new MXenes,  $\text{Nb}_2\text{C}$  and  $\text{V}_2\text{C}$ , was reported and their testing in Li-ion batteries presented (already published in *JACS*). At 1C, a reversible capacity of  $280 \text{ mAhg}^{-1}$  was obtained for the as-synthesized  $\text{V}_2\text{C}$ , which is more than double that for as-synthesized  $\text{Ti}_3\text{C}_2$ . However, once delamination of  $\text{Ti}_3\text{C}_2$  was achieved, a 4-fold increase in capacity was obtained ( $410 \text{ mAhg}^{-1}$  for additive-free electrodes of delaminated  $\text{Ti}_3\text{C}_2$ ). Thus, it is reasonable to assume that delaminated  $\text{V}_2\text{C}$  would achieve much higher capacities than  $400 \text{ mAhg}^{-1}$  at 1C. Work is ongoing on delamination of  $\text{V}_2\text{C}$  to produce flexible electrodes.

A new MXene,  $\text{Mo}_2\text{C}$ , was synthesized from a Mo-containing MAX phase. While etching resulted in a sample that contained only *ca.* 17 wt%  $\text{Mo}_2\text{C}$  due to incomplete conversion, this sample exhibited a reversible capacity of  $70 \text{ mAhg}^{-1}$  after more than 500 cycles at 1C. Since the unreacted MAX phase is an inactive material, the specific capacity of  $\text{Mo}_2\text{C}$  exceeds  $400 \text{ mAhg}^{-1}$  at 1C even before delamination. Work is ongoing to tune the synthesis parameters to make purer  $\text{Mo}_2\text{C}$ .

As discussed at the BATT AMR Anode meeting on May 17, one of the main challenges that face Si anodes is the low areal capacity; a focus group was formed to answer the question "how would it be possible to get to  $4 \text{ mAh/cm}^2$  electrodes?" MXene powders were pressed into  $300 \mu\text{m}$  discs (Fig. 1a). Since MXenes are electrical conductors, they do not need conductive additives, there is no extra deadweight of the Cu current collector, and since they are free-standing, there is no need for the binders used in conventional electrodes. Pressed  $\text{Nb}_2\text{C}$  MXene was tested as an anode material using the conditions suggested by the BATT Anode team leaders - cycling between 5 mV and 1.0 V, using a lithiation current of  $0.5 \text{ mA/cm}^2$  and delithiation current of  $0.75 \text{ mA/cm}^2$ . The areal capacity vs. cycle number is shown in Fig. 1b for two different cells (cell I loading was  $94 \text{ mg/cm}^2$ ; cell II loading was  $136 \text{ mg/cm}^2$ ). A reversible capacity of  $3.3 \text{ mAh/cm}^2$  was obtained after 60 cycles for cell I - more than double that reported for the Si baseline electrode after 20 cycles under the same conditions. By increasing the loading to  $136 \text{ mg/cm}^2$ , a reversible areal capacity of  $7 \text{ mAh/cm}^2$  was obtained after 11 cycles (cycling is still ongoing for cell II). The latter value is 5 times higher than what was reported for the Si baseline electrode after 11 cycles. The ratio of the areal capacity for the two cells after the same number of cycles was 7:4.6, very close to the loading ratio of 136:94. This suggests that even more loading can be achieved for MXenes to further increase the areal capacity without deteriorating the electrode performance, a crucial consideration for practical applications. The fact that such impressive figures have been obtained just two years after discovery of these 2D materials is simply remarkable, and bodes very well for the future. In the last year of this project, the team fully anticipates combining an areal capacity  $>5 \text{ mAh/cm}^2$ , at 1C rate, together with capacities  $>400 \text{ mAhg}^{-1}$  for more than 1000 cycles.

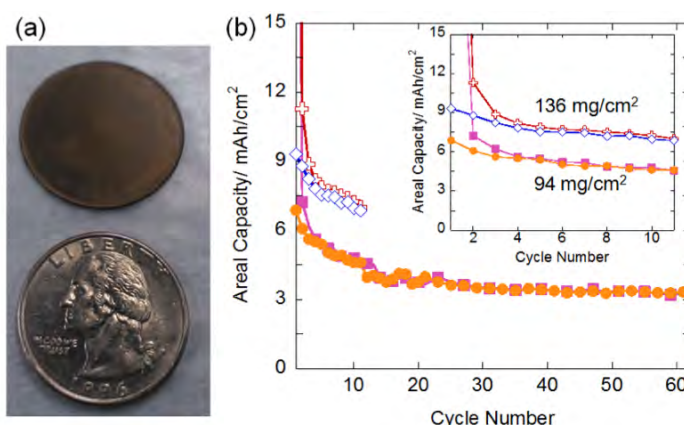


**Figure 1.** a) Free-standing additive-free  $\text{Nb}_2\text{C}$  MXene disc produced by pressing  $\text{Nb}_2\text{C}$  powder under 1 GPa at room temperature. b) Areal capacity vs. cycle number for pressed additives-free  $\text{Nb}_2\text{C}$ . The inset shows a zoom in the first 11 cycles for cells with two different loading ( $94$  and  $136 \text{ mg/cm}^2$ ). The squares and crosses are for lithiation capacities, while the circles and diamonds are for delithiation capacities for the loading of  $94$  and  $136 \text{ mg/cm}^2$ , respectively.

**Task 2.7-PI, INSTITUTION:** Donghai Wang and Michael Hickner, Pennsylvania State University

**TASK TITLE - PROJECT:** Anodes – Synthesis and Characterization of Structured Si/SiO<sub>x</sub>-based Nanocomposite Anodes and Functional Polymer Binders

**BASELINE SYSTEMS:** Conoco Philips CPG-8 Graphite/1 M LiPF<sub>6</sub>+EC:DEC (1:2)/Toda High-energy layered (NMC)

**BARRIERS:** Low energy, poor capacity cycling, large initial irreversible capacity.

**OBJECTIVES:** Obtain high-performance Si anode materials by developing novel-structured Si/SiO<sub>x</sub>-carbon nanocomposites and polymer binders to improve electrode kinetics and cycling life, and decrease initial irreversible capacity loss.

**GENERAL APPROACH:** Our approach is to synthesize Si/SiO<sub>x</sub>-carbon nanocomposites with controlled nanostructures to improve kinetics and cycling stability upon lithiation/delithiation. New polymer binders will be developed with controlled mechanical properties by variation in crosslinking and SiO<sub>x</sub> or carbon surface-binding functionality. These new binders are meant to help stabilize Si particles by providing a low-swelling polymer matrix with strong interactions with the anode particles and low electrolyte uptake.

**STATUS OCT. 1, 2012:** Silicon-carbon nanocomposites were developed with capacity above 800 mAh/g and capacity retention of 75% after 100 cycles. Evaluation of Si/SiO<sub>x</sub> nanoparticles with stable capacity of 650 mAh/g after 500 cycles has been completed. New materials strategies for low electrolyte uptake sulfonated binders with variable crosslinking are reported with their performance evaluated against CMC-SBR and Na-CMC controls. Capacity degradation is still observed within 50 cycles and new binder formulations are being developed.

**STATUS SEP. 30, 2013:** Synthesis, characterization and electrochemical performance evaluation of Si/SiO<sub>x</sub>-carbon nanocomposites will be completed to demonstrate optimized electrodes with stable cycle life and increased efficiency. Increased polymer binder performance with carboxylate-containing, cross-linked, mechanically stiff polymers will be demonstrated. Structure-property relationships for creating new, non-conductive binders that are soluble in benign solvents will be reported.

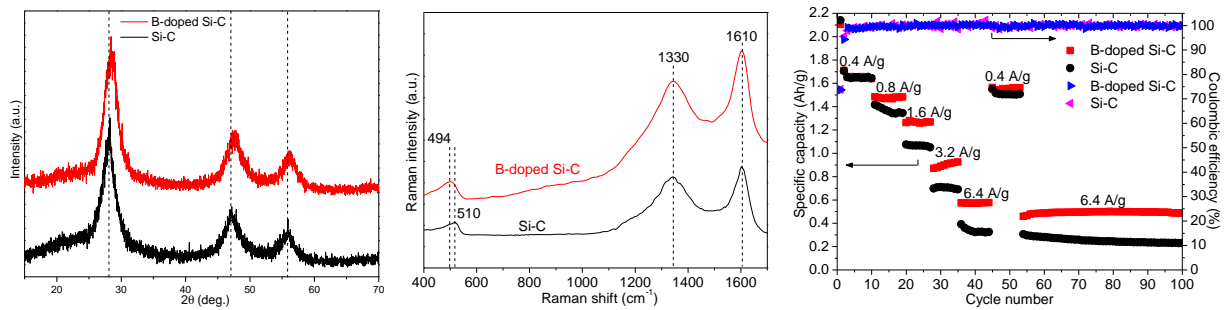
**RELEVANT USABC GOALS:** 200 Wh/kg (EV requirement); 96 Wh/kg, 316 W/kg, 3000 cycles (PHEV 40 mile requirement). Calendar life: 15 years. Improved abuse tolerance.

**MILESTONES:**

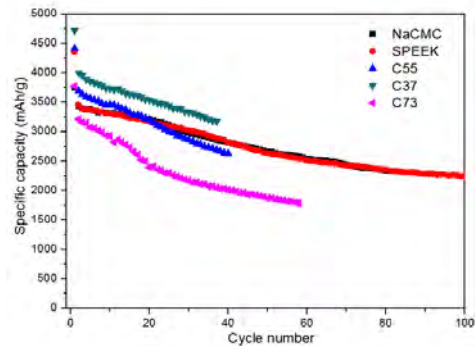
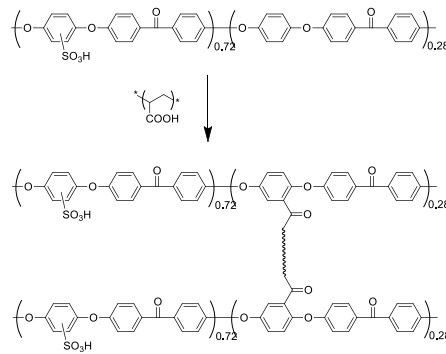
- (a) Synthesize and characterize three types of Si/SiO<sub>x</sub>-carbon nanocomposites. (Jan. 13) **Complete**
- (b) Demonstrate new crosslinking chemistry involving sulfonates, carboxylates, and azide chemistries for low-swelling polymer binders. (Sep. 13) **Complete**
- (c) Identify at least one Si/SiO<sub>x</sub>-carbon nanocomposite anode with a reversible specific capacity of at least 1000 mAh/g over 200 cycles. (May 13) **Complete**
- (d) Identify and optimize at least one polymer binder and processing solvent that shows better cycling performance than the reported binders with commercial Si nanoparticles. (Sep. 13) **Complete**
- (e) Supply laminates of the optimized electrodes with electrode capacity of 800 mAh/g that cycle 100 cycles to BATT PIs. (Aug. 13) **Complete**

## PROGRESS TOWARD MILESTONES

**Si-based anode materials:** The influence of boron doping on the electrochemical performance of the micro-sized Si-C composites reported in the FY13 Q1 report was further investigated. Boron doping was achieved by simply introducing dopant precursors ( $B_2O_3$ ) during the thermal disproportionation of SiO. Compared to undoped Si-C, the XRD peaks of B-doped Si-C shift to higher angles due to the replacement of Si atoms by smaller B atoms, which leads to a smaller lattice constant. This result, combined with the absence of Si-B alloy peaks, indicates the successful doping of B into Si. The Si Raman peak shifts from  $510\text{ cm}^{-1}$  for undoped Si to  $494\text{ cm}^{-1}$  for B-doped Si due to disorder in the Si structure caused by the stress developed in the surrounding Si atomic network after B doping, which is consistent with the XRD results. Boron in carbon was not detected as shifting of C peaks is not observed, which is due to the moderate carbon-coating temperature. The results above show only Si was doped with B in the composite. The B-doped Si-C composite shows much improved rate capability, delivering a capacity of  $575\text{ mAh/g}$  at  $6.4\text{ A/g}$  without any external carbon additive, 80% higher than that of undoped composite. The B-doped Si-C composite also exhibits better cycling stability at high rates. In contrast to the obvious capacity fading of Si-C, the capacity of B-doped Si-C was stable for about 50 cycles at  $6.4\text{ A/g}$ . The improved rate capability and cycling stability are attributed to lower charge transfer resistance of B-doped Si-C.



**Polymer binders:** Sulfonated poly(ether ether ketone) (SPEEK) binder has shown similar performance to NaCMC binder, but with higher rate capability, see previous reports. The crosslinking of SPEEK with PAA was investigated, see figure below, to decrease the swelling of the SPEEK binder in electrolyte. This strategy is different from PAA-type binders in that a mechanically robust network is formed between the SPEEK and PAA to constrain electrode swelling. The battery cycling performance demonstrated that the extent of crosslinking, denoted by samples C55, C37, and C73, had an influence on the specific capacity of the commercial Si-based nanoparticle electrode. In this formulation, the sample with 37 wt% PAA and 63 wt% SPEEK in the crosslinked binder had the best performance. There is still capacity fade in the cycling data at high capacity, but the performance of these new binders was increased over previously-reported commercial standards for Si in a number of SPEEK-based examples.



**TASK 2.8 - PI, INSTITUTION:** Yi Cui, Stanford University

**TASK TITLE - PROJECT:** Anodes – Wiring up Silicon Nanoparticles for High Performance Lithium-ion Battery Anodes

**BASELINE SYSTEMS:** Conoco Phillips CPG-8 Graphite/1 M LiPF<sub>6</sub>+EC:DEC (1:2)/Toda High-energy layered (NMC)

**BARRIERS:** Low energy density, low efficiency, short cycle life, and safety issues

**OBJECTIVES:** Overcome the charge capacity limitations of conventional carbon anodes by designing optimized nano-architected silicon electrodes as follows: 1) fabricate novel nanostructures that show improved cycle life, and 2) develop methods to study the lithiation/delithiation process to understand volume expansion for higher efficiency.

**GENERAL APPROACH:** This project explores 1) new types of nanostructured anodes, 2) methods for controlling SEI growth and electrode stability, and 3) the nature of volume changes in Si nanostructures. Over the course of the year, a variety of nanostructured electrodes will be developed, with particular emphasis placed on developing structures based on conductive frameworks and also making high performance electrodes with both nano- and micron-sized Si particles. In addition, hollow/porous nanostructures will be developed and optimized for SEI control in these electrode structures. Finally, separate efforts will be dedicated to understanding the fundamentals of volume expansion in Si nanostructures through *in situ* and *ex situ* single nanostructure observation; specifically, the fracture properties of Si with different crystallinity will be studied. This project was initiated January 1, 2011.

**STATUS OCT. 1, 2012:** A variety of conductive secondary additives (polymer, hydrogel, etc.) were developed. Nano- and micron-sized Si particle electrodes were fabricated with these additives. A variety of spherical, tubular, and porous Si nanostructures were fabricated and incorporated into Si anode architectures. Suitable amorphous and crystalline Si nanostructures with controlled sizes have been developed for study.

**STATUS SEP. 30, 2013:** Electrodes with cycle life >1000 cycles in a half cell and CE >99.5% will have been demonstrated from nano- and micron-sized Si particles. The critical size for fracture of amorphous nanostructures will have been found.

**RELEVANT USABC GOALS:** 200 Wh/kg (EV requirement); 96 Wh/kg, 316 W/kg, 3000 cycles (PHEV 40 mile requirement). Calendar life: 15 years. Improved abuse tolerance.

**MILESTONES:**

- (a) Develop conductive polymer additive/binder, incorporate into electrodes. (Jan 13) **Complete**
- (b) Determine the effect of electrode additives, coatings, and porosity on SEI thickness and properties. (Apr. 13) **Complete**
- (c) Optimize nano/micro particle electrodes for high capacity, >1000 cycles, >99.7% CE. (Jul. 13) **Complete**
- (d) Use *in situ* TEM and *ex situ* SEM to test critical size and rate for fracture for crystalline, polycrystalline, and amorphous Si nanostructures. (Jul. 13) **Complete**

## PROGRESS TOWARD MILESTONES

**Crab shells as sustainable templates from nature for Li-ion battery anodes.** A facile, scalable, and cheap method has been developed to fabricate high-performance Li-ion battery anodes by encapsulating Si nanoparticles in a carbon nano-channel array prepared from crab shells (*Nano Lett.* 2013, 13, 3385). Crab shells with the unique Bouligand structure consisting of highly mineralized chitin-protein fibers can be used as biotemplates to fabricate hollow carbon nanofibers. Typically, crab shell is calcined in air to remove the chitin-protein organic to form pure  $\text{CaCO}_3$  frameworks containing twisted hollow channels with *ca.* 60 nm inner diameter. As illustrated in Fig. 1b, a carbon thin-layer was then coated on the entire surface of the frameworks, followed by silicon deposition into the carbon channels. Finally, Si encapsulated carbon fibers are obtained after removing the  $\text{CaCO}_3$  with an HCl solution. The resulting nanostructured Si/C electrodes show high specific capacities (3060 mAh/g) and excellent cycling performance (up to 200 cycles with 95% capacity retention). The coulombic efficiency of cells after 200 cycles are 98.6% at C/2 and 98.9% at 1C (Fig. 1c). These results demonstrate the high stability of crab shell templated Si/C anode materials.

Since crab shells are readily available due to the 0.5 million tons produced annually as a byproduct of crab consumption, this waste-recycling preparation process is cheap and scalable for advanced re-chargeable Li ion batteries. In addition, this biotemplating concept will open a new avenue for producing nanostructured electrode materials from low-cost sustainable sources.

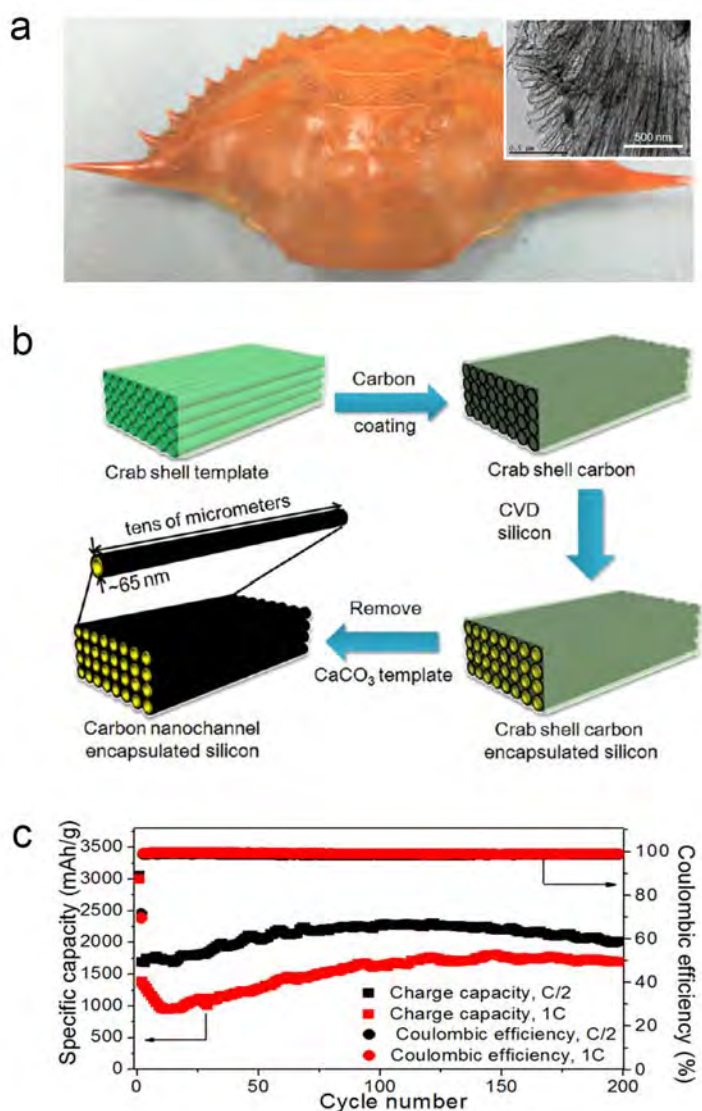


**Figure 1.** (a) Photo of a crab shell. The inset is TEM image of final carbon nano-channel arrays from crab shell. (b) Schematic illustration of the fabrication procedure for hollow carbon nanofiber arrays encapsulating silicon. Lithiation/delithiation capacity and CE of Si encapsulated crab shell-templated carbon channel.

**TASK 2.9 - PI, INSTITUTION:** Kwai Chan and Michael Miller, Southwest Research Institute

**TASK TITLE - PROJECT:** Anodes – Synthesis and Characterization of Silicon Clathrates for Anode Applications in Lithium-ion Batteries

**BASELINE SYSTEMS:** Conoco Phillips CPG-8 Graphite/1 M LiPF<sub>6</sub>+EC:DEC (1:2)/Toda High-energy layered (NMC)

**BARRIERS:** Low-energy density, low-power density, and short calendar and cycle lives

**OBJECTIVES:** The objectives are to synthesize and characterize silicon clathrate anodes designed to exhibit small volume expansion during lithiation, high specific energy density, while avoiding capacity fading and improving battery life and abuse tolerance.

**GENERAL APPROACH:** Our approach is to synthesize guest-free Type I silicon clathrate (Si<sub>46</sub>, space group  $Pm\bar{3}n$ ) using high-pressure and high-temperature experimental methods, including a newly-developed arc-melt technique. Concurrently, an investigational route for direct synthesis of guest-free clathrate is being explored, and *ab initio* and classical molecular dynamics (MD) computations will be performed to identify lithiation pathways. The silicon clathrates will be utilized to fabricate prototype silicon clathrate anodes. Electrochemical characterization will be performed to evaluate and improve, if necessary, anode performance including cyclic stability. The final year of the program will be directed at the design, assembly, and characterization of a complete (anode/cathode) small-scale, prototype battery suitable for concept demonstration.

**STATUS OCT. 1, 2012:** Possible reaction pathways for the formation of Si<sub>46</sub>, Li<sub>x</sub>Si<sub>46</sub>, Li<sub>15</sub>Si<sub>4</sub>, and Li<sub>x</sub>M<sub>y</sub>Si<sub>46-y</sub>l have been identified using first-principles methods. Several hundred grams of Type I silicon clathrates and metal-silicon clathrate alloys have been fabricated by two different processing methods (arc-melting and direct solution-synthesis) and have been characterized for purity. Several half-cells of Si anodes have been constructed and characterized for electrochemical properties.

**STATUS SEP. 30, 2013:** Several half-cells of silicon clathrate anodes will have been fabricated using Year 2 materials, in combination with best-case additives and electrolyte formulations. The electrochemical properties of prototype anodes will have been characterized using a half-cell test apparatus. A suite of techniques will have been utilized to obtain a comprehensive understanding of the electrochemical behavior of such anodes under cyclic Li<sup>+</sup> intercalation/de-intercalation conditions. An extensive post-mortem evaluation will be carried out to assess the structural and mechanical state of anode materials, and the experimental results will be compared against corresponding first-principles computations.

**RELEVANT USABC GOALS:** 200 Wh/kg (EV requirement); 96 Wh/kg, 316 W/kg, 3000 cycles (PHEV 40 mile requirement). Calendar life: 15 years. Improved abuse tolerance.

**MILESTONES:**

- (a) Construct and evaluate several electrochemical half cells using anode materials synthesized in Year 2, combined with best-case additives and electrolyte formulations. (Jan. 13) **Complete**
- (b) Characterize electrochemical properties of silicon clathrate anodes made from Year 2 materials. (Sep. 13) **Delayed until Dec. 13.**
- (c) Identify structural and mechanical states of silicon clathrate anodes during lithiation and delithiation processes and validate against theoretical calculations. (Jul. 13) **Complete**
- (d) Achieve a reversible capacity of 400 mAh/g after 50 cycles at C/15 for either Si<sub>46</sub> or A<sub>8</sub>M<sub>y</sub>Si<sub>46-y</sub> (A = Ba, Na; M = Al, Cu). (Sep. 13) **Delayed until Dec. 13.**

## PROGRESS TOWARD MILESTONES

### Task 1 – Synthesis of Type I Silicon Clathrates

During the previous quarter, the conditions for the phase transformation of fuel-grade sodium silicide were optimized to yield the highest purity of the Zintl phase possible, which was verified by XRD analysis. After successful scale-up of  $\text{Na}_4\text{Si}_4$  (ca. 10 g), this Zintl compound was employed during the present quarter in combination with a previously-synthesized alkylammonium- $\text{AlCl}_3$  ionic liquid (IL) in an attempt to synthesize empty silicon clathrate ( $\text{Si}_{46}$ ) in batch quantity via a Hofmann-type elimination-oxidation reaction scheme performed in solution. The XRD analysis (Fig. 1) of the reaction product indicates that the desired Type I clathrate was formed along with unreacted Zintl compound and the reaction by-products. The product will be further purified for subsequent electrochemical measurements as an anode material.

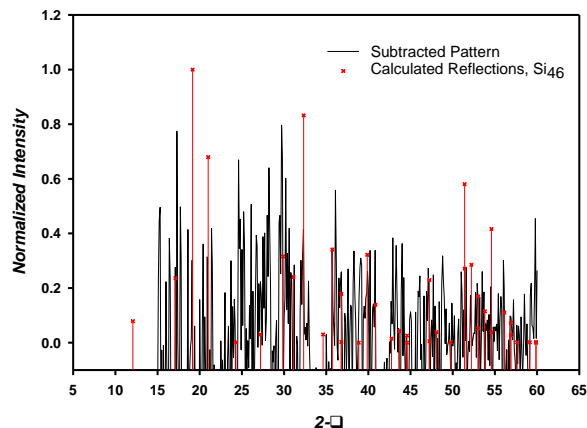


**Figure 1.** Overlay of powder XRD patterns for the synthesis product and the calculated reflections of empty clathrate ( $\text{Si}_{46}$ ), after subtraction of impurity phases.

### Task 3 – Prototypic Silicon Clathrate Anode Fabrication

Half-cell charge/discharge cycle tests on the intermetallic clathrate,  $\text{Ba}_8\text{Al}_8\text{Si}_{38}$ , combined with Super-P carbon (20 wt.%) and EC/DEC/FEC electrolyte are ongoing. The effect of higher than previous carbon loadings on overall capacity fade and coulombic efficiency will be determined from these measurements.

### Task 4 – Half-Cell Electrochemical Characterization

Long-term tests on an anode composed of the  $\text{Ba}_8\text{Al}_8\text{Si}_{38}$  intermetallic clathrate and 10 wt.% carbon loading (Super-P) were completed this quarter. The specific capacity and coulombic efficiency were recorded out to 200 cycles at  $C/2$ , allowing the half-cell to rest at OCP for ca. 8 hrs at the end of the 50<sup>th</sup> and 100<sup>th</sup> cycle (Fig. 2). These results show an initial capacity of 300 mAh/g (active material basis) on the 4<sup>th</sup> cycle, which decays to 54 mAh/g at near steady-state conditions upon reaching the 200<sup>th</sup> cycle. The average steady-state coulombic efficiency was  $98.79 \pm 0.14\%$ . Peak capacities much greater than the theoretical value (259 mAh/g for invariant lattice constant), along with marked improvements in the capacity fade, are expected from the use of greater than present carbon loadings (from Task 3).

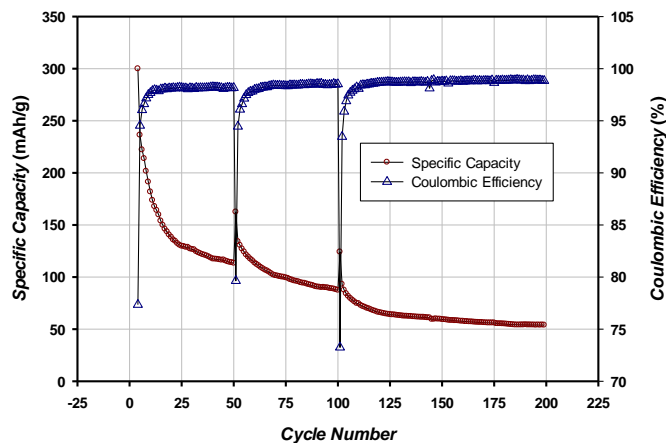


**Figure 2.** Long-term cyclic capacity and coulombic efficiency profiles measured for  $\text{Ba}_8\text{Al}_8\text{Si}_{38}$  anode (10 wt.% Super P + 10 wt.% PVDF) using ED/DEC/FEC (45:45:10). Cell was allowed to rest at OCP for ~8 hrs at end of 50<sup>th</sup> and 100<sup>th</sup> cycles before resuming test.

## BATT TASK 3

### ELECTROLYTES

**TASK 3.1 - PI, INSTITUTION:** John Kerr, Lawrence Berkeley National Laboratory

**TASK TITLE - PROJECT:** Electrolytes – Interfacial and Bulk Properties and Stability

**BASELINE SYSTEMS:** Conoco Philips CPG-8 Graphite/1 M LiPF<sub>6</sub>+EC:DEC (1:2)/Toda High-energy layered (NMC)

**BARRIERS:** Poor cycle and calendar life, low power and energy densities, particularly at low temperatures (-30°C).

#### OBJECTIVES:

1. Determine the role of electrolyte structure upon bulk transport and intrinsic electrochemical kinetics and how it contributes to cell impedance (Energy/ power density).
2. Determine chemical and electrochemical stability of electrolyte materials to allow elucidation of the structure of and the design of passivating layers (*e.g.*, SEI).

**GENERAL APPROACH:** A physical organic chemistry approach is taken to electrolyte design, where the molecular structure is varied to provide insight into the processes that may affect the performance of the battery. This involves model compounds as well as synthesis of new materials to test hypotheses which may explain battery behavior.

**STATUS, OCT. 1, 2012:** Carbon nanotubes and other carbonaceous conducting elements have been further modified with a broader range of chemical groups (PEGs, imide and malonato-difluoroborate anions) and the effects on composite electrode performance determined. Combination of these modifications with variations of binder polymers were studied to determine how electrode ink formulation affects the electrode morphology and electrode performance, particularly for thick, high energy electrodes.

**STATUS, SEP. 30, 2013:** The demonstration of the advantages and drawbacks of single-ion conductor materials will be complete. The exploration of surface functionalization of conducting additives and the effect of interfacial impedance will be complete. Measurement of the composite electrode thickness increases made possible by use of single-ion conductor electrolytes will provide data to estimate the potential energy and power density increases. Initial estimates of calendar and cycle life will be complete. A completely solid state battery will be constructed with no solvent.

**RELEVANT USABC GOALS:** *Available energy:* 56 Wh/kg (10 mile) and 96 Wh/kg (40 mile); *10 s discharge power:* 750 W/kg (10 mile) and 316 W/kg (40 mile); *Cycle life:* 5000 cycles (10 mile) and 3000 cycles (40 mile); *Calendar life:* 15 years (at 40°C); cold cranking capability to -30°C; abuse tolerance.

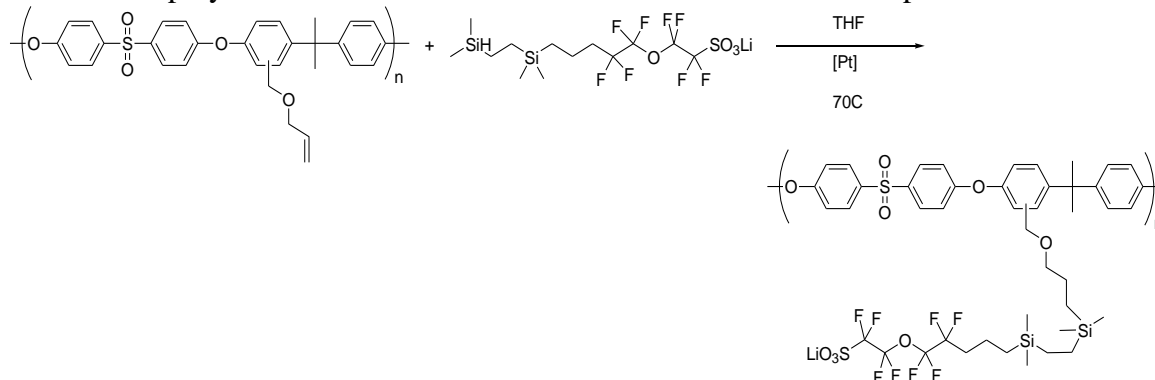
#### MILESTONES:

- (a) Complete construction and test of three different thicknesses of composite cathode electrode cells using gel electrolyte. (Sep. 13) **Delayed until Dec. 13**
- (b) Construct and test single-ion conductor solid-state cells with no free solvents and composite anodes and cathodes. (Sep. 13) **Delayed until Dec. 13**

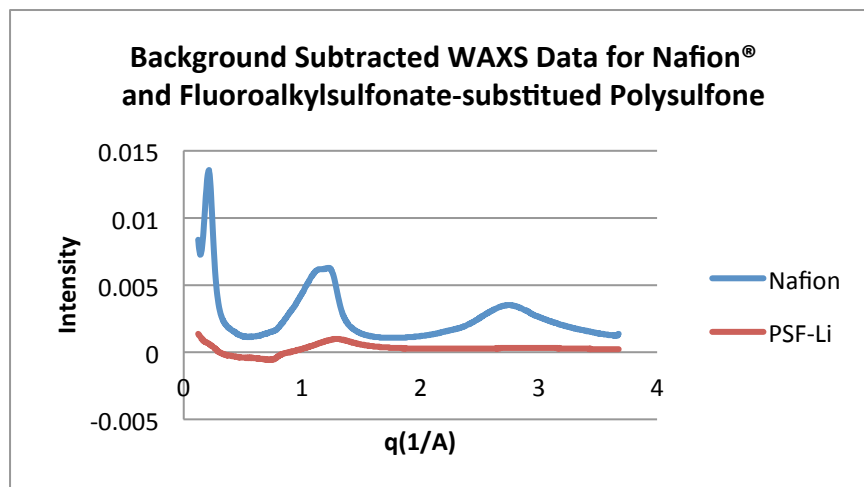
## PROGRESS TOWARD MILESTONES

Both milestones have been delayed due to unexpected difficulties in the synthesis of larger batches of material that are essential if a proper study of the performance of single-ion conducting materials is to be achieved.

Synthesis of the polysulfone and polyether materials continued in order to prepare sufficient material for the grafting of the anion species in the preparation of single-ion conductors. Scale-up of the polysulfone-base material was successfully achieved. The attachment of the anion to the polysulfone was successful for the fluorinated sulfonate species.



It was found that this reaction was easily terminated by the presence of water and other proton donors and had to be carried out under scrupulously dry conditions either in a glove box or under Schlenk line conditions. Nevertheless, the Li salt of the fluorosulfonate was examined by SAXS and WAXS measurements at the LBNL Advanced Light Source. The SAXS measurements showed very little scattering was expected from a polymer with such a small content of fluorine. However, the WAXS data (see below) did show some order which may be due to crystallinity or ordering in the amorphous phase. However, the DSC showed no sign of crystallinity.



Attempts to observe how the polymer behaved in the presence of carbonate solvents (EC/EMC) were thwarted due to the high solubility of the polymer in these solvents. It is necessary to cross-link the polymer in a membrane form before the solvent is added. This adds to the challenge of preparing uniform, composite electrodes, which will be reported in the next quarterly report.

**TASK 3.2 - PI, INSTITUTION:** Khalil Amine and Larry Curtiss, Argonne National Laboratory

**TASK TITLE - PROJECT:** Electrolytes — Advanced Electrolyte and Electrolyte Additives

**BASELINE SYSTEMS:** Conoco Philips CPG-8 Graphite/1 M LiPF<sub>6</sub>+EC:DEC (1:2)/Toda High-energy layered (NMC)

**BARRIERS:** Cycle/calendar life, abuse tolerance

**OBJECTIVES:** Develop advanced quantum chemical models to predict functional additives that form stable SEI on carbon anodes and cathodes and redox shuttles for overcharge protection. Synthesize suitable additives predicted by model, characterize, and perform extensive cycle and calendar life tests.

**GENERAL APPROACH:** Search for new electrolytic additives that react in a preferential manner to prevent detrimental decomposition of other cell components using experiment and theory. Use quantum chemical screening to predict oxidation and reduction potentials and decomposition pathways that form desirable coatings and prevent overcharge. Investigate SEI formation using a combination of computational and experimental techniques.

**STATUS OCT. 1, 2012:** Exploration of full decomposition pathways for selected additive candidates were carried out using advanced quantum chemical techniques. Experimental testing and characterization of the additives have been performed. Quantum chemical studies of the reaction energies for decomposition of shuttle candidates and experimental testing were carried out.

**STATUS SEP. 30, 2013:** Screening of redox shuttles based on tri- and quarter-phenyls with various functional groups using advanced quantum chemical calculations of redox potentials, exploration of full decomposition pathways, and surface interactions. Experimental testing and characterization of the selected shuttles will be performed. Computational and experimental investigations of the SEI structure and properties from oxalate based additives.

**RELEVANT USABC GOALS:** 10-s discharge power: 750 W/kg (10 mile) and 316 W/kg (40 mile.)

**MILESTONES:**

- (a) Screening of redox potentials and oxidative stabilities of derivatived ter- and quaterphenyls R-C<sub>6</sub>H<sub>4</sub>(C<sub>6</sub>H<sub>4</sub>)<sub>m</sub>C<sub>6</sub>H<sub>4</sub>-R (m=1,2), each with twelve different functional groups R, for use as redox shuttles for overcharge protection using advanced computational techniques. (Jan. 13) **Complete**
- (b) Synthesis of at least one ter- and quarterphenyl based shuttle from theoretical predictions. (Apr. 13) **Complete**
- (c) Characterization of synthesized redox shuttles from experiment and computational studies of spectroscopic properties. (Jun. 13) **Complete**
- (d) Demonstration of overcharge protection and cell balancing properties of selected redox candidates. (Sep. 13) **Complete**
- (e) Completion of modeling and characterization of polymeric SEI formed from an oxalate based additive on an anode surface. (Sep. 13) **Complete**

## PROGRESS TOWARD MILESTONES

The approach for the development of additives for SEI and redox shuttles for overcharge protection involves the screening of reduction and oxidation potentials through the use of accurate density functional theory (DFT) methods followed by investigation of the mechanism of decomposition through the investigation of the reaction pathways. The theoretical results are related to the performance of the additives and shuttles in a battery cell.

DFT methods were used to examine the oxidation potential and other properties of a potential redox shuttle 1-(2,2,2-trifluoroethoxy)-4-methoxy-2,5-di-*tert*-butylbenzene (F3-DDB) shown in Fig. 1. This molecule has less symmetry compared to previously studied shuttles, DDB (1,4-di-*t*-butyl-2,5-dimethoxybenzene) and F6-DDB (bis-(2,2,2-trifluoroethoxy)-2,5-di-*tert*-butylbenzene), also shown in Fig. 1. The calculated oxidation potential of F3-DDB is 4.02 V is in good agreement with the experimental value of 4.09 V from the work described below. This is smaller than that of F6-DDB (4.23 V, expt. 4.25 V), but larger than that of DDB (3.82 V, expt. 3.92 V). Calculated spin densities suggest that the less symmetric F3-DDB is slightly more prone to radical attack than the symmetric DDB and F6-DDB. Calculated ethyl radical binding energies  $E_b(ER)$  show that while F3-DDB has a slightly higher  $E_b(ER)$ , all three redox shuttles should be stable from this probe radical. Decomposition pathways were also examined. F3-DDB has three exergonic side arm reactions, F6-DDB has two, and the parent DDB has one. All proposed decomposition reactions have large activation barriers so they are unlikely to decompose. However, decomposition could be catalyzed by transition metal sites on the electrode surface.

The F3-DDB compound was synthesized for testing as a redox shuttle. This was done using commercially available precursors. The introduction of  $-OCH_2CF_3$  groups increases the oxidation potential compared to DDB. The compound was characterized using NMR. The F3-DDB compound displays a reversible redox potential at 4.09 V vs.  $Li/Li^+$  in carbonate-based electrolytes. F3-DDB also showed improved solubility in the carbonate-based electrolytes due to the introduction of the fluorinated alkoxy group. Up to 0.2 M solution of F3-DDB in 1.2 M  $LiPF_6$  in 3:7 EC/EMC was prepared. The overcharge effect was investigated in a  $LiFePO_4/Li_4Ti_5O_{12}$  cell containing 0.1 M F3-DDB. In this cell configuration, the F3-DDB shuttle can survive for | 73 cycles (>1000 h) at C/5 with 100% overcharge.

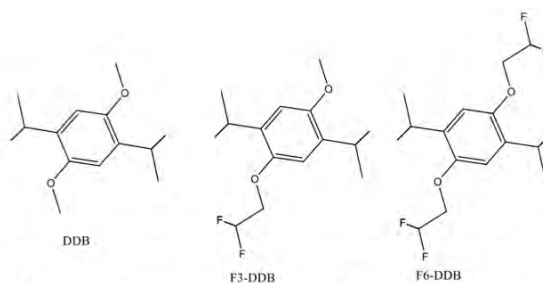


**Figure 1.** DDB and modified DDB redox shuttles.

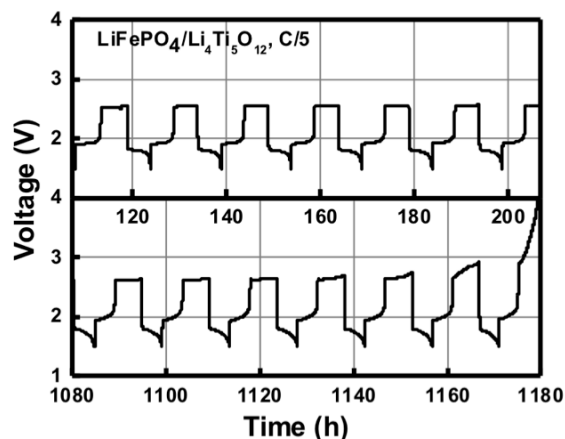


**Figure 2.** Voltage vs. time profile of  $LiFePO_4/Li_4Ti_5O_{12}$  cell containing 0.1 M F3-DDB during the overcharge test (C/5 charging rate, 100% overcharge).

**TASK 3.3 - PI, INSTITUTION:** Brett Lucht, University of Rhode Island

**TASK TITLE - PROJECT:** Electrolytes — Development of Electrolytes for Lithium-ion Batteries

**BASELINE SYSTEMS:** Conoco Philips CPG-8 Graphite/1 M LiPF<sub>6</sub>+EC:DEC (1:2)/Toda High-energy layered (NMC)

**BARRIERS:** Cell performance, life, cost: Calendar life: 40°C, 15 yrs; Survival Temp Range: -46 to +66°C; Unassisted Operating & Charging Temperature Range, -30 to + 52°C.

**OBJECTIVES:** Develop novel electrolytes with superior performance to SOA (LiPF<sub>6</sub> in carbonates). Develop an understanding of the source of performance fade in graphite/LiNi<sub>0.5</sub>Mn<sub>1.5</sub>O<sub>4</sub> cells cycled to high voltage (4.8 V vs Li). Develop an electrolyte formulation that allows for superior performance of graphite/LiNi<sub>0.5</sub>Mn<sub>1.5</sub>O<sub>4</sub> cells. Synthesize and characterize novel non-fluorinated Li salts for Li battery electrolytes.

**GENERAL APPROACH:** Investigate the surface of cathodes and anodes cycled with novel electrolytes, with or without additives, to develop a mechanistic understanding of interface formation and degradation. Develop additives for high voltage (~4.8 V) cathode materials which inhibit performance fade *via* reduction of Mn dissolution or cathode surface passivation. Use novel synthetic methods to prepare non-fluorinated lithium salts for lithium ion battery electrolytes.

**STATUS OCT. 1, 2012:** LiPF<sub>4</sub>(C<sub>2</sub>O<sub>4</sub>) electrolytes with optimized performance at low temperature after accelerated aging have been investigated. A better understanding of the role of electrolytes in the poor cycling efficiency and capacity fade of Li/LiNi<sub>0.5</sub>Mn<sub>1.5</sub>O<sub>4</sub> cells has been developed. Novel electrolyte formulations which optimize the performance of Li/LiNi<sub>0.5</sub>Mn<sub>1.5</sub>O<sub>4</sub> cells cycled to high voltage (4.8 V vs. Li) have been designed.

**STATUS SEP. 30, 2013:** A better understanding of the role of electrolyte in performance fade of graphite/LiNi<sub>0.5</sub>Mn<sub>1.5</sub>O<sub>4</sub> cells will have been developed. This understanding will be used to develop novel electrolyte formulations which improve the performance of graphite/LiNi<sub>0.5</sub>Mn<sub>1.5</sub>O<sub>4</sub> cells. One or more novel non-fluorinated salts will have been synthesized and the performance of the novel salt in electrolyte formulations in graphite/LiNi<sub>x</sub>Co<sub>1-2x</sub>Mn<sub>x</sub>O<sub>2</sub> cells will be investigated.

**RELEVANT USABC GOALS:** Calendar life: 40°C, 15 yrs; Survival Temp Range: -46–52°C; Cold cranking power at -30°C; Cycle life; Peak Pulse Discharge Power, 10 sec.

**MILESTONES:**

- (a) Develop an understanding of the role of electrolyte in capacity fade for graphite/LiNi<sub>0.5</sub>Mn<sub>1.5</sub>O<sub>4</sub> full cells cycled at moderately elevated temperature (55°). (Mar. 13) **Complete**
- (b) Design electrolyte formulations to decrease cell inefficiency (50% of SOA) and decrease capacity fade (50% of SOA) for graphite/LiNi<sub>0.5</sub>Mn<sub>1.5</sub>O<sub>4</sub> full cells. (Jul. 13) **Complete**
- (c) Synthesize and characterize novel non-fluorinated lithium salts and test novel electrolytes in graphite/LiNi<sub>x</sub>Co<sub>1-2x</sub>Mn<sub>x</sub>O<sub>2</sub> cells. (Sep. 13) **Incomplete due to change in project direction**

## PROGRESS TOWARD MILESTONES

The expected status for September 30, 2013 was achieved on completion of the first two milestones. The expected status for milestone three was not met; this is due to a change in research direction, as described below.

With regards to milestone (a): *Completed*. Please see the first two quarterly reports for details.

With regards to milestone (b): *Completed*. Please see the third quarterly report for details.

With regard to milestone (c): Synthetic methods to prepare novel salts were attempted. Two different novel salts were targeted, however, significant difficulties were experienced during the development of the synthetic methods. At the same time, a Silicon Focus Group was initiated within the BATT program. Thus, the focus of the final milestone was shifted from the development of novel non-fluorinated salts for Li-ion battery electrolytes, to the development of an understanding of the role of common additives, vinylene carbonate (VC), and fluoroethylene carbonate (FEC), on the capacity retention of Si nano-particle electrodes. Li/Si nano-particle cells were prepared with seven different electrolyte formulations. The baseline electrolyte was 1.2 M LiPF<sub>6</sub> in EC/DEC (1:1). The other electrolyte formulations included 3 and 6% VC and 5, 10, 15, and 25% FEC (wt%). The cycling performance of the different electrolytes is provided in Fig. 1. The best capacity retention was observed for cells containing 10 and 15% of FEC. Interestingly, the electrolytes with a lower concentration (5%) and a higher concentration (25%) of FEC showed inferior capacity retention. In addition, the cells with 3 and 6% VC had comparable cycling performance to the baseline electrolyte. *Ex situ* analysis of the Si nano-particle electrodes with XPS, SEM, and FT-IR is currently being conducted and will be presented in FY 14 reports.

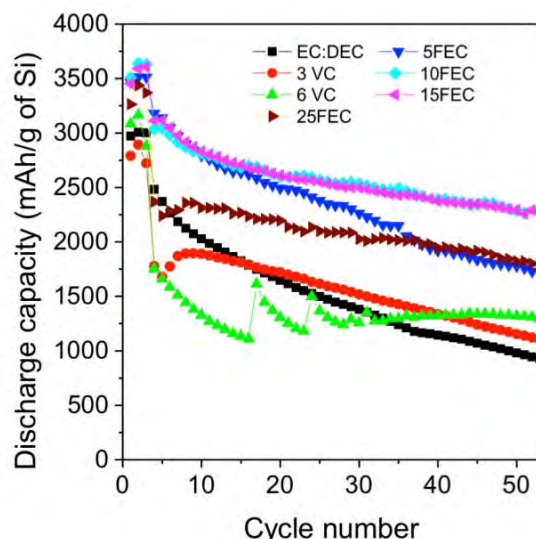


**Figure 1.** Capacity retention of Li/Si nano-particle cells cycled with different electrolytes

**Collaborations:** D. Abraham (ANL), M. Smart (NASA-JPL), V. Battaglia, G. Chen, and J. Kerr (LBNL), A. Garsuch, M. Payne (BASF), and the Silicon Focus Group.

### Publication and Presentation:

“Improving the Performance of Graphite/LiNi<sub>0.5</sub>Mn<sub>1.5</sub>O<sub>4</sub> Cells at High Voltage and Elevated Temperature with added Lithium bis(oxalato) borate (LiBOB),” M. Xu, L. Zhou, Y. Dong, Y. Chen, A. Garsuch, B.L. Lucht *J. Electrochem. Soc.* **2013**, *160*, A2005-A2013.

“Improved performance of graphite/LiNi<sub>0.5</sub>Mn<sub>1.5</sub>O<sub>4</sub> cells with electrolyte additives,” *6th International Conference on Advanced Lithium Batteries for Automotive Applications*, Argonne, IL, September 2013.

**TASK 3.4 - PI, INSTITUTION:** Daniel Scherson and John Protasiewicz, Case Western Reserve University

**TASK TITLE - PROJECT:** Electrolytes — Bifunctional Electrolytes for Lithium-ion Batteries

**BASELINE SYSTEMS:** Conoco Philips CPG-8 Graphite/1 M LiPF<sub>6</sub>+EC:DEC (1:2)/Toda High-energy layered (NMC)

**BARRIERS:** Abuse tolerance

**OBJECTIVES:** Design, synthesize, and characterize physical, electrochemical, and interfacial characteristics of functionalized Li-salt anions containing phosphorus moieties known to impart materials with flame retardant properties (Flame Retardant Ions or FRIONs) and additional functional redox active groups capable of providing overcharge protection. Develop and implement ATR-FTIR spectroscopic methods for monitoring *in situ* products generated at Li-ion battery anodes.

**GENERAL APPROACH:** Develop methods for the chemical functionalization of anions known to improve the performance of Li-ion batteries with covalently linked groups displaying flame retardant and/or overcharge protection attributes. Establish guidelines for the rational design and synthesis of optimized FRIONs and FROPs based on the analysis of results of testing in actual Li-ion batteries. Develop new *in situ* tactics for the application of attenuated total reflection Fourier transform infrared ATR-FTIR for the characterization of solution products generated at Li-ion battery anodes and solid electrolyte interfaces formed therein.

**STATUS OCT. 1, 2012:** Complete synthesis and purification of four cyclic triol borate (CTB) salts and determination of their flammability. Development of methods for the preparation of 100g of CTB-type compound for testing in actual batteries finished. Develop methods for depositing a thin layer of metal onto the diamond window for ATR measurements and thus avoid problems with electrolyte contributions due to migration effects of IRAS.

**STATUS SEP. 30, 2013:** Complete synthesis and characterization of new FRION materials based on diphosphonato-catecholate ligand (DPC) including flammability and electrochemical testing. Scale up synthesis of Li[B(DPC)<sub>2</sub>] and Li[B(DPC)(oxalato)] salts for testing in cells. Establish structure-electrochemical performance relationships and comparisons with previously studied anion families. Systematic *in situ* ATR-FTIR spectroscopic and impedance studies involving selected solvent formulations incorporating Case FRIONs both as main salts and additives.

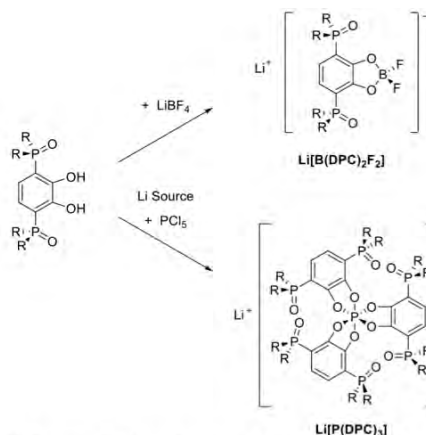
**RELEVANT USABC GOALS:** No fire or rapid disassembly of cells during abuse conditions.

**MILESTONES:**

- (a) Prepare and fully characterize the electrochemical and flammability properties characteristics of Li[B(DPC)<sub>2</sub>] and Li[B(DPC)(oxalato)] salts. (Oct. 12) **Complete**
- (b) Expand the Li[B(DPC)<sub>2</sub>] and Li[B(DPC)(oxalato)] salts-type libraries of compounds (Mar. 13) **Complete; expanded library salts have shown promise in electrolyte solutions, synthetic goals will focus on continuing to expand this library.**
- (c) Synthesize and characterize a Li[P(DPC)<sub>3</sub>] FRION. (Sep. 13) **Complete**
- (d) Complete characterization of the effect of Case additives by cyclic voltammetry and impedance measurements with the most promising materials as determined from milestone (e) below. (Sep 13) **Delayed, due Dec. 13**
- (e) Perform full testing of all Case salts as full fledged electrolytes and/or as additives in actual batteries at Novolyte (Oct 12), and LBNL and ANL. (Sep 13) **Complete**
- (f) Improve cycling by at least 15% to reach the same decay/end of life *vs.* the control electrolyte.(Sep 13) **Complete. Cycling performed by LBNL.**
- (g) Construct and optimize cell for *in situ* ATR measurement with metal-coated diamond window. (Sep. 13) **Delayed, due Dec. 13**

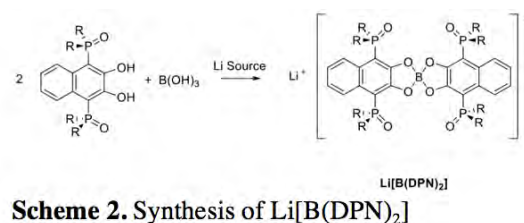
## PROGRESS TOWARD MILESTONES

**Synthesis and characterization of FRIONS** – Work in this quarter focused on expanding the FRION library. Specifically, (a) gram scale quantities of pure  $\text{Li}[\text{P}(\text{DPC})_3]$  were synthesized (Scheme 1, bottom. 97.8% yield) and characterized by TGA and microcombustion calorimetry. This material displayed thermal properties similar to the previously reported FRIONS  $\text{Li}[\text{B}(\text{DPC})_2]$  and  $\text{Li}[\text{B}(\text{DPC})(\text{oxalato})]$ . (b) A pure, new, naphthalene analogue of DPC (DPN) was synthesized and utilized to prepare a novel lithium DPN borate salt  $\text{Li}[\text{B}(\text{DPN})_2]$  (see Scheme 2. 78.2% yield).  $\text{Li}[\text{B}(\text{DPN})_2]$ . (c) The lithium DPC difluoroborate salt  $\text{Li}[\text{B}(\text{DPC})\text{F}_2]$  was prepared (Scheme 1, top. 54.4% yield) and characterized by  $^1\text{H}$ ,  $^{31}\text{P}$ ,  $^{13}\text{C}$ , and  $^{19}\text{F}$  NMR spectroscopy.



**Scheme 1.** Synthesis of  $\text{Li}[\text{B}(\text{DPC})_2\text{F}_2]$  and  $\text{Li}[\text{P}(\text{DPC})_3]$

Some aspects of the electrochemistry of the newly synthesized compounds were examined by CV in de-aerated EC/EMC (50/50 by volume) recorded at 10 mV/s using a Ni wire as the working electrode and a piece of metallic Li as the counter-reference electrode. In all cases the materials were dissolved to saturation. The voltammetric curves shown in Fig. 1 illustrate some of the changes induced by the structure of the material. In particular, the B-containing material (left) displays features reminiscent of those obtained in the standard 1M  $\text{LiPF}_6$  in the same solvent mixture. In stark contrast, the response of the phosphorous analogue yielded a resistive type behavior (right) over a wide potential range which is indicative of the formation of a film on the Ni electrode.



**Scheme 2.** Synthesis of  $\text{Li}[\text{B}(\text{DPN})_2]$

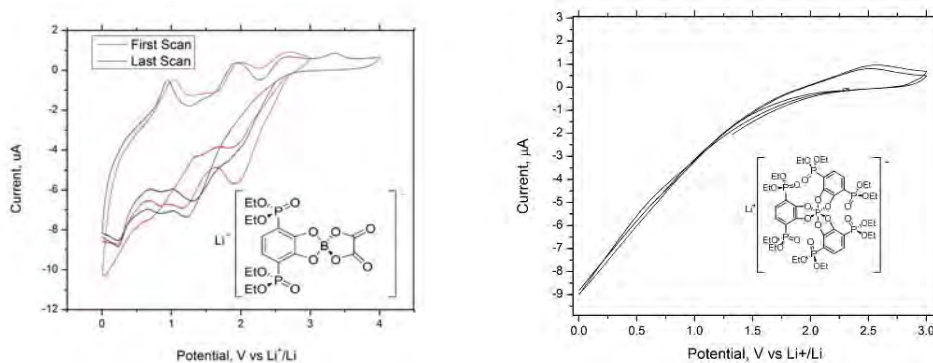


**Figure 1.** Cyclic voltammetric curves of a Ni wire electrode in EC/EMC (50/50 by volume) solutions containing the materials showed in the insets recorded at a rate of 10 mV/s. Other experimental details are given in the text.

**TASK 3.5 - PI, INSTITUTION:** Austen Angell, Arizona State University

**TASK TITLE - PROJECT:** Electrolytes – Sulfone Liquids and Sulfate/Triflate Solids for High Voltage Electrolytes

**SYSTEMS:** Conoco Philips CPG-8 Graphite/1 M LiPF<sub>6</sub>+EC:DEC (1:2)/Toda High-energy layered (NMC)

**BARRIERS:** Electrolyte needs increased oxidation resistance with decreased ionic resistance, and improved safety. Safety will follow increased ionic liquid or superionic solid content.

**OBJECTIVES:** To devise new electrolyte types (sulfone mixtures and superionic glasses or plastic solid derivatives) that will permit cell operation at high voltages without solvent oxidation and with adequate overcharge protection, and to provide optimized nanoporous supporting membranes for this electrolyte.

**GENERAL APPROACH:** The approach has been twofold: (i) A suite of electrolyte studies, beginning with cell-performance testing of additive protected sulfone electrolytes, extending to the design of novel Li<sup>+</sup>-conducting media is planned. The latter will retain the high oxidation resistance known for noncyclic sulfones, and conductivity of EC-DMC solutions, but will have Li<sup>+</sup> transport number unity. Novel Li<sup>+</sup>-conducting silicon based solid-state conductors and rubbery polymers will be tested for compatibility with the chosen Li (Ni,Mn) spinel cathode. Finally, some novel ionic liquid electrolytes will be tested; and (ii) the further development of the “Maxwell slats” approach to synthesis of nanoporous supports. A hot water-soluble reversibly-self-assembling net has now been abandoned in favor of a successful stronger-bonded model that successfully self-assembles in hot ionic liquid and hydrogen bonding solvents.

**STATUS OCT. 1, 2012:** Half-cell and full-cell tests with the Li(NiMn) high voltage cathode using our newly developed graphite-compatible all-sulfone, and part sulfone electrolyte solvents, now completed, will begin examination. Progress towards understanding the nature of new Li conducting complex anion solid and liquid-state conductors will have been made. A range of different rigid and non-rigid struts for nano-porous nets (now called amorphous MOFs) will have been explored. Non-calorimetric strategies for determining softening temperatures will have been decided (by collaboration if preferable.)

**STATUS SEP. 30, 2013.** A go-no-go point will have been passed on sulfone-solvent-based high voltage cell development. An alternative solvent system of even higher voltage window and comparable conductivity, based on “ionic liquid” solvents, will have been tested for performance with the Li(Ni,Mn)O<sub>4</sub> cathode, and variants of the superionic glass and metastable crystal variety will have been examined. The best cases of the latter will have been tested with the Li(Ni,Mn)O<sub>4</sub> cathode and the expected absence of side reactions verified. The nanoporosity of aqueous self-assembling models of the Maxwell slat concept will have been assessed, and study of more practical (stronger-bonding) variants will have been commenced.

**RELEVANT USABC GOALS:** 1000 cycles (80% DoD); 10 year life. An electrolyte with electrochemical window 5.2 volts and conductivity 20 mS/cm.

**MILESTONES:**

- (a) Decide go-no-go on cathode half cells with sulfone electrolytes with HFiP additive. (Feb. 13)  
**On-going, due Dec. 13**
- (b) Produce new plastic Li-conducting phases of  $\sigma(25^{\circ}\text{C}) > 10$  mS/cm. (Jun. 13) **On-going, due Dec. 13**
- (c) Achievement of glassy or viscous liquid single-ion Li-conducting versions of (b). (Jun. 13)  
**On-going, due Dec. 13**
- (d) Production of new mixed 3 and 4-bonding covalent nanoporous nets (amorphous MOFs.) (Jun. 13) **Complete**
- (e) Go-no-go development of mechanically robust nanoporous covalent networks for novel solution and plastic alkali-ion conductors. (Aug. 13) **Delayed to Dec. 13**

## PROGRESS TOWARD MILESTONES

(a) **Go/no-go on cathode half-cells with sulfone electrolytes with HFIP additive, postponed to May 2013.** Last report showed half-cell CV and current efficiency data for the LMNO cathode using ethylmethylsulfone EMS with co-solvent DMC, which were pleasing. This half-cell has now been tested with HFIP and LiBOB additives out to 80 cycles and only marginal improvement was found (Fig. 1). JECS paper is submitted.

(b) **Production of new plastic Li-conducting phases of  $\sigma(25^\circ\text{C}) > 10 \text{ mS/cm}$ , delayed to Mar. 2014.** This milestone has not been met. At the beginning of the year it was found that artifacts could not be excluded (due to inaccuracies in assessment of residual acid contents in the plastic phases) as the source of the impressive conductivities earlier reported. In order to ensure completion of the reactions in question, it has been necessary to totally overhaul the preparative procedures, creating closed system syntheses. This has been achieved with  $-30^\circ\text{C}$  cold finger condensers and internal product traps, using the apparatus in Fig. 2.

The products, which are the intermediates to the formation of lithiated materials described earlier, are solid acids with a white waxy appearance, from which all reactant acid has been eliminated. The solid acids have high proton mobilities that permit  $^1\text{H}$  NMR resonances to be



Figure 2. Apparatus

determined without resource to solid state NMR. A spectrum (for preparation H4) is shown in Fig. 3, where it is compared to that for pure  $\text{H}_2\text{SO}_4$ : ( $\text{HTf}$ ,  $\text{H}_3\text{PO}_4$  lie at 10.5, 9.6).

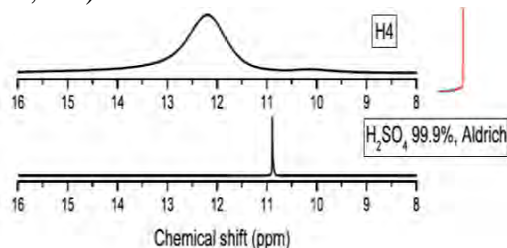


Figure 3.  $^1\text{H}$  NMR spectra for solid acid

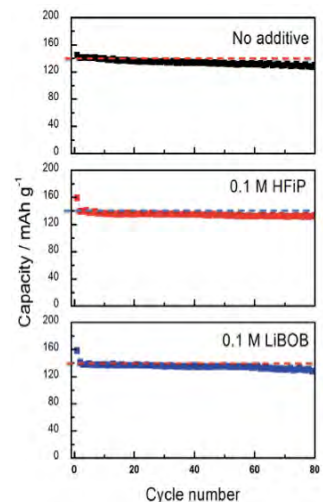


Figure 1. Cycling and with and w/o additives.

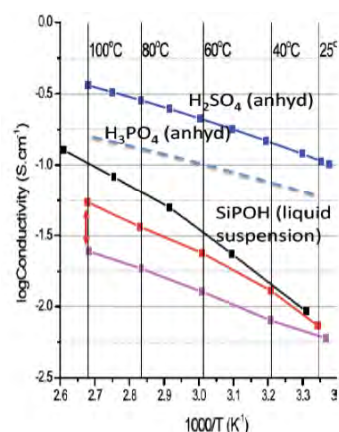


Figure 4. Conductivities

(c) **Achievement of glassy or viscous liquid single-ion Li-conducting versions of (b). (Jun. 13) delayed to Mar 2014.** The conductivities of some alternative preparations are seen in the lower two curves of Fig. 4. Comparison is made with three liquids: the recent fuel cell electrolyte SiPOH, and (upper curves) pure  $\text{H}_3\text{PO}_4$  and  $\text{H}_2\text{SO}_4$ . The solid acids have conductivities approaching  $10 \text{ mS/cm}$  at ambient temperature and are likely important in themselves. Conversions to lithiated states will be revisited in the final stages of our project. *Revised milestone Dec.2013.*

(d) **Production of new mixed 3 and 4-bonding covalent nanoporous nets (amorphous MOFs) by June 2013.** These have been achieved, but so far fail on robustness (see next).

(e) **Go/no-go development of mechanically robust nanoporous covalent networks for novel solution and plastic alkali-ion conductors, by August 2013.** So far the team is unable to solve the mechanical problem, which is like that found earlier (and largely solved) for sol-gel glasses.

## BATT TASK 4

### CATHODES

**Task 4.1 - PI, INSTITUTION:** Michael Thackeray, Argonne National Laboratory

**TASK TITLE:** Cathodes – Novel Cathode Materials and Processing Methods

**SYSTEMS:** Conoco Philips CPG-8 Graphite/1M LiPF<sub>6</sub>+EC:DEC(1:2)/Toda NMC  
Conoco Philips CPG-8 Graphite/High voltage electrolyte/Li-Ni-Mn-O spinel

**BARRIERS:** Low energy, cost and abuse tolerance limitations of Li-ion batteries

**OBJECTIVE:** To develop low cost, high-energy and high-power Mn-oxide-based cathodes.

**APPROACH:** Li<sub>2</sub>MnO<sub>3</sub>-stabilized composite electrode structures, such as ‘layered-layered’ xLi<sub>2</sub>MnO<sub>3</sub>•(1-x)LiMO<sub>2</sub> (M=Mn, Ni, Co), ‘layered-spinel’ xLi<sub>2</sub>MnO<sub>3</sub>•(1-x)LiM<sub>2</sub>O<sub>4</sub> and more complex ‘layered-layered-spinel’ y{xLi<sub>2</sub>MnO<sub>3</sub>•(1-x)LiMO<sub>2</sub>}•(1-y)LiM<sub>2</sub>O<sub>4</sub> systems are receiving international attention because they can provide rechargeable capacities between 200 and 250 mAh/g between 4.6 and 2.0 V vs. Li. These electrodes suffer from voltage decay and surface instability on cycling, thereby compromising the energy and power of the Li-ion cells and preventing their implementation in practical systems. A novel, simple, and versatile processing technique, using Li<sub>2</sub>MnO<sub>3</sub> as a precursor, to synthesize composite electrode structures is advocated; it offers the possibility of tailoring composite electrode structures and enhancing their electrochemical properties to meet Li-ion battery performance targets for PHEVs and EVs.

**STATUS OCT. 1, 2012:** Significant progress in exploiting a new synthesis approach using Li<sub>2</sub>MnO<sub>3</sub> as a precursor to fabricate high-capacity (200-250 mAh/g), structurally-integrated lithium-metal-oxide composite electrode materials, such as ‘layered-layered’, ‘layered-spinel’, ‘layered-rocksalt’ systems and more complex types, was made in FY 2012. The project focused predominantly on evaluating detailed structural, electrochemical, and surface properties of ‘layered-layered’ electrodes; the structural information was obtained from experiments conducted at Argonne’s Advanced Photon Source.

**STATUS SEP. 30, 2013:** Progress will be made in enhancing the electrochemical and structural stability of ‘layered-layered’ xLi<sub>2</sub>M’O<sub>3</sub>•(1-x)LiMO<sub>2</sub> electrodes at high potentials, with improvements in rate capability and cycle life.

**RELEVANT USABC GOALS:** 200 Wh/kg (EV requirement); 96 Wh/kg, 316 W/kg, 3000 cycles (PHEV 40 mile requirement). Calendar life: 15 years. Improved abuse tolerance.

#### MILESTONES:

- (a) Identify at least three promising, high-capacity (200-250 mAh/g) xLi<sub>2</sub>M’O<sub>3</sub>•(1-x)LiMO<sub>2</sub> compositions with a high Mn content using Li<sub>2</sub>MnO<sub>3</sub> or LiMn<sub>0.5</sub>Ni<sub>0.5</sub>O<sub>2</sub> as a precursor, determine their structures, and evaluate their electrochemical properties. (Sep. 13) **Complete**
- (b) Improve the surface stability of the electrode materials at high charging potentials by coating methodologies. (Sep. 13) **Complete**
- (c) Model surface structures and interfacial phenomena of coated electrodes. (Sep. 13) **Delayed until Sep. 14. This milestone was not worked on because the team member (Benedek) was assigned to an ABR project.**

## PROGRESS TOWARD MILESTONES

**Collaborators:** J. R. Croy, Brandon Long, Mahalingam Balasubramanian, Matthew Suchomel

Milestone (a) addressed: Evaluate the structural properties of  $x\text{Li}_2\text{M}'\text{O}_3 \cdot (1-x)\text{LiMO}_2$  ('layered-layered') electrode structures with a high Mn content.

Significant progress was made during FY2013 in evaluating and understanding: 1) synthesis-structure-electrochemical property relationships in 'layered-layered'  $x\text{Li}_2\text{MnO}_3 \cdot (1-x)\text{LiMO}_2$  materials, and 2) coated electrodes using sonochemical approaches, as highlighted in previous quarterlies (the January 2014 report will cover the sonochemical results, which have been submitted for publication). Two milestones, (a) and (b), have been completed for FY2013.

During this quarter, a detailed study was undertaken to understand relationships between synthesis and composition and transition metal ordering in Li- and Mn-rich  $x\text{Li}_2\text{MnO}_3 \cdot (1-x)\text{LiMO}_2$  electrodes. Several compositions were selected, including  $0.5\text{Li}_2\text{MnO}_3 \cdot 0.5\text{LiCoO}_2$ . Transition metal precursors were prepared by co-precipitation, followed by mixing and firing with lithium carbonate at  $550^\circ\text{C}$ . Subsequently, the as-prepared precursor was divided into three batches and annealed at  $850^\circ\text{C}$ , and cooled by different methods: 1) *Quenching*, 2) *Uncontrolled furnace cooling*, and 3) *Controlled slow-cooling* by a programmed temperature profile. Samples were characterized by ICP MS, synchrotron XRD, and absorption (EXAFS) at the Advanced Photon Source. ICP analyses of the baseline precursor and the final products showed that all samples had their intended stoichiometry (Table 1). Therefore, structural differences in these materials would likely be due to differences in synthesis conditions. However, Fig. 1a shows that the synchrotron XRD patterns of all samples overlap, identically. Furthermore, the Mn and Co K-edge EXAFS data in Fig. 1b and c, respectively, are essentially identical for all samples. These data provide important information about structure/synthesis relationships; electrochemical studies of these materials are currently underway to determine if their electrochemical properties are also independent of these synthesis conditions. Phenomena such as voltage fade and hysteresis are known to persist in samples prepared by different methods. The findings suggest that  $x\text{Li}_2\text{MnO}_3 \cdot (1-x)\text{LiMO}_2$  structures may be largely insensitive to the synthesis conditions described in this report and to a relevant electrochemically-active space. Atomic-scale investigations of electrochemical mechanisms that occur in these materials are in progress.

**Table 1.** ICP analyses of characterized samples

Sample	ICP Composition (O = 2)
Baseline ( $550^\circ\text{C}$ )	$\text{Li}_{1.19}\text{Mn}_{0.39}\text{Co}_{0.42}\text{O}_2$
Quenched	$\text{Li}_{1.19}\text{Mn}_{0.39}\text{Co}_{0.42}\text{O}_2$
Uncontrolled	$\text{Li}_{1.19}\text{Mn}_{0.39}\text{Co}_{0.42}\text{O}_2$
Controlled ( $\sim 1^\circ\text{C}/\text{min}$ )	$\text{Li}_{1.2}\text{Mn}_{0.39}\text{Co}_{0.41}\text{O}_2$

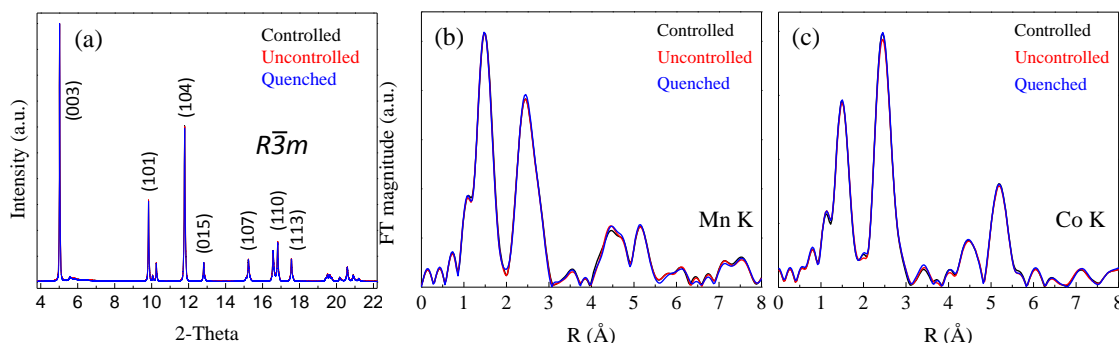


**Figure 1.** a) XRD; b, c) Mn and Co EXAFS of  $0.5\text{Li}_2\text{MnO}_3 \cdot 0.5\text{LiCoO}_2$  after various annealing treatments.

**TASK 4.2 - PI, INSTITUTION:** Marca Doeff, Lawrence Berkeley National Laboratory

**TASK TITLE:** Cathodes – Design of High Performance, High Energy Cathode Materials

**SYSTEMS:** Conoco Philips CPG-8 Graphite/1 M LiPF<sub>6</sub>+EC:DEC (1:2)/Toda High-energy layered (NMC)

**BARRIERS:** Cost, power and energy density, cycle life

**OBJECTIVES:** To develop high energy, high performance cathode materials including composites and coated powders, using spray pyrolysis and related synthesis techniques.

**GENERAL APPROACH:** High-energy cathode materials such as modified NMCs and LiNi<sub>0.5</sub>Mn<sub>1.5</sub>O<sub>4</sub> (LNMS) are synthesized *via* spray pyrolysis and related techniques, as well as composites containing these materials, and coated particles. For comparison, materials are also made by conventional techniques such as solid-state synthesis and the mixed hydroxide method. An array of physical and electrochemical techniques is used to characterize their behavior, in conjunction with members of the diagnostics team. Emphasis is placed on increasing energy density without sacrificing stability, safety, or cycle life.

**STATUS OCT. 1, 2012:** Phase-pure samples of LiNi<sub>0.5</sub>Mn<sub>1.5</sub>O<sub>4</sub> spinel (LNMS) have been produced by spray pyrolysis, and work on composite materials has begun. The survey of Li[Ni, Co, Ti, Mn]O<sub>2</sub> compounds was completed, allowing selection of the most promising compositions for further work to be carried out.

**STATUS SEP. 30, 2013:** Synthetic parameters for producing hollow LNMS particles (useful for making composites) and solid particles (for coated materials) will have been worked out. Work on NMCs will be directed towards understanding the mechanism of improvement in capacities and cycling behavior observed in some compounds when Ti is partially substituted for Co.

**RELEVANT USABC GOALS:** High energy, thermal stability, cycle life, cost (EV, PHEV).

**MILESTONES:**

- (a) Synthesize and electrochemically characterize composites consisting of spray-pyrolyzed LNMS hollow particles containing and coated with LiFePO<sub>4</sub> or a manganese oxide spinel. (Sep. 13) **Delayed to Jan. 14**
- (b) Produce and electrochemically characterize thin-film electrodes of a high-energy Ti-substituted NMC suitable for synchrotron studies. (Sep. 13). **Discontinued. Milestone was dropped because the study could be completed without producing thin films. The Ti-substituted NMC effort is being transferred to a newly funded ABR project.**

## PROGRESS TOWARD MILESTONES

(1) LNMS materials were prepared by spray pyrolysis with relatively high yield *via* several modifications of the previous set-up. The materials were electrochemically characterized and exhibited great dependence on the synthetic parameters. Figures 1a and 1b show the results for a typical LNMS material synthesized by spray pyrolysis, where a noticeable amount of  $\text{Mn}^{3+}$  exists in the material. Effort is being implemented to achieve phase-pure LNMS materials and their derivatives. Meanwhile, parallel efforts are being made to synthesize surface-protected LNMS materials using, but not limited to, atomic layer deposition (Fig. 1c). Several other coating techniques are being considered in order to integrate the functionalities (*e.g.*, electro-catalytic effect) of the coatings to electrochemical processes. In addition, controllable crystallinity is being investigated for the surface coating.

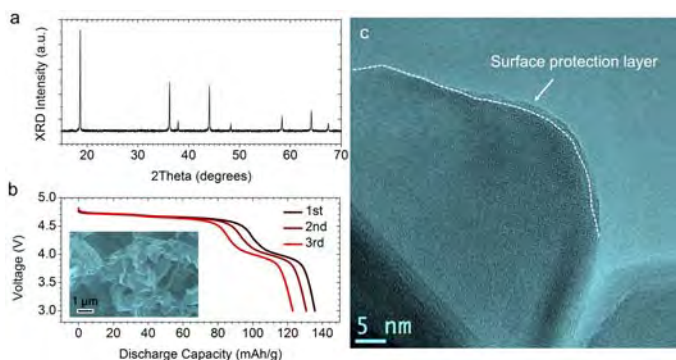


**Figure 1.** (a) XRD pattern of a typical LNMS material synthesized by spray pyrolysis. (b) Voltage-discharge capacity profile for the same material, and the corresponding SEM image is provided in the inset. (c) TEM image of a LNMS particle partially coated with a surface protection layer.

(2) Correlated ensemble-averaged XAS and spatially resolved STEM/EELS were performed in parallel to analyze the chemical evolution of the surface reaction layer for NMC materials under carbonate-based  $\text{LiPF}_6$  electrolyte. The dynamic evolutions of chemical species and layer thickness are monitored. So far, it was found that the surface reaction layer is primarily composed of  $\text{LiF}$  imbedded in a complex organic matrix (Fig. 2). The layer is rather sensitive to electrochemical processes. It is necessary to further investigate the impacts of surface reaction layer on the impedance buildup of operating cells that is widely observed in  $\text{Li}/\text{NMC}$  half-cells. This portion of the work is in collaboration with D. Nordlund and T. -C. Weng of SSRL/SLAC and H. L. Xin of BNL.

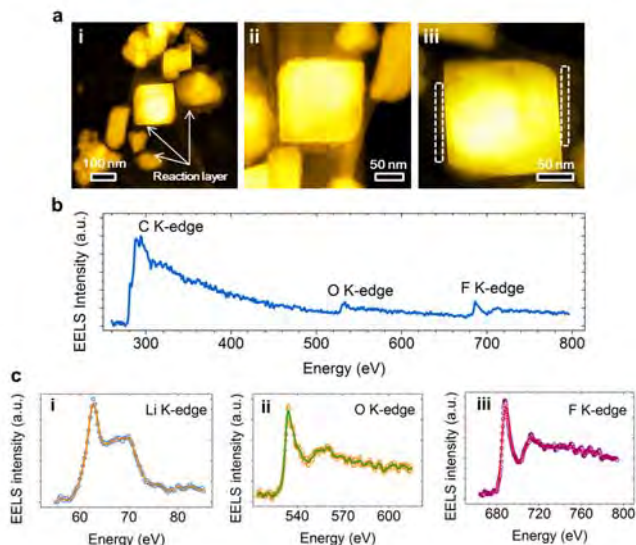


**Figure 2.** Spatially resolved STEM-EELS investigation of surface reaction layer on NMC materials. The EELS spectra were collected in the boxed areas labeled in (a) (iii).

**TASK 4.3 - PI, INSTITUTION:** Arumugam Manthiram, University of Texas at Austin

**TASK TITLE - PROJECT:** Cathodes – High-capacity, High-voltage Cathode Materials for Lithium-ion Batteries

**BASELINE SYSTEM:** Conoco Philips CPG-8 Graphite/1 M LiPF<sub>6</sub>+EC:DEC (1:2)/Toda High-energy layered (NMC)

**BARRIERS:** Cost, energy density, power density, cycle life, and safety

**OBJECTIVES:** To develop (i) low-cost cathodes based on polyanions that can offer a combination of high energy and power with excellent thermal stability and safety, and (ii) low-cost, high-voltage spinel cathodes that can offer high power and energy along with long cycle life.

**GENERAL APPROACH:** Our focus is on the design and development of cathode materials based on polyanions that have the possibility for reversibly inserting/extracting more than one Li<sup>+</sup> ion per transition metal ion, M<sup>n+</sup>, and/or operating above 4.3 V. Some example systems to be pursued are Li<sub>2</sub>MSiO<sub>4</sub> and Li<sub>2</sub>MP<sub>2</sub>O<sub>7</sub> (M = Mn, Fe, Co, and Ni) and their solid solutions. However, there are technical challenges in achieving the theoretical energy densities of many of these cathode materials. Synthesis and processing conditions play a critical role in realizing the full capacities of these polyanion cathodes with more than one Li<sup>+</sup> ion per M<sup>n+</sup> ion. Novel solution-based synthesis approaches, such as microwave-assisted solvothermal methods that can offer controlled nanomorphologies, are pursued to maximize the electrochemical performance. The synthesized nanostructured polyanion cathodes are characterized by a variety of techniques including *ex situ* and *in situ* X-ray diffraction, electron microscopy (SEM, TEM, and STEM), X-ray photoelectron spectroscopy, time of flight–secondary ion mass spectroscopy, and in-depth electrochemical measurements. In addition, the role of cation doping, segregation of certain doped cations to the surface, cation ordering, morphology, and surface planes on the electrochemical properties of high-voltage spinel cathodes are investigated. Based on the characterization data gathered, a fundamental understanding of structure-composition-property-performance relationships is developed.

**STATUS OCT. 1, 2012:** Developed (i) novel synthesis approaches to obtain high-capacity, high-voltage polyanion (silicate and phosphate) cathodes with unique nanomorphologies, (ii) an understanding of the factors that control the performance of high-voltage (4.7 V) spinel oxide cathodes, and (iii) an understanding of their structure-composition-property-performance relationships.

**STATUS SEP. 30, 2013:** (i) Synthesis by novel solution-based synthesis approaches and characterization of Li<sub>2</sub>MP<sub>2</sub>O<sub>7</sub> (M = Fe, Mn, Co, and Ni) and their solid solutions, as well as Li<sub>2</sub>MSiO<sub>4</sub> (M = Mn, Fe, Co, and Ni) and their solid solutions, and (ii) an understanding of the influence of morphology and crystal planes on the performance of high-voltage spinel cathodes.

**RELEVANT USABC GOALS:** 300,000 shallow discharge cycles, 10-year life, < 20% capacity fade over a 10-year period

**MILESTONES:**

- (a) Understand the influence of morphology and crystal planes on the electrochemical performance of high-voltage spinels. (Dec. 12) **Complete**
- (b) Synthesize and characterize Li<sub>2</sub>MP<sub>2</sub>O<sub>7</sub> (M = Fe, Mn, Co, and Ni) as well as their solid solutions. (Jun. 13) **Complete**
- (c) Assess surface segregation in Li<sub>2</sub>M<sub>1-x</sub>Fe<sub>x</sub>SiO<sub>4</sub> and Li<sub>2</sub>M<sub>1-x</sub>Fe<sub>x</sub>P<sub>2</sub>O<sub>7</sub> (M = Co, Mn, and Ni.) (Sep. 13) **Complete**

## PROGRESS TOWARD MILESTONES

This quarter,  $\text{Li}_2\text{MnSiO}_4/\text{C}$  nanocomposite cathodes that have the potential to reversibly extract more than one Li per transition-metal ion were synthesized with unique morphologies, employing poly(methyl methacrylate) (PMMA) crystals as a hard-template and a phenolic-resin polymer as the carbon source. The PMMA template is easy to synthesize and decomposes readily to gaseous products at elevated temperatures during the formation of the desired compound without requiring any extra step to remove the template unlike other hard-templates, such as silica. A long-range, ordered, macroporous structure resulted, as seen in the SEM picture in Fig. 1a, due to the close-packed nature of the PMMA template. The first two charge-discharge profiles of  $\text{Li}_2\text{MnSiO}_4/\text{C}$ , shown in Fig. 1b, suggest a possible structural rearrangement during the first cycle. The

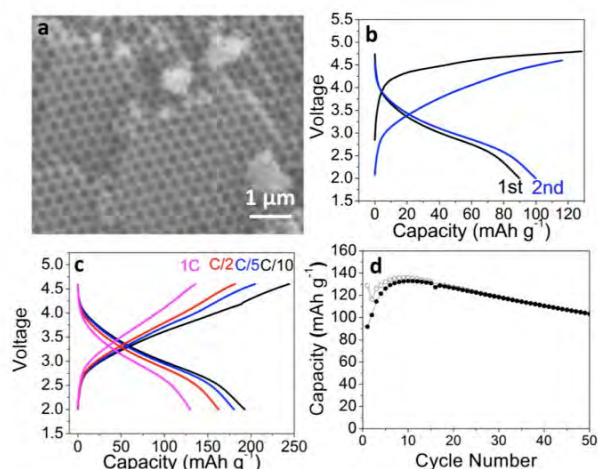


**Figure 1.** (a) SEM image, (b) first two charge-discharge profiles, (c) the highest capacity obtained at various rates, and (d) cycling performance at 1C rate of the  $\text{Li}_2\text{MnSiO}_4/\text{C}$  nanocomposite cathode material.

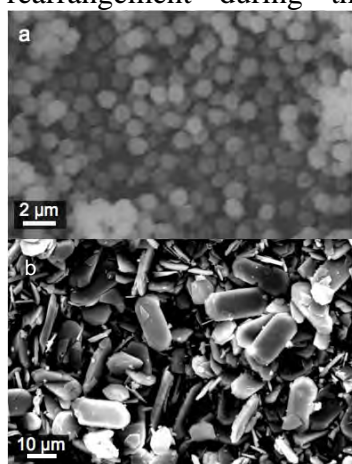


**Figure 2.** SEM photographs of (a)  $\text{Li}_2\text{Fe}_{0.9}\text{Mn}_{0.1}\text{SiO}_4$  and (b)  $\text{Li}_2\text{MnP}_2\text{O}_7$ .

sample exhibited a reversible capacity of *ca.*  $200 \text{ mAh g}^{-1}$  (Fig. 1c) at  $55^\circ\text{C}$  corresponding to the extraction of 1.2 Li per Mn. However, the cathode exhibited some capacity fade as seen in Fig. 1d (at a rate of 1C at  $55^\circ\text{C}$ ) after an initial increase in capacity during the first 10 cycles. Also,  $\text{Li}_2\text{Fe}_{0.9}\text{Mn}_{0.1}\text{SiO}_4$  was synthesized by a hydrothermal process at  $200^\circ\text{C}$  followed by heating at  $650^\circ\text{C}$ , but the particle size was larger (*ca.*  $1 \mu\text{m}$ ), as seen in Fig. 2a. In addition, the pyrophosphate  $\text{Li}_2\text{MnP}_2\text{O}_7$  was obtained at  $300^\circ\text{C}$  by a microwave-assisted solvothermal (MW-ST) process, but the particle size was too large, as seen in Fig. 2b. Unfortunately, the analogous  $\text{Li}_2\text{FeP}_2\text{O}_7$  could not be made under similar conditions, so the possible surface segregation in  $\text{Li}_2\text{Mn}_{1-x}\text{Fe}_x\text{P}_2\text{O}_7$  could not be verified. Also, *ca.*  $100 \text{ mAh g}^{-1}$  was achieved with  $\text{LiVP}_2\text{O}_7$  obtained by a MW-ST process.

Furthermore, the voltage variations in polyanion cathodes have largely been explained in the past for isostructural materials. Therefore, a crystal-chemical guide was provided for understanding how factors such as the crystal structure and covalency of the polyanion affect the  $\text{M}^{2+/3+}$  redox energies in polyanion cathodes having different structures. It was demonstrated that an accurate prediction of the voltage can be made based on a basic understanding of how the coordination of the transition-metal ion affects the covalency of the M-O bond. Additionally, a new method for assessing the covalency of the polyanion (beyond the electronegativity of the counter-cation) was presented and used to explain why the voltage delivered by  $\text{Li}_2\text{MP}_2\text{O}_7$  cathodes is higher than that of  $\text{LiMPO}_4$  for a given M. A comparison of the silicate and phosphate structures revealed that edge sharing between transition-metal polyhedra and other cation polyhedra has an opposite effect on the voltage delivered by these materials. It was also shown that crystal-field theory alone is not sufficient to explain the voltages of polyanion cathodes, demonstrating the necessity of considering the structural effects to fully understand the voltage trends.

**TASK 4.4 – PI, INSTITUTION:** Ji-Guang (Jason) Zhang and Jie Xiao, Pacific Northwest National Laboratory

**TASK TITLE:** Cathodes – Development of High Energy Cathode Materials

**BASELINE SYSTEM:** Conoco Philips CPG-8 Graphite/1 M LiPF<sub>6</sub>+EC:DEC (1:2)/Toda High-energy layered (NMC)

**BARRIERS:** Low energy density, high cost, limited cycle life

**OBJECTIVES:** To develop high-energy, low-cost, and long-life cathode materials.

**GENERAL APPROACH:** To develop high energy-density cathode materials through cost-effective methods. Appropriate doping, surface treatment, and appropriate electrolytes/additives will be used to improve the electrochemical performances of both high-voltage spinel LiNi<sub>0.5</sub>Mn<sub>1.5</sub>O<sub>4</sub> and Mn-based Li-rich layered composite. The fundamental reaction mechanisms of cathode materials during electrochemical processes will be systematically investigated to understand/address the challenges in these cathode materials.

**STATUS OCT. 1, 2012:** High-voltage LiNi<sub>0.5</sub>Mn<sub>1.5</sub>O<sub>4</sub> was synthesized by a facile approach, while the content of disordered phase in the spinel was precisely controlled through reheating, element substitution, or different cooling rates. Several other “inactive” components in the electrode, including cell cans, separators, and carbon additives, were also systematically re-examined for their stability in a high-voltage system. Using the optimized electrolyte and stable components, the high-voltage spinel cathode has achieved more than 500 cycles with less than 20% capacity fade (half cells.) Synthesis of the Li<sub>2</sub>MnO<sub>3</sub> baseline has been completed. Surface treatment, doping, and electrolyte additives will be applied in the layered composite system coupled with advanced characterizations to understand/mitigate the degradation issues.

**STATUS SEP. 30, 2013:** High-energy cathodes for Li-ion battery applications will be further explored. Synthesis of xLi<sub>2</sub>MnO<sub>3</sub>•(1-x)LiMO<sub>2</sub> (M = Mn, Ni, Co; 0 ≤ x ≤ 1) will be optimized and their degradation mechanism will be investigated. Manganese dissolution issue in both layered composite and spinel will be studied and mitigated to improve the cell performance. Appropriate electrolyte additives will be identified in the layered composite system to improve the cycling stability. Safety, power rate, and cycling stability of these cathode materials will be improved to satisfy the need for HEV/EV applications.

**RELEVANT USABC GOALS:** >96 Wh/kg (for PHEVs), 5000 deep-discharge cycles, 15-year calendar life, improved abuse tolerance, and less than 20% capacity fade over a 10-year period.

**MILESTONES:**

- (a) Identify the key factors related to the oxygen release in layered composite xLi<sub>2</sub>MnO<sub>3</sub>•(1-x)LiMO<sub>2</sub> (M = Mn, Ni, Co; 0 ≤ x ≤ 1). (May 13) **Complete**
- (b) Demonstrate the effects of different treatments (doping, coating, and electrolyte additive) on cathode and improve their cyclability by more than 20% as compared with untreated samples. (Sep. 13) **Complete**
- (c) Identify electrolyte additives that can improve the cycling stability of layered composite to more than 200 mAh/g in 100 cycles at C/3 rate. (Sep. 13) **Complete**

## PROGRESS TOWARD MILESTONES

All the milestones for FY13 have been completed in this quarter. Tris(pentafluorophenyl)borane ( $(C_6F_5)_3B$ , TPFPB) was found to effectively enhance the cycling stability and alleviates the voltage fading of LMR cathode  $Li[Li_{0.2}Ni_{0.2}Mn_{0.6}]O_2$ , probably through the modification of interfacial reactions on the cathode surface. The synthesis route of LMR was also modified by adding a hydrothermal treatment step, which promoted the homogenous mixing of starting materials at the atomic level.

The effects of TPFPB additive are compared in Fig.1a. After the first three formation cycles, an initial discharge capacity of *ca.* 200 mAh  $g^{-1}$  was achieved in all cells at C/3. However, fast capacity fading was observed for  $Li[Li_{0.2}Ni_{0.2}Mn_{0.6}]O_2$  in the baseline electrolyte during cycling. With the addition of TPFPB, the cycling stability of LMR was largely improved. After 300 cycles, the discharge capacities were maintained at 157 mAh/g for LMR cathodes tested with 0.1 M TPFPB in the electrolyte, corresponding to a capacity retention of 80.6%. Increasing the TPFPB concentration to 0.2 M did not further improve the cycling performance of LMR. TPFPB itself is stable up to 5 V (data not shown here), thus it will not decompose in the first charge. It was proposed that TPFPB effectively confines the highly active oxygen species released from the lattice through its strong coordination ability and high oxygen solubility. The electrolyte decomposition caused by the oxygen attack is therefore largely mitigated, forming reduced amount of byproducts on the cathode surface.

The effects of hydrothermal treatment on the starting materials are also reported in this quarter. It was revealed that homogenous mixing of the starting material is critical to prevent the previously observed Ni segregation at some surface regions and grain boundaries, which initiated side reactions between a highly active surface  $Ni^{4+}$  and the electrolyte at high voltage. Figure 1b demonstrates that through synthesis modification, the cycling stability of LMR was remarkably improved (no additive was used), delivering greater than 200 mAh/g capacity in 100 cycles at a C/3 cycling rate.

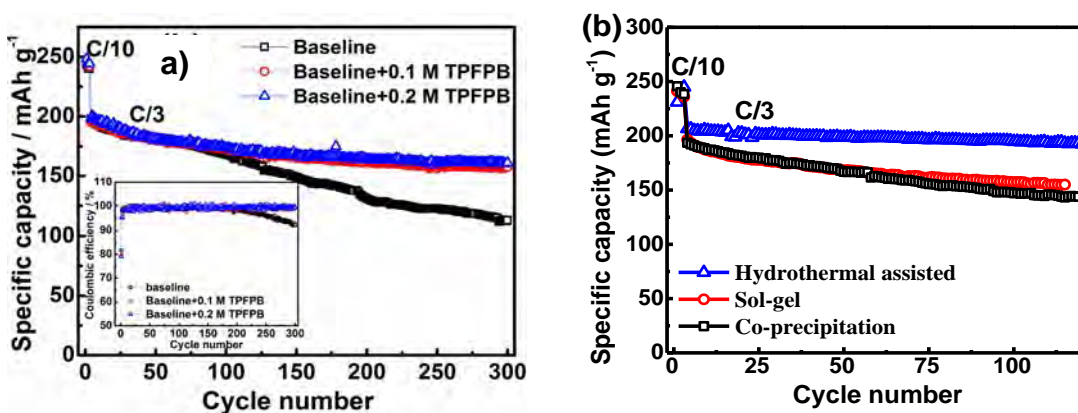


**Figure 1.** a) Effects of TPFPB on the cycling performance of  $Li[Li_{0.2}Ni_{0.2}Mn_{0.6}]O_2$ . The inset of (a) is the corresponding Coulombic efficiency during cycling. b) Effects of synthesis modification (No additive was used). A hydrothermal treatment was included in the synthesis step of LMR. For the first three cycles, a slow rate at C/10 was used followed by C/3 in the subsequent cycling in all cell tests.

**Presentation:** J.Zheng, M.Gu, J.Xiao, P.Zuo, C.Wang and J.Zhang, "LMR cathode: its structure evolution and performance improvement", *Beijing 2013 International Forum on Li-ion Battery*, Beijing, China, 2013.

**Task 4.6 - PI, INSTITUTION:** Patrick Looney and Feng Wang, Brookhaven National Laboratory

**TASK TITLE:** Cathodes – *In situ* Solvothermal Synthesis of Novel High Capacity Cathodes

**BASELINE SYSTEM:** Conoco Philips CPG-8 Graphite/1 M LiPF<sub>6</sub>+EC:DEC (1:2)/Toda High-energy layered (NMC)

**BARRIERS:** Low energy density and cost

**OBJECTIVE:** Develop low-cost cathode materials that offer high energy density (>660 Wh/kg) and electrochemical properties (cycle life, power density, safety) consistent with USABC goals.

**GENERAL APPROACH:** Our approach is to develop and utilize a specialized *in situ* reactor designed to investigate synthesis reactions in real-time using synchrotron techniques. This capability will allow us to identify intermediate or transient phases and better control phase nucleation, reaction rates, and material properties. These new tools and insights will be used to prepare novel high energy density lithium cathode materials ( $\geq 660$  Wh/kg).

**STATUS OCT. 1, 2012:** In FY12 work was initiated on the synthesis and electrochemical testing of the high capacity cathode Cu<sub>0.95</sub>V<sub>2</sub>O<sub>5</sub>. By the end of FY12 a synthesis procedure for the preparation of pure, nano-scale Cu<sub>0.95</sub>V<sub>2</sub>O<sub>5</sub> was identified and electrochemical testing was performed. The development of an improved *in situ* synthesis reactor for synchrotron studies and a 2<sup>nd</sup> generation reactor is complete.

**STATUS SEP. 30, 2013:** In Year 2 investigation of Cu-V-O compounds will continue. By the end of FY13 multiple Cu-V-O compounds will have been synthesized. The optimal procedure for the synthesis of Cu<sub>0.95</sub>V<sub>2</sub>O<sub>5</sub> will be determined by evaluating a variety of precursors (Cu source, V source and reducing agents) and reaction conditions (temperature and time). Electrochemical studies (*in situ* and *ex situ*) along with material characterization (*e.g.*, particle size and morphology) will be determined to identify mechanism(s) of capacity fade. The feasibility of using ion exchange reactions will also be determined.

**RELEVANT USABC GOALS:** 200 Wh/kg (EV requirement); 96 Wh/kg, 3000 cycles (PHEV 40 mile requirement); lower cost batteries.

**MILESTONES:**

- (a) Determine optimal procedure for the synthesis of Cu<sub>0.95</sub>V<sub>2</sub>O<sub>5</sub>. This will involve an evaluation of precursors, reducing agents and synthesis conditions. (Jan. 13) **Complete**
- (b) Identify mechanism(s) responsible for poor cycling in Cu<sub>0.95</sub>V<sub>2</sub>O<sub>5</sub> and identify a pathway for reducing capacity fade with cycling. (Mar. 13) **Complete**
- (c) Synthesize and electrochemically characterize at least one other Cu-V-O compound using hydrothermal/solvothermal and/or ion-exchange reactions. (May. 13) **Complete**
- (d) Determine the feasibility of using hydrothermal and/or ion-exchange reactions to prepare polyanion cathodes. (Sep. 13) **Complete**

## PROGRESS TOWARD MILESTONES

The low-temperature, soft-chemistry-based, hydrothermal/solvothermal method was used in previous quarters for synthesis of high-capacity Cu-V-O cathodes. In this quarter, hydrothermal-based methods for preparing polyanion-type cathodes were explored, either *via* direct chemical reaction or lithium substitution in iso-structural, Na-containing precursors in an aqueous solution. Some of the results are reported on the ion-exchange synthesis of high-capacity lithium metal fluorophosphates,  $\text{Li}(\text{Na})_{1+x}\text{MPO}_4\text{F}_x$ , in which more than one Li may be (de)intercalated.

Synthesis of the fluorophosphates  $\text{Li}_x\text{Na}_{2-x}\text{MnPO}_4\text{F}$  and  $\text{Li}_x\text{Na}_{1.5-x}\text{VPO}_5\text{F}_{0.5}$  *via* ion exchange was typically performed in a sealed autoclave at elevated temperatures, using  $\text{Na}_2\text{MnPO}_4\text{F}$  or  $\text{Na}_{1.5}\text{VPO}_5\text{F}_{0.5}$  as the precursor, LiBr as the Li source, and 1-hexanol as the solvent. The extent of exchange was maximized *via* tuning reaction conditions, such as temperature and the concentration of the Li source. Fig. 1 provides XRD patterns of synthesized  $\text{Li}_x\text{Na}_{2-x}\text{MnPO}_4\text{F}$  and  $\text{Li}_x\text{Na}_{1.5-x}\text{VPO}_5\text{F}_{0.5}$  that exhibit similar structures as their precursors but smaller volumes. Subtle structural changes, and possibly a reduction in particle size, are suggested by the change in the relative intensity and broadening of diffraction peaks. The results demonstrate the feasibility of using ion exchange method to prepare metastable phosphates that are mostly inaccessible by direct chemical reactions.

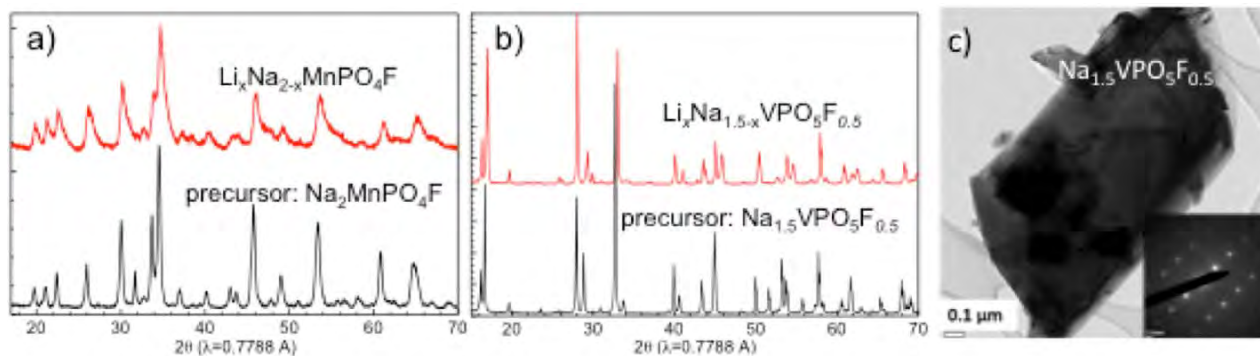


**Figure 1.** Structural characterization of precursors and Li-exchanged final products by synchrotron XRD (a, b), bright-field TEM imaging and electron diffraction (c).

A new type of *in situ* reactor was developed for studying ion-exchange reactions and used for studies of the structural change in single-crystalline,  $\mu\text{m}$ -sized,  $\text{Na}_{1.5}\text{VPO}_5\text{F}_{0.5}$  particles (see Fig. 1c for TEM examination) throughout the entire Li-exchange process. One set of time-resolved XRD patterns is provided in Fig. 2. Interestingly, a gradual phase transformation (blue region) occurred in the early stage, followed by solid solution (red), and then stabilization of a final phase (green), which suggests a complicated reaction process with more than one phase involved. Systematic *in situ* measurements and structure refinements have been completed for studies of the phase transformations and reaction kinetics during hydrothermal ion-exchange of  $\text{Na}_{1.5}\text{VPO}_5\text{F}_{0.5}$ .

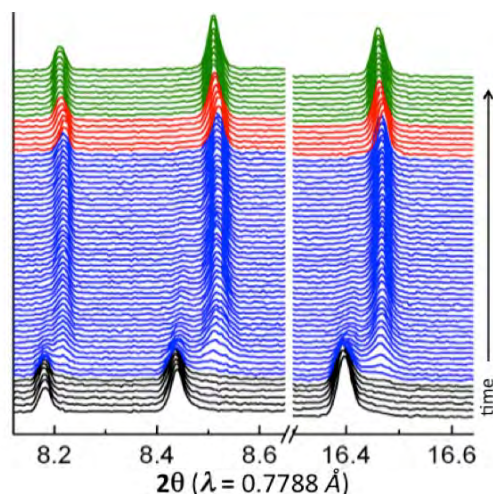


**Figure 2.** Time-resolved XRD patterns from ion exchange process in  $\text{Na}_{1.5}\text{VPO}_5\text{F}_{0.5}$ .

All milestones for FY13 have been met or exceeded.

**Task 4.7 - PI, INSTITUTION:** Jim Kiggans and Andrew Kercher, Oak Ridge National Laboratory

**TASK TITLE:** Cathodes – Lithium-bearing Mixed Polyanion (LBMP) Glasses as Cathode Materials

**BASELINE SYSTEM:** Conoco Philips CPG-8 Graphite/1 M LiPF<sub>6</sub>+EC:DEC (1:2)/Toda High-energy layered (NMC)

**BARRIERS:** Cathodes for Li-ion batteries require lower cost materials and improved energy density, safety, and cycling stability.

**OBJECTIVE:** Develop lithium-bearing mixed polyanion (LBMP) glasses as potential cathode materials for Li-ion batteries with superior performance to lithium iron phosphate for use in electric vehicle applications. Modify compositions of LBMP glasses to provide higher electrical conductivities, higher redox potentials, and higher specific energies than similar crystalline polyanion framework materials. Test LBMP glasses for performance and cyclability. The final goal is to develop LBMP glass compositions with the potential to provide specific energies up to near 1000 mWh/g.

**GENERAL APPROACH:** The experimental approach combines: (1) structure and property modeling, (2) glass processing, (3) glass characterization, (4) conventional cathode production, and (5) electrical and electrochemical testing. Computer modeling will be used to suggest the most promising LBMP glass compositions in terms of electrochemical performance and glass processing capability. Classical heat-quench glass forming and sol gel processing will be used to make the LBMP glasses. Electrochemical performance will be demonstrated on coin cells with LBMP glass cathodes using cycle testing and variable discharge rate testing.

**STATUS OCT. 1, 2012:** An experimental test matrix for initial cathode glass compositions has been developed. Materials and equipment have been purchased for initial glass compositions. Initial work with TGA-DTA analyses of glass precursors is in progress.

**STATUS SEP. 30, 2013:** One or more promising glass compositions will be selected from an initial experimental screening. CALPHAD simulation will be developed and verified against initial experimental results. Optimization and examining the interrelation of properties, compositions, and synthesis methods will be underway.

**RELEVANT USABC GOALS:** Reduce the cost of electrochemical energy storage by developing Li-ion batteries and other advanced energy-storage technologies that afford higher energy densities without sacrificing safety and performance.

**MILESTONES:**

- (a) Setup CALPHAD database and perform initial simulation for one glass composition. (Jan. 13) **Complete**
- (b) Synthesize, characterize, and perform electrochemical testing on at least four different glass compositions. (Sep. 13) **Complete**
- (c) Create CALPHAD thermodynamic database and verify results with comparison to initial experimental glass compositions and electrochemical performance. (Sep. 13) **Complete**

## PROGRESS TOWARD MILESTONES

Lithium-manganese-phosphate-vanadate (LMPV) glasses were produced with the goal of demonstrating multi-valent intercalation reactions in a mixed polyanion glass cathode. Unfortunately, even with exceptionally high vanadate substitution, the LMPV glasses did not achieve high specific capacity by intercalation reactions (Fig. 1). However, these LMPV glasses did have an unknown high capacity reaction at low voltages similar to what was previously observed in iron phosphate vanadate glasses. Including both the intercalation reaction and the unknown high capacity reaction, an LMPV glass discharged down to 1V had nearly 3 Li atoms electrochemically active per Mn atom in the glass (299 mAh/g). Ongoing research efforts are focused on: (a) producing polyanion glasses with other transition metal cations in order to achieve multi-valent intercalation reactions and (b) understanding the mechanism of the unknown high capacity reaction with the aim of designing glasses where this electrochemical reaction occurs at higher voltages.

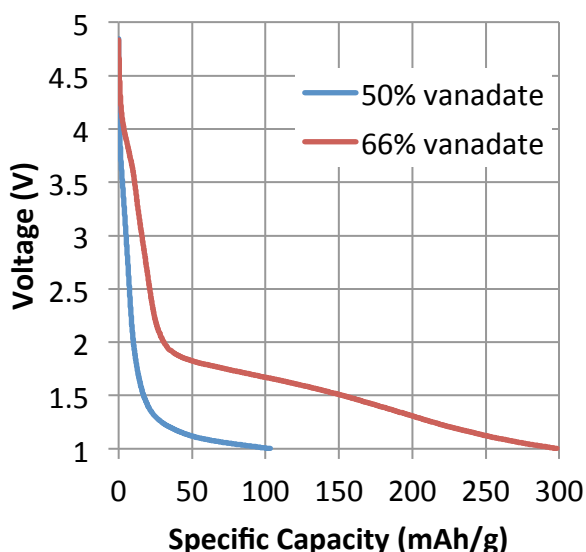


**Figure 1:** Discharge curves (8  $\mu$ A) of lithium manganese phosphate vanadate glasses with 50% and 66% of the polyanions as vanadate.

A computational thermodynamic model of 50% vanadate-substituted iron pyrophosphate glass was further refined to improve agreement with experimental results with the introduction of interaction parameters to describe non-ideal mixing extrapolated from the constituents. A symmetric, sub-regular solution model was needed to express the non-ideality between the mixing of Li and vacancies in the dedicated sublattice.  ${}^0L$  and  ${}^2L$  interaction parameters in the Redlich-Kister polynomial were used to predict the electrochemical performance of polyanion glasses.

All three milestones for FY2013 were accomplished. Thermodynamic modeling using the CALPHAD approach simulated the electrochemical response of a mixed polyanion glass cathode. Modeled discharge curves were compared to an actual battery discharge curve for an iron phosphate vanadate glass. Four different iron-containing polyanion glasses were synthesized, characterized, and electrochemically tested. Using processing and property insights from the Fe-containing glasses, Mn-containing glasses were produced and electrochemically tested.

**Collaborators:** Dongwon Shin, Joanne Ramey, Lynn Boatner, Fred Montgomery, Nancy Dudney

## BATT TASK 5 DIAGNOSTICS

**Task 5.1 - PI, INSTITUTION:** Robert Kostecki, Lawrence Berkeley National Laboratory

**TASK TITLE:** Diagnostics – Interfacial Processes

**BASELINE SYSTEMS:** Conoco Philips CPG-8 Graphite/1 M LiPF<sub>6</sub>+EC:DEC (1:2)/Toda High-energy layered (NMC)

**BARRIERS:** Low energy (related to cost), poor lithium battery calendar/cycle lifetimes.

**OBJECTIVES:** (i) Establish direct correlations between electrochemical performance of high-energy Li-ion composite cathodes, and surface chemistry, morphology, topology and interfacial phenomena, (ii) improve the capacity and cycle life limitations of Li<sub>x</sub>Si anodes

**GENERAL APPROACH:** Design and employ novel and sophisticated *in situ* analytical methods to address the key problems of the BATT baseline chemistries. Proposed experimental strategies combine imaging with spectroscopy aimed at probing electrodes at an atom, molecular, or nanoparticulate level to unveil structure and reactivity at hidden or buried interfaces and determine electrode performance and failure modes in baseline Li<sub>x</sub>Si-anodes and high-voltage LMNO cathodes. The proposed methodologies, *in situ* and *ex situ* Raman, FTIR and LIBS far- and near-field spectroscopy/microscopy, SPM, spectroscopic ellipsometry, SEM, HRTEM, standard electrochemical techniques, and model single particle and/or monocrystal model electrodes will be used to probe and characterize bulk and surface processes in Si anodes and high-energy cathodes.

**STATUS OCT. 1, 2012:** This is a new project initiated October 1, 2012. Some insight into the mechanism of electrolyte decomposition at the surface of model anode and cathode materials has been gained and its impact on the electrode long-term electrochemical behavior evaluated. The composition and (re)formation dynamics of the surface layer on model monocrystal Sn and Si intermetallic anodes, and on model single particle and composite high-voltage cathodes, were determined using various complementary spectroscopy techniques. A unique strategy involving the use of *in situ* techniques (AFM, ellipsometry, Raman and fluorescence imaging, FTIR and AP-XPS) in conjunction with *ex situ* techniques (XAS, RBS and NRA) were applied to monitor and identify surface processes. Preliminary evaluation of near-field optical spectroscopy and imaging techniques for fundamental interfacial studies of Li-ion systems were carried out.

**STATUS SEP. 30, 2013:** Insight into the mechanism of surface phenomena on thin-film and monocrystal Sn and Si intermetallic anodes will be gained and their impact on the electrode long-term electrochemical behavior will be evaluated. Comprehensive fundamental study of the early stages of SEI layer formation on polycrystalline and single crystal face Sn and Si electrodes will be carried out. *In situ* and *ex situ* far- and near-field FTIR and Raman spectroscopy will be employed in conjunction with AFM surface imaging to detect and monitor surface phenomena at the intermetallic anodes. Similar experimental methodology will be used to detect and characterize surface and bulk processes in high-voltage (>4.3V) model and composite cathodes.

**RELEVANT USABC GOALS:** *Cycle life:* 5000 (deep) and 300,000 (shallow) cycles. *Available energy:* 200 Wh/kg. *Calendar life:* 15 years.

### **MILESTONES:**

- (a) Resolve SEI layer chemistry of Si model single-crystal anodes (collaboration with the *BATT Anode Group*. (Jul. 13) **Complete**
- (b) Characterize interfacial phenomena in high-voltage composite cathodes (collaboration with the *BATT Cathode Group*. (Jul. 13) **Complete**
- (c) Incorporate an *in situ* electrochemical cell into existing ultrafast laser beam delivery/automated translation stage/spectrometer LIBS system. (Aug. 13) **Complete**

## PROGRESS TOWARD MILESTONES

In the fourth quarter of FY2013, the main efforts toward milestone (c) focused on the development, testing, and optimization of an *in situ* cell for the analysis of interfacial layers formed on model electrode systems using ultrafast Laser Induced Breakdown Spectroscopy (LIBS). A UV-transmissive, three-electrode cell configuration with all-optical access (photon excitation/photon detection) was built and integrated into an ultrafast, laser-beam,

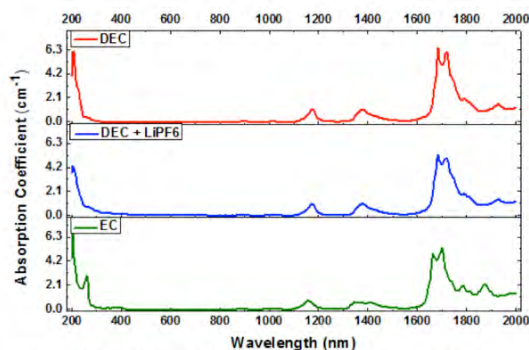


**Figure 1.** Absorption coefficient of different components of a 1M LiPF<sub>6</sub> EC:DEC [1:1] solution.

(minimally absorbed by the electrolyte) was chosen as an excitation source. The laser pulse duration was  $500 \times 10^{-15}$  sec.

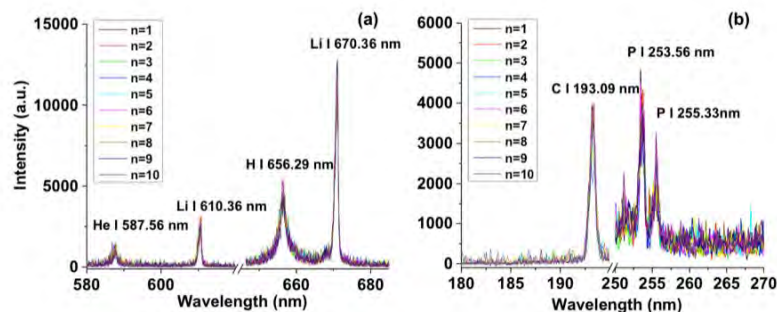


**Figure 2.** Ultrafast LIBS emission intensity from the Si electrode/organic electrolyte system as a function of wavelength in the (a) 580 to 685nm and (b) 180-270 nm spectral region.

rate as well as organic electrolyte thickness above the working electrode to control the contribution of the electrolyte in the emission signal. It was found that higher repetition rates can contribute significantly towards improvement of the Si signal-to-noise ratio, a phenomenon associated with cavitation in the electrolyte due to the laser material interaction in the examined laser energy regime.

Further near-field IR spectroscopy/imaging experiments are underway to investigate the SEI layer (re)formation process and composition on Si monocrystals as well as fluorescence spectroscopy and imaging measurements to determine the origin of fluorescence compounds in Li-ion systems.

delivery/translation stage and detection system (Czerny Turner Spectrometer/ICCD). Figure 1 shows the absorption coefficient of the individual components of the 1M LiPF<sub>6</sub> EC:DEC [1:1] electrolyte system in the 200 to 2000 nm spectral range obtained using UV/Vis spectrophotometry. This step was critical in identifying the optical absorption properties of different components of the electrolyte system and controlling the way that radiation, both transmitted from the laser and emitted from the liquid electrolyte. A femtosecond laser source with an emission wavelength at 343 nm

Figure 2 depicts the ultrafast LIBS spectral emission originating from a 1M LiPF<sub>6</sub> EC:DEC [1:1] electrolyte in contact with a Si wafer with (100) crystal orientation. All major elements of interest (C, P, Li, H) were successfully detected from the electrolyte for the first 10 laser pulses. Subsequent experiments involved optimization of laser parameters including laser energy/pulse and laser repetition

**Task 5.2 - PI, INSTITUTION:** Xiao-Qing Yang and Kyung-Wan Nam, Brookhaven National Laboratory

**TASK TITLE:** Diagnostics – Advanced *In situ* Diagnostic Techniques for Battery Materials

**BASELINE SYSTEM:** Conoco Philips CPG-8 Graphite/1 M LiPF<sub>6</sub>+EC:DEC (1:2)/Toda High-energy layered (NMC)

**BARRIERS:** PHEV: Energy density, Cycle life; HEV: Power density, Abuse tolerance

**OBJECTIVE:** The primary objective is to determine the contributions of electrode materials changes, interfacial phenomena, and electrolyte decomposition to cell capacity and power decline in helping the development of high energy density Li battery with better safety characteristics and longer life.

**GENERAL APPROACH:** To use various synchrotron based X-ray techniques to characterize electrode materials and electrodes taken from baseline BATT Program cells. The following approaches will be used: *in situ* synchrotron XRD and hard XAS at transition metal K-edges during cycling; soft XAS on L-edges of Mn, Ni and Co and K-edges of C, O, and F using electron yield (surface) and fluorescence yield (bulk) detectors after cycle; high resolution transmission electron microscopy (HRTEM) coupled with electron energy loss spectroscopy (EELS) after cycle; *in situ* TR-XRD coupled with MS during heating of charged cathode materials (thermal stability study); *in situ* and *ex situ* Si K-edge XAS of Si based anode materials during cycling; *in situ* quick XAS of the cathode materials for dynamic study during cycling.

**STATUS OCT. 1, 2012:** This is a new project initiated October 1, 2012. Structural studies on the high energy density Li<sub>2</sub>MnO<sub>3</sub>-LiMO<sub>2</sub> (M = Ni, Mn, Co) layered materials have been carried out (in collaboration with ANL) and *in situ* XRD studies on different types of lithium iron phosphate cathode materials with mesoporous structure. *In situ* XRD and XAS diagnostic studies of high voltage LiMn<sub>2-x</sub>M<sub>x</sub>O<sub>4</sub> (M = Ni, Cu etc.) have also been performed with spinel structure during cycling.

**STATUS SEP. 30, 2013:** Thermal stability studies of high-voltage LiMn<sub>2-x</sub>Ni<sub>x</sub>O<sub>4</sub> with ordered (*P4<sub>3</sub>32*) and disordered (*Fd-3m*) spinel structure will have been carried out using time-resolved XRD coupled with MS and XAS during heating. The XAS studies on high energy density Si-based anode materials during cycles also will have been started.

**RELEVANT USABC GOALS:** 15-year calendar life, <20% capacity fade over a 10-year period, improved abuse tolerance.

**MILESTONES:**

- (a) Complete the *in situ* time-resolve XRD studies of LiMn<sub>2-x</sub>Ni<sub>x</sub>O<sub>4</sub> cathode material with ordered (*P4<sub>3</sub>32*) spinel structure during heating. (Apr. 13) **Complete**
- (b) Complete the XAS studies of LiMn<sub>2-x</sub>Ni<sub>x</sub>O<sub>4</sub> cathode material with ordered (*P4<sub>3</sub>32*) spinel structure during heating. (Apr. 13) **Complete**
- (c) Complete the *in situ* time-resolve XRD studies of LiMn<sub>2-x</sub>Ni<sub>x</sub>O<sub>4</sub> cathode material with disordered (*Fd-3m*) spinel structure during heating. (Sep. 13) **Complete**
- (d) Complete the XAS studies of LiMn<sub>2-x</sub>Ni<sub>x</sub>O<sub>4</sub> cathode material with disordered (*Fd-3m*) spinel structure during heating. (Sep. 13) **Complete**
- (e) Complete the *ex situ* Si K-edge XAS studies of Si-based high energy density anode materials after cycles. (Sep. 13) **Complete**

## PROGRESS TOWARD MILESTONES

In the 4th quarter of FY2013, all milestones were successfully completed. During this period, BNL was focused on studying the thermal stability of high voltage  $\text{LiMn}_{2-x}\text{Ni}_x\text{O}_4$  ( $x=0.5$ , LNMO) spinel cathode materials with disordered ( $Fd-3m$ ) structure during heating and electronic structure changes of Si-based anode materials after cycling using XAS. These studies correspond to the completion of milestones (d) and (e).

To study local structural variations around Ni and Mn during thermal decomposition of charged  $\text{Li}_x\text{Ni}_{0.5}\text{Mn}_{1.5}\text{O}_4$  (LNMO), *in situ* extended EXAFS spectra for both disordered (d-) and ordered (o-) charged LNMO during heating up to  $370^\circ\text{C}$  were analyzed. The Fourier-transformed (FT) EXAFS spectra at Ni and Mn K-edge are shown in Fig. 1a and b. In Fig. 1a, it can be seen that the Ni-O bond length (*i.e.*, the first peak at *ca.*  $1.5 \text{ \AA}$ ) abruptly expanded between  $220^\circ\text{C}$  and  $320^\circ\text{C}$  upon oxygen release observed by mass spectroscopy (not shown here), indicating a marked reduction of  $\text{Ni}^{4+}$ . The second peak at *ca.*  $2.5 \text{ \AA}$  follows the same trend as the first one.

Interestingly, this Ni reduction occurred at higher temperatures for the *o*-LNMO (red curve) compared with the *d*-LNMO (black curve) suggesting better thermal stability of LNMO with ordered structure. The EXAFS spectra of both samples at  $370^\circ\text{C}$  showed similar features to that of the reference  $\text{NiMn}_2\text{O}_4$ -spinel phase revealing the formation of  $\text{NiMn}_2\text{O}_4$ -type spinel phase and migration of Mn cations (mostly  $\text{Mn}^{2+}$ ) to the tetrahedral sites after thermal decomposition. For the Mn K-edge EXAFS results (Fig. 1b), there were less changes in either the FT peak-intensity or position compared to the Ni K-edge results, suggesting less local structural changes around Mn than Ni. However, the EXAFS feature changes can be observed clearly between  $270$  and  $370^\circ\text{C}$  showing that the Mn local structure transformed from the initial LNMO spinel to the final  $\text{NiMn}_2\text{O}_4$ -type spinel structure with the tetrahedral sites being occupied by  $\text{Mn}^{2+}$  formed during thermal decomposition. The temperatures for certain local structure changes around Mn in *o*-LNMO caused by the thermal decomposition were higher than those in *d*-LNMO, demonstrating the better thermal stability of the *o*-LNMO than the *d*-LNMO.

Using Si K-edge XANES, the electronic structure changes of a Si anode were studied during the first cycle as shown in Fig. 2. During lithiation, the spectra showed continuous edge shift to lower energy, probably due to the expansion of the Si-Si bonds. The intensity of the  $1s \rightarrow 2p$  transition peak (A) also decreased during lithiation, revealing increased local structural disordering around Si. The evolution of peak B was found to originate from the formation  $\text{Li}_x\text{Si}$  alloy, as supported by DFT calculations. After the 1<sup>st</sup> cycle, the XANES feature nearly changed completely back to its original pristine spectrum, showing the irreversible lithiation/delithiation behavior of the Si anode studied in this work.

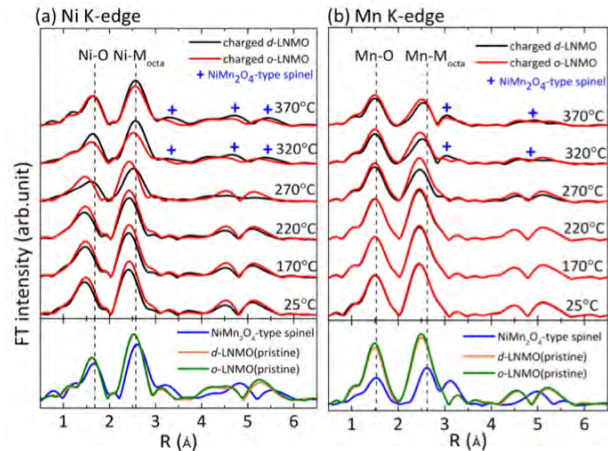


**Figure 1.** Fourier-transformed magnitude of (a) Ni and (b) Mn K-edge EXAFS spectra for the fully charged *d*- and *o*- LNMO upon heating. Bottom panel shows data for the (uncharged) pristine *d*- and *o*- LNMO along with the reference spinel  $\text{NiMn}_2\text{O}_4$  oxides.

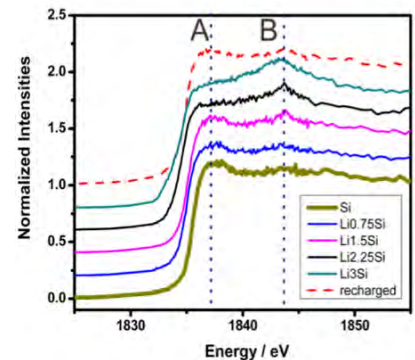


**Figure 2.** Si K-edge XANES spectra of Si anode at different states of lithiation and delithiation.

**Task 5.3 - PI, INSTITUTION:** Clare Grey, Cambridge University

**TASK TITLE:** Diagnostics – NMR and Pulse Field Gradient Studies of SEI and Electrode Structure

**BASELINE SYSTEM:** Conoco Philips CPG-8 Graphite/1 M LiPF<sub>6</sub>+EC:DEC (1:2)/Toda High-energy layered (NMC)

**BARRIERS:** Capacity fade due to significant SEI formation (focusing on Si); reduced rate performance due to SEI formation; high energy density; high power

**OBJECTIVE:** Identify major SEI components and their spatial proximity, and how this changes with cycling. Contrast SEI formation on Si vs. graphite and high voltage cathodes. Correlate Li<sup>+</sup> diffusivity in particles and composite electrodes with rate. Investigate local structural changes of high voltage/high capacity electrodes on cycling.

**GENERAL APPROACH:** Multinuclear NMR of local structure; *in situ* NMR studies of Li<sup>+</sup> transport. Pulse Field Gradient (PFG) measurements of electrolyte diffusivity and tortuosity; SIMS and XPS of SEI composition

**STATUS OCT 1, 2012:** This is a new project initiated April 1, 2013.

**STATUS SEP. 30, 2013:** The <sup>13</sup>C NMR studies of the enriched carbonate electrodes will be ongoing, along with comparison studies with FEC and VC additives. Basic quantification studies of SEI formation vs. cycle number and depth of discharge will have been completed.

**RELEVANT USABC GOALS:** Specific power 300 W/kg, 10 year life, < 20% capacity fade

**MILESTONES:**

- (a) Identify major (NMR active) inorganic components (LiF, phosphates, carbonates) in Si SEI by NMR methods. (May 13) **Complete**
- (b) Establish viability of TOF-SIMS measurements to identify SEI components on Si. (Sep. 13) **Complete**

## PROGRESS TOWARD MILESTONES

### 1. Application of *In situ* NMR studies to study lithium-ion mobility in paramagnetic cathode materials – application to Li

A new NMR methodology was applied to study the cathode  $\text{Li}_{1+x}\text{Mn}_{2-x}\text{O}_4$  (chosen as a model cathode material to develop the technique). This is challenging primarily due to three factors: (1) the resonance lines are broadened severely; (2) spectral analysis is made more complicated by bulk magnetic susceptibility (BMS) effects, which depend on the orientation and shape of the object under investigation; (3) the difficulty in untangling the BMS effects induced by the paramagnetic and metallic components on other (often diamagnetic) components in the system. In an important finding, it was shown that the BMS-induced shift could be minimized by orienting the cell at an angle of  $54.7^\circ$ , facilitating the interpretation of the *in situ* NMR spectra of a working battery containing paramagnetic electrodes.<sup>1</sup> Importantly, it was shown that the NMR spectra (Fig. 1) were highly sensitive to changes of Li dynamics and cation ordering as the battery was cycled, and two-phase reactions *vs.* solid solutions could be separated in this system.

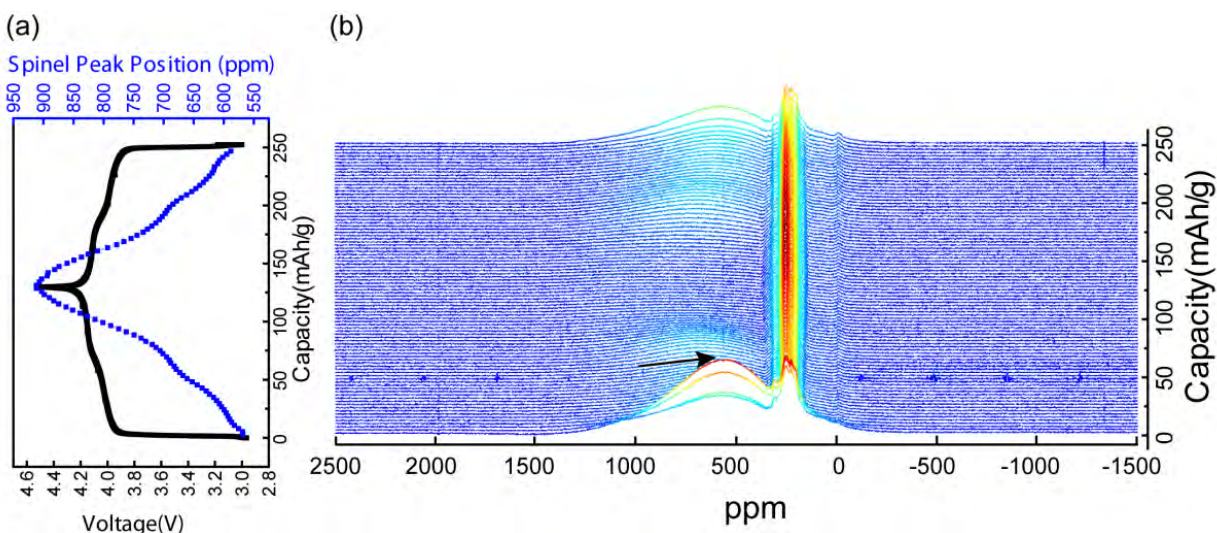


**Figure 1.** *In situ*  $^{7}\text{Li}$  static NMR spectra for the first cycle of a  $\text{Li}_{1.08}\text{Mn}_{1.92}\text{O}_4$  *vs.*  $\text{Li}/\text{Li}^+$  bag cell. (a) Voltage profiles and  $\text{Li}_{1.08}\text{Mn}_{1.92}\text{O}_4$  isotropic shifts *vs.* capacity plots. (b) Stacked plot of the  $^{7}\text{Li}$  spectra. The *in situ* cell was cycled galvanostatically with a C/50 rate between 3.0 and 4.5 V during the spectral acquisition. Note the increase of intensity following 50% Li extraction (at the end of the 1<sup>st</sup> process) consistent with cation ordering.

#### Silicon and its SEI:

The  $^{13}\text{C}$  NMR studies of the enriched carbonate electrodes were started. Since the focus has been on establishing a protocol and identifying key SEI components, studies with FEC and VC were yet to be initiated. These will commence in the next quarter. The effects of this analysis will be ongoing, along with comparison studies with FEC and VC additives. The effect of cycle number and depth of discharge on reversible capacity were explored. New Si coatings were also explored electrochemically and with NMR studies.

<sup>1</sup>L. Zhou, M. Leskes, A. J. Ilott, N. M. Trease, and C. P. Grey, *J. Magn. Reson.*, **234**, 44-57 (2013).

**TASK 5.4 - PI, INSTITUTION:** Nitash Balsara, University of California, Berkeley

**TASK TITLE - PROJECT:** Diagnostics – Simulations and X-ray Spectroscopy of Li-S Chemistry

**BASELINE SYSTEM:** Conoco Philips CPG-8 Graphite/1 M LiPF<sub>6</sub>+EC:DEC (1:2)/Toda High-energy layered (NMC)

**BARRIERS:** (1) Elucidating the mechanism by which the redox reactions in a sulfur cathode proceed. (2) Development of unique diagnostic tools based on X-ray spectroscopy and molecular modeling.

**OBJECTIVES:** A mechanistic understanding of the redox reactions and diffusion of reaction intermediates in a model sulfur cathode based on experimentally-verified models that incorporate both statistical and quantum mechanics.

**GENERAL APPROACH:** (1) A model Li-S cell will be built with a simple cathode comprising a binder that conducts both electrons and ions on the 10 nm length scale and sulfur nanoparticles. (2) The cells will be fabricated in a manner that facilitates the use of soft and hard X-ray spectroscopy during charge-discharge cycles. (3) Detailed (first-principles or empirical force-field) molecular dynamics simulations will be used to sample molecular configurations at finite temperature, interpret associated X-ray spectra and obtain models of (electro-)chemical reaction pathways in the cells.

**STATUS OCT. 1, 2012:** New project initiated October 1, 2012. Begin measurements of X-ray spectra of polysulfides and electrolyte salts in polymer electrolytes. Begin simulations of polysulfides and electrolyte salts in polymer electrolytes that enable predicting X-ray spectra and simulate reference X-ray spectra for molecular and homogeneous condensed-phase components of interest.

**STATUS SEP. 30, 2013:** The synthesis procedure for PEDOT-PEO block copolymers that are predicted to serve as ion- and electron-conducting binders for sulfur cathodes will have been worked out. Definite spectral fingerprints of the lithiated compounds (polysulfides and salts) of interest near the absorption edges of interest (Li, O, S, C, etc.) will have been obtained.

**RELEVANT USABC GOALS:** Fundamental study to determine the factors that underlie limited cycle life of high energy couples such as Li-S cells.

**MILESTONES:**

- (a) Obtain first-simulation results of molecular S<sub>8</sub>, Li<sub>2</sub>S<sub>x</sub>, and Li salts in SEO PEO (or short-oligomer analogs) (Mar. 13) **Complete**
- (b) Make initial predictions of X-ray spectroscopy signatures of Li<sub>2</sub>S<sub>x</sub> and other components in the model Li-S cell. (Mar. 13) **Complete**
- (c) Work out the synthesis procedure for poly(dihexylpropylenedioxythiophene)-polyethylene oxide, PEDOT-PEO, (ProDOT). (Mar. 13) **Complete**
- (d) Measure X-ray spectroscopy signatures of Li<sub>2</sub>S<sub>x</sub> and other components in the model Li-S cell (e.g., salt) in SEO and PEDOT-SEO. (Sep. 13) **Complete**
- (e) Design model Li-S cells appropriate for measurement of X-ray spectroscopy measurements as a function of state of charge of the cathode. (Sep. 13) **Complete**

## PROGRESS TOWARD MILESTONES

**Milestone a.** Molecular dynamic simulations of  $\text{Li}_2\text{S}_x$  molecules dissolved in tetraglyme show that lithium polysulfide molecules elect to form nano-agglomerates in solution, and are not poly-dispersed as is commonly assumed. The thermodynamics of agglomeration were investigated by calculating the free energy of agglomeration for two  $\text{Li}_2\text{S}_8$  molecules in tetraglyme. The agglomerates are the thermodynamically stable state with a 0.4 kcal/mol (0.5 eV) barrier, which is accessible at room temperature.

**Milestone b.** Spectroscopic signatures for both single polysulfide molecules in tetraglyme and multi-polysulfide molecules were obtained. Due to computational limitations, the nano-agglomerates were modeled as solid phase structures to allow for the calculation of the Sulfur K-edge X-ray absorption spectra. As shown in Fig. 1,  $\text{Li}_2\text{S}_8$  nano-agglomerate is in closer agreement with experiment than isolated  $\text{Li}_2\text{S}_8$ . The separation between pre-edge and main-edge peak (labeled a and b) is significant in the isolated molecule but absent in the  $\text{Li}_2\text{S}_8$  solid and experiment. This result connects the experimental and computational spectra.

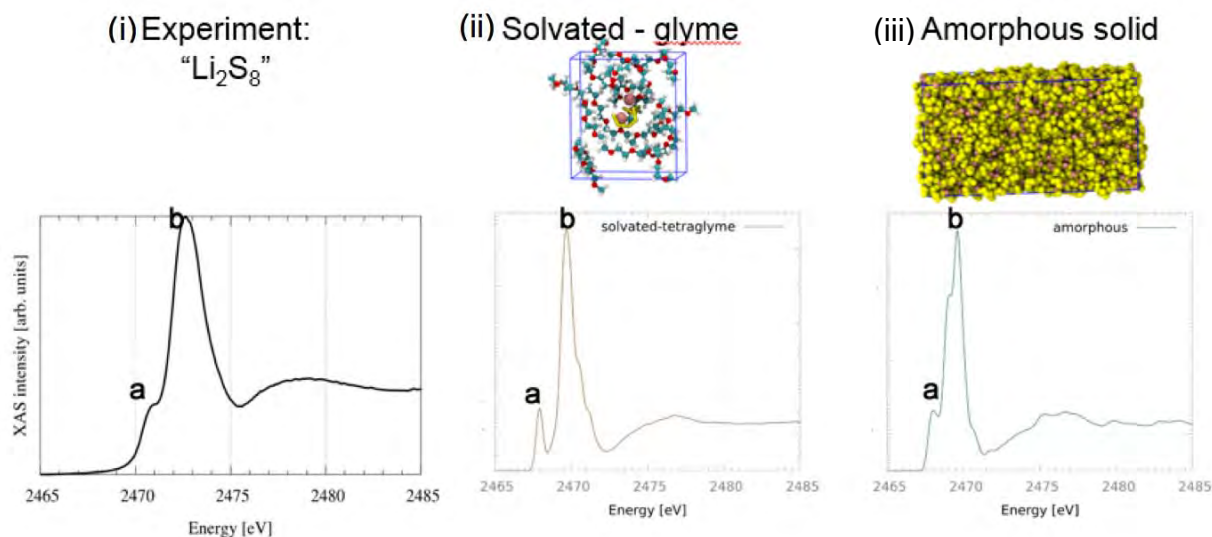


**Figure 1.**  $\text{Li}_2\text{S}_8$  X-ray absorption Sulfur K-edge spectra from (i) experimental measurements (ii) theoretical calculations of the isolated molecule in tetraglyme (iii) theoretical calculations of the amorphous solid. Pre-edge (a) and main edge (b) peak are labeled.

**Milestone c.** PEDOT-PEO synthesis has been accomplished.

**Milestone d.**  $\text{Li}_2\text{S}_x$  X-ray spectra in PEO and SEO has been found to be influenced by the polymer thickness as a result of X-ray self-absorption. To avoid this effect, samples were spin-cast to be between 120 and 180 nm. Within this range, obtained  $\text{Li}_2\text{S}_8$  in SEO spectra was found to be similar and independent of sample preparation.

**Milestone e.** Batteries made of Li metal/SEO electrolyte/sulfur-based cathode were assembled. The battery design for *in situ* X-ray spectroscopy will use electrolyte films with thicknesses in the 120 to 180 nm range. The anode will have a width that is 1 mm smaller than that of the cathode and the incident X-ray beam will be positioned within the exposed electrolyte film.

**Task 5.6 - PI, INSTITUTION:** Guoying Chen, Lawrence Berkeley National Laboratory

**TASK TITLE:** Diagnostics – Design and Synthesis of Advanced High-Energy Cathode Materials

**BASELINE SYSTEM:** Conoco Philips CPG-8 Graphite/1 M LiPF<sub>6</sub>+EC:DEC (1:2)/Toda High-energy layered (NMC)

**BARRIERS:** Available energy (Goal: 11.6 kWh); Cycle life (Goal: 5,000 cycles/58 MWh).

**OBJECTIVES:** Obtain new insights into electrode materials by utilizing state-of-the-art analytical techniques. Gain fundamental understanding on structural, chemical and morphological instabilities during Li extraction/insertion and extended cycling. Establish and control the interfacial chemistry between the cathode and electrolyte at high operating potentials. Determine transport limitations at both material and electrode levels. Develop and synthesize next-generation electrode materials based on rational design as opposed to more conventional empirical approaches.

**GENERAL APPROACH:** Prepare single crystals of Li-rich layered composites and Ni/Mn spinels with well-defined physical attributes and perform advanced diagnostic and mechanistic studies at both bulk and single crystal levels. Global properties and performance of the samples will be established from the bulk analyses, while the single-crystal-based studies will utilize time and spatial-resolved analytical techniques to probe solid-state chemistry and solid-electrolyte interfacial processes at the crystallite level.

**STATUS OCT. 1, 2012:** This is a new project initiated October 1, 2012.

**STATUS SEP. 30, 2013:** A large collection of single-crystal samples with the layered Li<sub>1+x</sub>M<sub>1-x</sub>O<sub>2</sub> and spinel LiNi<sub>x</sub>Mn<sub>2-x</sub>O<sub>4</sub> structures will have been synthesized. Structural, chemical, and morphological changes during first charge/discharge, particularly the activation process in the layered composites, and after extended cycling prompted deteriorated performance and stability will have been examined. Bulk and surface changes associated with metal dissolution in the active materials will have been evaluated and the dissolution mechanism examined. The impact of physical properties on these changes and subsequently the performance and stability of the oxide cathodes established. Approaches to characterize the side reaction products formed on the cathode crystal surface will have been developed.

**RELEVANT USABC GOALS:** PHEV: 96 Wh/kg, 5000 cycles; EV: 200 Wh/kg; 1000 cycles (80% DoD)

**MILESTONES:**

- (a) Synthesize single-crystal samples of Li-excess layered composites and Ni/Mn spinels. (Apr. 13) **Complete**
- (b) Determine structural, chemical, and morphological changes resulting from initial Li extraction/insertion and extended cycling. Correlate these changes to crystal physical attributes. (Jul. 13) **Complete**
- (c) Evaluate transition-metal dissolution in crystal samples and examine its mechanism. (Aug. 13) **Ongoing, due Mar. 14**
- (d) Develop approaches to characterize the cathode-electrolyte interfacial layer. (Sep. 13) **Complete**

## PROGRESS TOWARD MILESTONES

**Transition-metal dissolution:** Collaboration with Prof. Lucht was established to investigate the effect of particle surface properties on transition-metal dissolution.  $\text{LiNi}_{0.5}\text{Mn}_{1.5}\text{O}_4$  crystal samples with different surface facets were delivered to URI. After a series of aging and cycling treatments, metal contents in the solids and electrolyte solutions will be analyzed.

**Cathode-electrolyte interfacial layer:** In this quarter, two synchrotron techniques with high spatial resolution were used to characterize the cathode/electrolyte interface and to distinguish the local changes in the electrode particles. In collaboration with Drs. Phil Ross and Zhi Liu at beamline 9.3.1 at the Advanced Light Source, tender X-ray photoelectron spectroscopy (TXPS), with excellent surface sensitivity as well as depth-profiling capability, was used to nondestructively probe the atomic and chemical compositions of the species at variable sampling depth. Initial studies were performed with an incident photoelectron energy between 3 and 4 keV that probes particle surfaces at a depth of 10 and 15 nm, respectively. The results from a cycled, binder- and carbon-free  $\text{LiMn}_{1.5}\text{Ni}_{0.5}\text{O}_4$  electrode showed significant attenuation to Li 1s, Mn 3p and  $\text{O}^{2-}$  intensities originating from the  $\text{LiMn}_{1.5}\text{Ni}_{0.5}\text{O}_4$ , suggesting cycling leads to the deposition of solid products that suppress the detectable signals from the oxide underneath. A large amount of new carbon species with higher binding energies were revealed, and the presence of organic containing ‘surface’ species was further confirmed by the broadening of the higher binding energy O 1s peak. The chemical nature and thickness of this organic surface layer, as well as the role of particle surface features, are the topics of further investigation.

With a high spatial resolution of 25 nm and an energy range of 95 to 2000 eV, scanning transmission X-ray microscopy (STXM) at beamline 11.0.2 is a powerful tool for the investigation of the local structural and chemical variations occurring at the crystal level. In collaboration with the beamline scientist, Dr. Tolek Tyliszczak, layered  $\text{Li}_{1-x}\text{M}_{1-x}\text{O}_2$  ( $\text{M} = \text{Ni}, \text{Mn}, \text{Co}$ ) single crystals were chemically delithiated/relithiated or electrochemically cycled and then examined by STXM at the O *K*-edge as well as the Ni, Mn and Co *L*-edges. Figure 1 shows the preliminary single-pixel (25nm x 25nm) Ni *L*-edge spectra collected on a plate-shaped  $\text{Li}_{1.2}\text{Ni}_{0.13}\text{Mn}_{0.54}\text{Co}_{0.13}\text{O}_2$  crystal that was charged to 4.8 V in a binder- and carbon-free electrode. The variation of Ni oxidation state within the particle was evident as the predominate 4+ state at the center of the crystal gradually lowered in oxidation state upon moving towards the edge, signaled by the increasing intensity of the peak at 853 eV (Fig. 1). Since the large surfaces and the edges of the plates are composed of different surface facets, this variation may be a result of the facet-dependent reactivity between the oxide particles and the electrolyte. Local structural and chemical changes as a function of Li content and cycle number will be further investigated to explore the intrinsic failure mechanisms in the oxide cathodes.

**Collaborations this quarter:** Drs. T. Tyliszczak, L. Zhi, P. Ross, V. Zorba, R. Kostecki and M. Doeff (LBNL); Profs. B. Lucht (URI) and Y.-M. Chiang (MIT); SSRL and ALS.

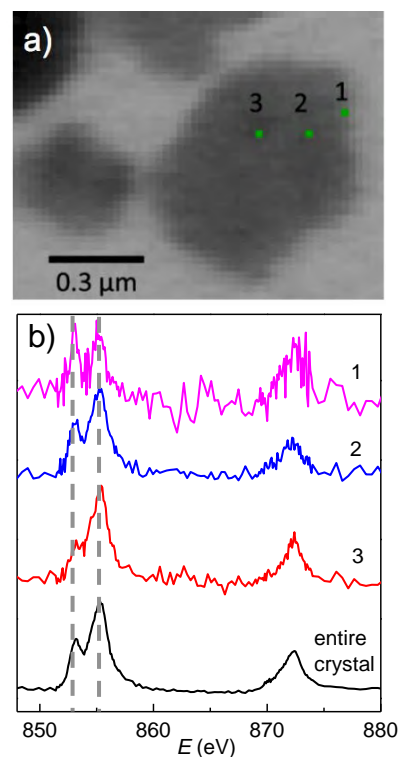


**Figure 1.** a) STXM image of a  $\text{Li}_{1.2}\text{Ni}_{0.13}\text{Mn}_{0.54}\text{Co}_{0.13}\text{O}_2$  crystal and b) Ni *L*-edge X-ray absorption spectra collected at the indicated single-pixel and the entire crystal.

**Task 5.7 - PI, INSTITUTION:** Shirley Meng, University of California, San Diego

**TASK TITLE:** Diagnostics – Optimization of Ion Transport in High-Energy Composite Cathodes

**BASELINE SYSTEM:** Conoco Philips CPG-8 Graphite/1 M LiPF<sub>6</sub>+EC:DEC (1:2)/Toda High-energy layered (NMC)

**BARRIERS:** The Li-rich oxides offer considerably higher energy density than the baseline cathode materials, but they suffer severely from the lack of lithium mobility and unstable voltage discharge profiles upon cycling.

**OBJECTIVE:** The ultimate goal of the proposed diagnostic work is to control and optimize Li-ion transportation, TM migration, and oxygen activity in the high-energy Li rich composite cathodes so that their power performance and cycle life can be significantly improved.

**GENERAL APPROACH:** The approach uniquely combines atomic resolution scanning transmission electron microscopy (a-STEM) & Electron energy loss spectroscopy (EELS), X-ray photoelectron spectroscopy (XPS) and first-principles computation to elucidate the dynamic changes of the bulk and surface structural changes in the complex oxide materials during electrochemical cycling. A systematic study with powerful analytical tools is necessary to pin down the mechanisms of surface coating and determine the optimum surface characteristics for high rate and long life, and to help the synthesis efforts to produce the materials at large scale with consistently good performance.

**STATUS OCT. 1, 2012:** This is a new project initiated April 1, 2013.

**STATUS SEP. 30, 2013:** Establish the coherent interface between layer-layer phases and layer-spinel phases in first-principles modeling. Identify the key samples for in-depth diagnostic study by completing the electrochemical measurements. Due to the complexity of the problem, a suite of surface sensitive diagnostic tools will be applied.

**RELEVANT USABC GOALS:** PHEV: 96 Wh/kg, 5000 cycles; EV: 200 Wh/kg; 1000 cycles (80% DoD)

**MILESTONES:**

- (a) Identify dynamic structure changes, quantify voltage stability upon cycling. Identify at least two best Li rich candidate materials as focused samples (among UCSD synthesized samples and other BATT teammate samples.) (Sep. 13) **Complete**
- (b) Demonstrate the chemical sensitivity and special resolution of the suite of surface characterization tools, including STEM/EELS, XPS and first-principles computation models. (Sep. 13) **Complete**

## PROGRESS TOWARD MILESTONES

**Morphology control of samples** A non-spherical  $\text{Li}[\text{Li}_{1/5}\text{Ni}_{1/5}\text{Mn}_{3/5}]\text{O}_2$  powder and a morphologically controlled  $\text{Li}[\text{Li}_{1/5}\text{Ni}_{1/5}\text{Mn}_{3/5}]\text{O}_2$  powder were both successfully prepared by co-precipitation methods. The morphologically controlled particles are uniformly, spherically shaped with a diameter distribution of roughly 2 to 3  $\mu\text{m}$  (Fig. 1). Although the spherical material delivers a smaller initial discharge capacity when compared to the non-spherical control sample, it exhibits a more stable capacity and voltage.

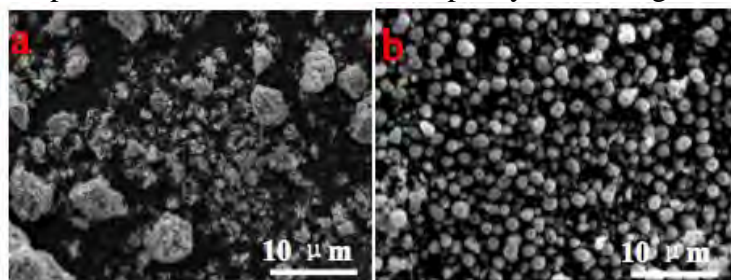
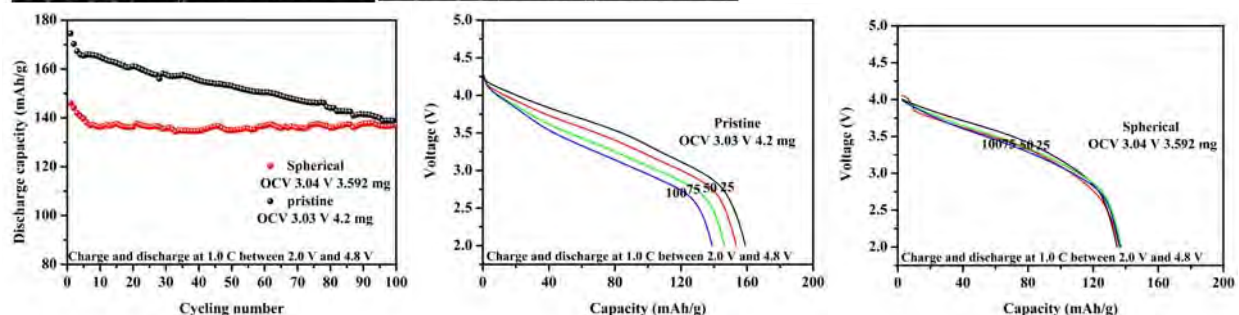


**Figure 1.** (Up) SEM images of the samples  $\text{Li}[\text{Li}_{1/5}\text{Ni}_{1/5}\text{Mn}_{3/5}]\text{O}_2$ : (a) non spherical pristine material, and (b) homogeneously spherical material, both prepared by a co-precipitation method. Graphs compare cycling performance of the samples  $\text{Li}[\text{Li}_{1/5}\text{Ni}_{1/5}\text{Mn}_{3/5}]\text{O}_2$  with different morphologies.



**XPS and STEM/EELS diagnosis.** In order to evaluate the effect that bulk substitution of a TM has on the Li-rich layered oxide, a series of samples with various substitutional elements were prepared. In particular,  $\text{Li}_{7/6}\text{Ni}_{1/6}\text{Mn}_{1/2}\text{Co}_{1/6}\text{O}_2$  was studied in detail by XPS, STEM/EELS, and first principles computation. From XPS, the bonding energy shift of the Ni 3s peak identified  $\text{Ni}^{2+}/\text{Ni}^{4+}$  as the redox couple during cycling.

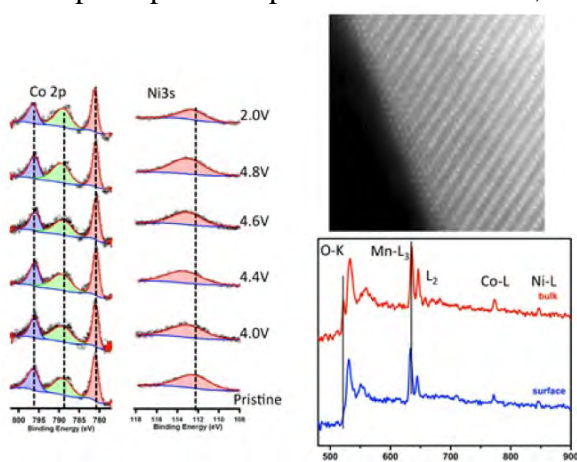


**Figure 2.** (Left): XPS of surface transition metal ions oxidation status changes; (Right) up: HRSTEM images of surface phase transformation; (Right) bottom: EELS spectrum from cycled samples.

During the 4.5 V plateau region, both the Co 2p satellite relative area and the Ni 3s bonding energy showed that the oxidation states of surface Co and Ni were reduced and that oxygen vacancies may have formed. After cycling, a defect spinel phase was visualized by high resolution STEM. Chemical differences can be identified from the EELS spectra. While the bulk spectra (red) has an oxygen pre-peak and indicates that Mn was not reduced, the oxygen pre-peak was absent in the surface spectra (blue) and surface Mn was reduced. This result from a Co-substituted sample is consistent with other Co-free Li excess layered materials such as  $\text{Li}_{6/5}\text{Ni}_{1/5}\text{Mn}_{3/5}\text{O}_2$ .

**Publications:** 1. C. R. Fell, D. Qian, ... Y. S. Meng, "Correlation between oxygen vacancy, microstrain, and cation distribution in Lithium-excess layered oxides," *Chemistry of Materials*, **25**(9), p1621, (2013).

2. K. J. Carroll, D. Qian, ... Y. S. Meng, "Probing the electrode/electrolyte interface in the Li-excess material  $\text{Li}_{1.2}\text{Ni}_{0.2}\text{Mn}_{0.6}\text{O}_2$ ," *Phys. Chem. Chem. Phys.*, **15**, p.11128, (2013).

**Task 5.8 - PI, INSTITUTION:** Gabor Somorjai, UC Berkeley and Philip Ross, Lawrence Berkeley National Laboratory

**TASK TITLE:** Diagnostics – Analysis of film formation chemistry on silicon anodes by advanced *in situ* and *operando* vibrational spectroscopy

**BASELINE SYSTEM:** Conoco Philips CPG-8 Graphite/1 M LiPF<sub>6</sub>+EC:DEC (1:2)/Toda High-energy layered (NMC)

**BARRIERS:** High energy density Si anodes have large irreversible capacity and are not able to cycle. These failures are due in part to loss of electrolyte by reduction and an SEI that is not stable on the surface with repeated cycling.

**OBJECTIVE:** To understand the composition, structure, and formation/degradation mechanisms of the SEI on the surfaces of Si during charge/discharge cycles and how the properties of the SEI contribute to failure of electrochemical systems for vehicular applications.

**GENERAL APPROACH:** Si anode materials including single crystals, e-beam deposited polycrystalline films, and nanostructures with baseline electrolyte and promising electrolyte variations will be studied. A combination of *in situ* and *operando* Fourier Transform Infrared (FTIR), Sum Frequency Generation (SFG), and UV-Raman vibrational spectroscopies will be used to directly monitor the composition and structure of electrolyte reduction compounds formed on the Si anodes. Pre-natal and post-mortem chemical composition is identified using X-ray photoelectron spectroscopy. The Si films and nanostructures are imaged using scanning and transmission electron microscopies.

**STATUS OCT. 1, 2012:** New project initiated October 1, 2012. A spectroelectrochemical FTIR cell was constructed for the Si anode system based on a previous design. The design phase of the SFG cell is on track. Control studies of SEI formation on Au films were performed using *operando* FTIR.

**STATUS SEP. 30, 2013:** Complementary *operando* FTIR and SFG studies of electrolyte reduction on Si(100) wafers and Si polycrystalline films, using the baseline electrolyte, are expected to have been conducted. At this time point Si nanostructures will have been prepared to complement the Si structures of larger dimensions.

**RELEVANT USABC GOALS:** EV: >200 wH/kg with > 1000 cycles to 80% DOD

**MILESTONES:**

- (a) Complete construction of SFG spectroelectrochemical cell. (Jan. 13) **Complete**
- (b) Perform *operando* FTIR and SFG analyses of electrolyte reduction products on doped and undoped 100-nm thick single crystalline Si using baseline electrolyte. (May 13) **Complete**
- (c) Develop procedure to create Si thin films on current collector. (May 13) **Delayed until Jul. 14**
- (d) Perform *operando* FTIR and SFG analyses of electrolyte reduction products on at least three Si film thicknesses (*e.g.*, 10 nm, 50 nm, and 100 nm) using baseline electrolyte. (Sep. 13) **Delayed until Jul. 14**
- (e) Choose promising electrolyte additive(s) for further study to evaluate how it (they) impact the surface chemistry. (Sep. 13) **Complete**

## PROGRESS TOWARD MILESTONES

The new *in situ* ATR-FTIR cell described in the previous quarterly report was employed to analyze the chemistry of electrolyte reduction at the surface of a p-type Si (100) single crystal (doped). By varying the penetration depth variation of the IR radiation, both the near-surface (<1  $\mu\text{m}$ ) and boundary layer (>10  $\mu\text{m}$ ) regions could be analyzed. The wide wave number range (4000 to 800  $\text{cm}^{-1}$ ) allows the stretching vibration of  $\text{PF}_6^-$  anion to be probed, which would indicate a change in the Li-ion solvation state across the solid electrolyte interphase. With different depth into the electrolyte, it was found that the  $\text{PF}_6^-$  vibration peak shifts. Interpretation of these shifts in terms of solvation states will require quantum chemical modeling.

The electrochemical properties of Si (100), Si (110), Si (111), both doped and undoped wafers (450 microns thickness), were characterized during charging-discharging cycles, using primarily CV (at 0.1 mV/s equivalent to *ca.* 4 hr. constant current cycling). The kinetics of Li diffusion was observed to be dependent on crystal orientation and, more importantly, changes in depth of lithiation; number of cycles was also orientation dependent. Typically, the charge for delithiation increased progressively in the first few cycles and achieved a quasi-equilibrium value (after about 30 cycles) as a result of the competition between Li diffusion rate and potential scanning rate. The level of and type of dopant (N or P) strongly affected the bulk electrical conductivity and also the Li capacity of the Si wafers: increasing N-type dopant concentration decreased capacity; while P-type dopant density demonstrated the opposite trend. These results are consistent with some reports in the literature, *e.g.* *J. Phys. Chem. C*, 2011, **115**, 18916-18921. The correlation between the electrochemical properties of model Si wafers and real world Si may therefore be problematic, as the nature of the bulk impurities is typically unknown and/or uncontrolled.

Following the Anode Focus Group meeting last month, and at the recommendation of the focus group, FEC, the monofluorinated version of EC, was chosen as the additive for future study by SFG and ATR-FTIR. This completes Milestone (e) on schedule. Si thin-film samples of various film thicknesses were received from NREL. This will re-establish progress towards Milestone (d) in the next quarter.

## BATT TASK 6

### MODELING

**Task 6.1 - PI, INSTITUTION:** Venkat Srinivasan, Lawrence Berkeley National Laboratory

**TASK TITLE – PROJECT:** Modeling – Model-Experimental Studies on Next-generation Li-ion Battery Materials

**BASELINE SYSTEM:** Conoco Philips CPG-8 Graphite/1 M LiPF<sub>6</sub>+EC:DEC (1:2)/Toda High-energy layered (NMC)

**BARRIERS:** Low calendar/cycle life; Low energy, High cost

**OBJECTIVES:** (1) Quantify power limitations in porous cathodes and its relationship to design; (2) Measure concentration dependent transport properties of the baseline electrolyte of the BATT Program [LiPF<sub>6</sub> in EC:DEC (1:1)]; (3) Quantify polarization losses at single ion conductor (ceramic) / liquid electrolyte interface; (4) Develop a model to predict the onset of mechanical damage to particle-binder interfaces in porous electrodes.

**GENERAL APPROACH:** Develop mathematical models for candidate Li-ion chemistries. Design experiments to test theoretical predictions and to estimate properties needed for the models. Use models to connect fundamental material properties to performance and degradation modes and provide guidance to material-synthesis and cell-development PIs. Use models to quantify the ability of the candidate chemistry to meet DOE performance goals.

**STATUS OCT. 1, 2012:** New project initiated October 1, 2012. A mathematical model that accounts for the concentration and reaction distributions in the porous electrode will be developed. A simulation of a spherical particle, surrounded by a binder layer and undergoing large volume changes when charging and discharging, will be complete, and a modified kinetic expression incorporating the influence of deformation will be obtained.

**STATUS SEP. 30, 2013:** The porous-electrode model that predicts the performance of NMC cathode will be completed and compared with the experiments. Measurement of concentration dependent transport properties for the baseline electrolyte of the BATT Program [LiPF<sub>6</sub> in EC:DEC (1:1)] will be complete. Polarization losses at the single ion conductor (ceramic)/liquid electrolyte interface will be quantified. Stress calculations in 2D domains, simulating multiple interacting particles embedded in binder, will be complete.

**RELEVANT USABC GOALS:** *Available energy:* 56 Wh/kg (10 mile) and 96 Wh/kg (40 mile); *10-s discharge power:* 750 W/kg (10 mile) and 316 W/kg (40 mile).

#### MILESTONES:

- (a) Measure concentration dependent transport properties (diffusion coefficient, conductivity, transference number) of LiPF<sub>6</sub> in EC: DEC (1:1 by weight); Quantify polarization losses at the single ion conductor (ceramic) / liquid electrolyte interface; Construct a simple two-dimensional system consisting of a region of active material in contact with a region of binder. Using a large-deformation intercalation model to describe the active material behavior during charge and discharge, calculate stresses at the interface between the two regions. (May 13) **Complete**
- (b) Find out baseline parameters for the porous-electrode model and compare the model results with experimental data to understand solution-phase limitation; Quantify the rate of side reactions for NMC cathodes and extract kinetic parameters; Use the large-deformation model to approximately represent a system of particles dispersed in a binder matrix, calculating stresses throughout the system. (Sep. 13) **Delayed until Jan. 14**

## PROGRESS TOWARD MILESTONES

### Understanding limitations in the solution phase of NMC electrode:

A systematic approach has been applied to study rate limitations in an NMC cathode. The exchange current density of Li metal was extracted from Li-Li symmetric cell cycling data. The NMC cathode exchange current density and Li diffusion coefficient were obtained from OCV and rate experiments, respectively, on thin NMC electrodes. Figure 1 shows model-experiment comparison of an NMC electrode at different rates. The electrode behavior is well predicted at rates  $<1C$ . For rates  $>1C$ , the model is able to predict the electrode potential at the beginning of discharge, but not the capacity loss near the end of discharge. It is because electrolyte concentration increases at the Li anode and extrapolation of the literature values might not reflect the actual electrolyte properties towards the end of discharge. Figure 2 shows the estimate of potential drop in the NMC electrode. The electrolyte resistance contributes to most of the potential drop from the equilibrium state, and the diffusion resistance contributes to both potential drop and capacity loss at 5C. It is evident that the electrode performance is limited by the electrolyte phase of the porous electrode. This September milestone is complete and future studies will focus on investigating electrolyte transport properties to better understand electrode performance.

### Quantifying the rate of side reactions for NMC cathodes

is important for predicting capacity fade in Li-ion batteries. NMC half-cells were formed and then charged from 3.7 to 4.6 V in increments of 0.1 V at C/25 and then discharged similarly. The cell voltage was kept constant and current monitored with time. Any residual current in the cell was due to side reactions. The side reaction exchange current density was extracted by fitting a Tafel expression to experimental data. This September milestone is complete and similar exercises will be carried out in the future for other Li-ion chemistries.

**Stress calculations for particle-binder interactions:** The two-dimensional large-deformation model of a Si cylinder attached to binder regions has seen continued development, and simulations have produced interesting results that deserve further study. Figures 3 and 4 show typical results on partial cross-sections of the active material particle, with initial radius  $R$  and height  $2Z$ . These plots show simulated results near the end of Li insertion, with and without the presence of a binder. The binder region has a clear mechanical influence, which in turn is subtly connected to the distribution of Li within the particle. Stresses and strain energies are computed throughout these systems and may be used to estimate where and when material damage is likely to arise. Due to this shift in focus, the milestone involving simulation of a system of particles has been postponed to January in favor of further study of single-particle systems, which will provide better context when investigating the multiple-particle systems.

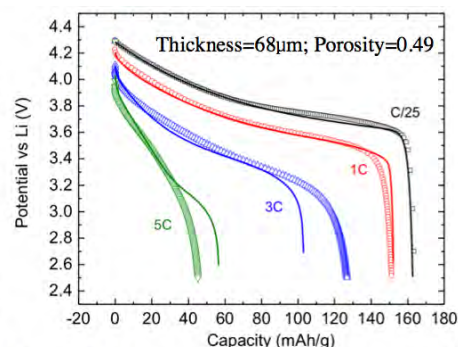


**Figure 1.** Experimental potentials of NMC electrode discharged at different rates.

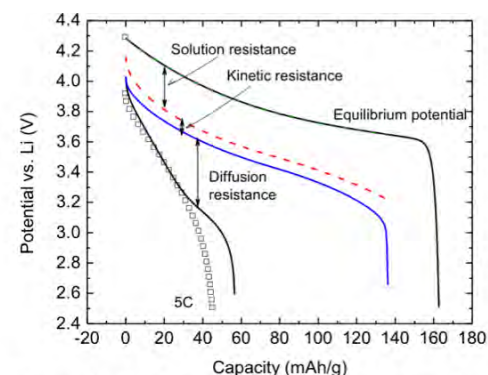
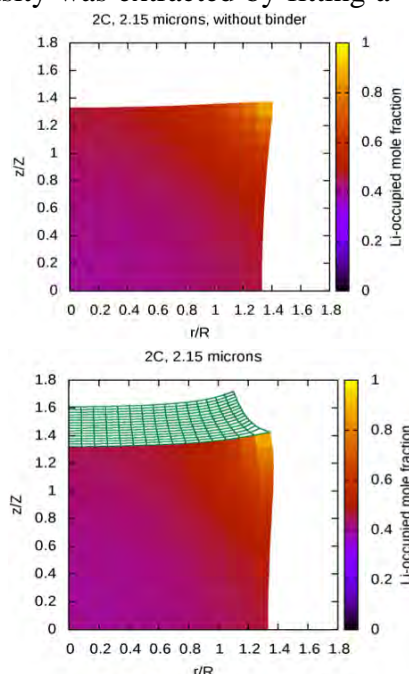


**Figure 2.** Estimation of potential drops in NMC electrode at 5C.



**Figures 3 and 4.**

**Task 6.2 - PI, INSTITUTION:** Kristin Persson, Lawrence Berkeley National Laboratory

**TASK TITLE – PROJECT:** Modeling – Predicting and Understanding Novel Electrode Materials From First-Principles

**SYSTEMS:** Conoco Philips CPG-8 Graphite/1 M LiPF<sub>6</sub>+EC:DEC (1:2)/Toda High-energy layered (NMC)

**BARRIERS:** High cost, low energy, low rate, poor cyclability.

**OBJECTIVES:** 1) Understand the atomistic mechanisms underlying the behavior and performance of the Li-excess as well as related composite cathode materials underlying, and 2) make recommendations for modifications to mitigate voltage and capacity fade.

**GENERAL APPROACH:** First-principles atomistic simulations and statistical mechanics approaches will be used to study the thermodynamic and kinetic processes that govern the electrochemical behavior of the lithium excess and related composite layered-layered or layered-spinel materials. Phase stability, defect formations in the Li, oxygen and cation lattices will be studied, as well as the migration paths for the mobile species.

**STATUS OCT. 1, 2012:** New project initiated October 1, 2012. First-principles calculations utilized to map out the layered Li<sub>2</sub>MnO<sub>3</sub> (LMR), layered LiMnO<sub>2</sub> and LiMn<sub>2</sub>O<sub>4</sub> phase diagrams, and structures including defect cation compositions to yield the possible stable and metastable delithiation and lithiation paths from the first charge and onwards. This will yield an understanding of the thermodynamically accessible phase space as a function of the oxygen release and possible cation rearrangements.

**STATUS SEP. 30, 2013:** Comprehensive phase diagrams as function of Li, O, Mn and defect (vacancies) in layered and spinel (defect) structures to inform on the stability as a function of SOC.

**RELEVANT USABC GOALS:** Specific power 300 W/kg, 10 year life, <20% capacity fade

**MILESTONES:**

- (a) Map phase diagram including relevant bulk Li, O and Mn and defect phases in layered Li<sub>2</sub>MnO<sub>3</sub>. (Jun. 13) **Complete**
- (b) Map phase diagram including relevant bulk Li, O and Mn and defect phases in layered LiMnO<sub>2</sub> (Sep. 13) **Complete**
- (c) Map phase diagram including relevant bulk Li, O and Mn and defect phases in spinel LiMn<sub>2</sub>O<sub>4</sub> (Sep. 13) **Complete**

## PROGRESS TOWARD MILESTONES

**Collaborations:** Gerbrand Ceder (MIT), Clare Grey (U Cambridge, UK). Mike Thackeray (ANL), Guoying Chen (LBNL).

Layered  $\text{Li}_2\text{MnO}_3$  is one of the components in the layered-layered and layered-spinel composite cathode materials. It is believed that the activation of  $\text{Li}_2\text{MnO}_3$  involves formation of new phases which are electrochemically more active than the original material. The possible phase transformations of  $\text{Li}_2\text{MnO}_3$ , including defect spinel and layered phases, is being investigated using first-principles methods. It has been found that the original structure is thermodynamically unstable towards transformation and deformation to spinel-like domains, especially at low Li content. In cases of large deformation, there exist a significant driving force for Mn ions to migrate from the Mn layer into the Li layer. An example of resulting in local re-arrangement is illustrated in Fig. 1. The Mn migration results in spinel-like structures, as the major difference between the layered structure and the spinel is the existence of Mn tetrahedron formation spanning the Mn layer and Li layer.

The degree of Mn migration is determined by thermodynamic as well as kinetic factors, which means that the migration could be slow enough for material to retain its original structure during fast Li-extraction even if the structure is thermodynamically unstable. Hence, further calculations of the energy barriers of Mn migration were performed. The elastic band method is employed for several different hypothesized Mn migration paths at three different Li contents,  $x = 0$ , 0.5, and 1. For low Li content, a favorable Mn migration path is found which implies a correlation between high charge and increased spinel transformation.

Analyzing the charge and positions of the oxygen around each path will provide further understanding on the phase transformation mechanism. Further studies also include oxygen migration.

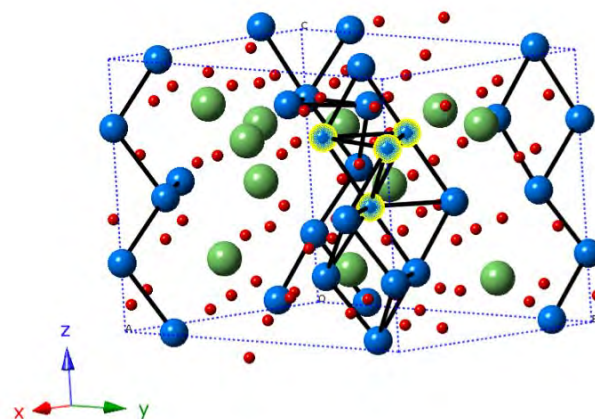


**Figure 1.** An example of a defect phase with a spinel-like domain. Mn ions are distributed over both the Mn-layer and Li-layer. One Mn tetrahedron, composed of four nearest neighbor Mn ions, is highlighted.

**Task 6.3 - PI, INSTITUTION:** Gerbrand Ceder, Massachusetts Institute of Technology

**TASK TITLE:** Modeling — First Principles Calculations of Existing and Novel Electrode Materials

**BASELINE SYSTEM:** Conoco Philips CPG-8 Graphite/1 M LiPF<sub>6</sub>+EC:DEC (1:2)/Toda High-energy layered (NMC)

**BARRIERS:** Low rate capabilities; high cost; poor stability; low energy-density

**OBJECTIVE:** Develop more stable high capacity Li-excess layered cathodes. Develop high-capacity, high-rate Na-intercalation electrodes. Generate insight into the behavior of alkali-intercalating electrode materials.

**GENERAL APPROACH:** Use first-principles calculations (density functional theory) to identify redox-active metals, relative stability of different structures, mobility of Li- and transition-metal ions, and the effect of structure on rate capability. Anticipate possible instabilities in materials at high states of charge by using calculations.

**STATUS OCT. 1, 2012:** This is a new project initiated April 1, 2013.

**STATUS SEP. 30, 2013:** Models for Li transport in partially disordered Li-excess NMC materials will have been initiated. The phase diagram calculation of this material will have been started by studying the ground states of the Li-Ni-Mn-O and Li-Co-Mn-O system. An understanding of what determines the structure selection of Na<sub>x</sub>MO<sub>2</sub> materials and its effect on rate will be reached.

**RELEVANT USABC GOALS:** Specific power 300 W/kg, 10 year life, <20% capacity fade

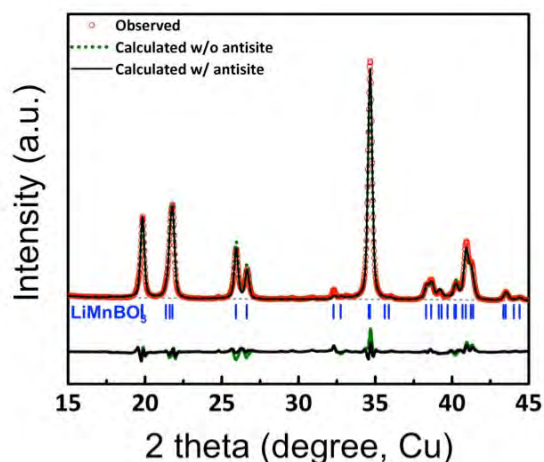
**MILESTONES:**

- (a) Obtain relative stability of Na<sub>x</sub>MO<sub>2</sub> materials in different structures: P2, P3, O3, O2 for M = single metal (Jun. 13) **Complete**
- (b) Obtain ground state structures in the Li-Co-Mn-O and Li-Ni-Mn-O system covering layered, spinel, and the known ternary compounds in this space. (Sep. 13) **Delayed to Dec. 13**
- (c) Initiate model study to understand Li transport in overcharged Li-excess materials. (Sep. 13) **Delayed to Dec. 13**
- (d) Understand Na mobility difference between P2 and O3 structures (Sep. 13) **Complete**

## PROGRESS TOWARD MILESTONES

The particle size dependence of the Li transport in Li intercalating cathodes was investigated. Our modeling system is monoclinic  $\text{LiMnBO}_3$ , which is another example of a one-dimensional Li-ion conductor.<sup>[1]</sup> In such a case, Li transport can be impeded by antisite defects which block the migration path (Mn in Li sites).<sup>[1,2]</sup> In addition, assuming homogeneous distribution of the defects, this clogging of the channel will become more serious in large particles than in small ones since Li will have a higher probability to encounter the defect as the particle becomes larger.<sup>[2]</sup>

The experimentally achievable capacity ( $100 \text{ mAh g}^{-1}$ ) of  $\text{LiMnBO}_3$  so far has been limited to 50% of its theoretical value ( $222 \text{ mAh g}^{-1}$ ).<sup>[1]</sup> Considering both Mn and Li sites are trigonal-bipyramidal with similar ionic radii in  $\text{LiMnBO}_3$ , a fair amount of antisites are expected.<sup>[3]</sup> Indeed, a refined XRD pattern of the as-synthesized  $\text{LiMnBO}_3$  revealed that more than 4% of the Mn occupy the Li sites. After firing at  $500^\circ\text{C}$ , the average particle size of  $\text{LiMnBO}_3$  was 100 nm with a wide distribution ranging from 20 to 230 nm.



Small particles (less than 50 nm) were not likely to be affected by the channel blockage, but its portion to the overall volume is insignificant. On the other hand, particles larger than 150 nm may not contribute to the Li intercalation reaction at all because almost all of the diffusion channels will be effectively shut off by the antisite defects. In the particles with intermediate sizes, Li migration can occur even if the migration path is blocked since there is a chance for Li to detour the blockage *via* neighboring channels. Although possible, however, this rate is estimated to be very low. All in all, the limited capacity of monoclinic  $\text{LiMnBO}_3$  results from the particle size dependency of Li transport rooted in the channel blockage in large particles due to the antisite defects.

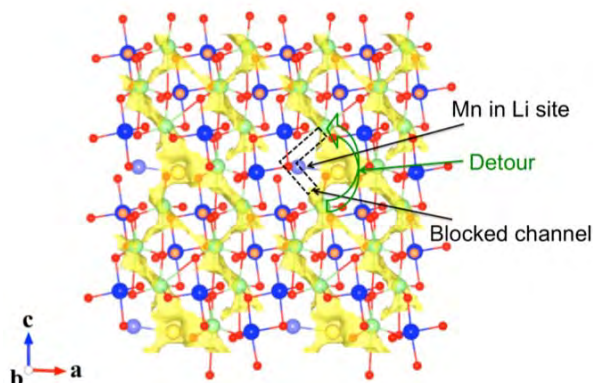


**Figure 2.** Li trajectory as calculated by *ab initio* computation.

**Figure 1.** Profile matching of XRD pattern of monoclinic  $\text{LiMnBO}_3$  with and without considering antisite defects in the unit cell.

Work is continuing to gauge the actual diffusivity values of  $\text{LiMnBO}_3$  by using standard diffusion analysis.

<sup>[1]</sup> Kim et al., *J. Electrochem. Soc.*, **2011**, 158, A309-A315.

<sup>[2]</sup> Malik et al., *J. Electrochem. Soc.*, **2013**, 160, A3179-A3197.

<sup>[3]</sup> Shannon et al., *Acta Crystallogr. A*, **1976**, 32, 751-767.

**Task 6.4 - PI, INSTITUTION:** Perla Balbuena, Texas A&M University

**TASK TITLE:** Modeling — First-principles Modeling of SEI Formation on Bare and Surface/additive Modified Silicon Anode

**BASELINE SYSTEM:** Conoco Philips CPG-8 Graphite/1 M LiPF<sub>6</sub>+EC:DEC (1:2)/Toda High-energy layered (NMC)

**BARRIERS:** Modeling different surface terminations; characterization of electron transfer through the SEI layer; description of SEI structure and evolution.

**OBJECTIVE:** Develop fundamental understanding of the molecular processes that lead to the formation of a SEI layer due to electrolyte decomposition on Si anodes, and use such new knowledge for a rational selection of additives and/or coatings.

**GENERAL APPROACH:** Focus is placed SEI layer formation and evolution during cycling and subsequent effects on capacity fade using two models: 1) SEI layers on bare Si surfaces, and 2) SEI layers on coated surfaces. Reduction reactions will be investigated with quantum chemistry (cluster-based) calculations on simplified models of electrodes; static ultra-high vacuum type DFT calculations of model electrodes with one electrolyte solvent/salt molecule; ab initio molecular dynamics simulations of the liquid-solid interface; and ab initio-Green's function theories to evaluate rates of electron transfer.

**STATUS OCT. 1, 2012:** This is a new project initiated on April 1, 2013. Preliminary DFT evaluations of Li<sub>x</sub>Si<sub>y</sub> surfaces will be initiated. A large pool of data has been obtained through literature search regarding current knowledge of Li<sub>x</sub>Si<sub>y</sub> cluster structures evaluated with quantum chemistry methods.

**STATUS SEP. 30, 2013:** Most stable Li<sub>x</sub>Si<sub>y</sub> surfaces will have been identified and adsorption of most common solvents characterized. Adhesion of common surface oxides (*i.e.*, SiO<sub>2</sub>, Li<sub>4</sub>SiO<sub>4</sub>) on Li<sub>x</sub>Si<sub>y</sub> surfaces and reactivity of the composite surface will be evaluated. Assessment of electron transfer through simple models of SEI layers on model electrodes; surface effects on reduction reactions of EC, VC, FEC, including solvation effects characterized through cluster models, will be carried out.

**RELEVANT USABC GOALS:** Additives/coatings for improved SEI layers in Si anodes

**MILESTONES:**

- (a) Identify most favorable surfaces of bare Li<sub>x</sub>Si<sub>y</sub> periodic structures and characterize their reactivity. (Jun. 13) **Complete**
- (b) Characterize geometric, electronic, and Li<sup>+</sup> transport properties of surfaces coated with thin layers of SiO<sub>2</sub> and Li<sub>4</sub>SiO<sub>4</sub> oxides. (Jun. 13) **Complete**
- (c) Estimate maximum SEI layer thickness for electron transfer in model SEI films. (Jun. 13) **Complete**
- (d) Characterize surface effects on EC, VC, FEC decomposition using cluster models of bare Li<sub>x</sub>Si<sub>y</sub> structures. (Sep. 13) **Complete**

## PROGRESS TOWARD MILESTONES

**(a) Identify most favorable surfaces of bare  $\text{Li}_x\text{Si}_y$  periodic structures and characterize their reactivity.** Effects of degree of lithiation and nature of the exposed surface on the reduction of EC and FEC were fully characterized. At intermediate lithiation ( $\text{LiSi}$ ), two different  $2\text{-e}^-$  EC reduction mechanisms (simultaneous *vs.* sequential) were found, independent of surface functionalization or nature of exposed facets. On less lithiated surfaces (quasi-amorphous  $\text{LiSi}_4$  and  $\text{LiSi}_2$ ), the simultaneous  $2\text{ e}^-$  reduction was found more frequently, where EC reduction starts by formation of a C-Si bond that allows adsorption of the intact molecule to the surface, and is followed by electron transfer and ring opening. Strongly lithiated  $\text{Li}_{13}\text{Si}_4$  surfaces were found to be highly reactive. Reduction of adsorbed EC molecules occurred *via* a  $4\text{-e}^-$  mechanism yielding as reduction products  $\text{CO}^{2-}$  and  $\text{O}(\text{C}_2\text{H}_4)\text{O}^{2-}$ . Direct transfer of  $2\text{ e}^-$  to EC molecules in the liquid phase was also found, resulting in  $\text{O}(\text{C}_2\text{H}_4)\text{OCO}^{2-}$  anions in the liquid phase. FEC was much more reactive, and very fast processes involving sequential 4 or 5  $\text{e}^-$  were found independently of surface functionalization or degree of lithiation. Bonds were broken in the order CO/CF/CH/CO yielding  $\text{CO}^-$  and  $\text{C}_2\text{O}_2\text{H}_2^-$ , or  $\text{CO}_2^-$  and  $\text{C}_2\text{OH}_3^-$ , with F and H adsorbed. VC reduction mechanisms were found similar to those of EC (although yielding double-bonded products).

**(b) Characterize geometric, electronic, and  $\text{Li}^+$  transport properties of surfaces coated with thin layers of  $\text{SiO}_2$  and  $\text{Li}_4\text{SiO}_4$  oxides.** A preliminary attempt was performed at modeling  $1\text{-e}^-$  attacks on FEC in the presence of a  $\text{Li}_{13}\text{Si}_4$  electrode, with each surface coated with a 7 Å thick  $\text{Li}_4\text{SiO}_4$  layer so that FEC liquid is no longer in contact with the  $\text{Li}_{13}\text{Si}_4$  surface. FEC is found to decompose in picosecond time scales. Despite the expectation that the oxide should slow down electron transfer and enhance  $1\text{-e}^-$  attack on FEC over  $2\text{-e}^-$  reduction, Bader charge decomposition analysis shows that the products are still consistent with  $2\text{-e}^-$ -induced reactions. However, EC and FEC reductions tested on slabs of pure  $\text{Li}_4\text{SiO}_4$  and  $\text{Li}_2\text{Si}_2\text{O}_5$  were found not possible. These results suggested a critical role of the oxide thickness on surface reactivity.

**(c) Estimate maximum SEI layer thickness for electron transfer in model SEI films.** Electron transfer was calculated through electrode/SEI/EC interfaces. SEI layers were represented by one component ( $\text{Li}_2\text{O}$  or  $\text{LiF}$ ) and the electrode state of lithiation was modeled by Si,  $\text{LiSi}$ , and Li clusters respectively. Calculations were done for variable thicknesses and configurations of the SEI layer. Gold tips were attached at each end of the interfacial system and a bias voltage was applied to determine electron transfer. It was found that the rate of electron transfer followed the expected trend depending on the type of electrode ( $\text{Li} > \text{LiSi} > \text{Si}$ ), and both model SEI layers showed similar degrees of electron transfer resistance. At constant applied voltage (2V), the electron current was found to decay exponentially by *ca.* 94% at SEI thicknesses of *ca.* 21 Å.

**(d) Characterize surface effects on EC, VC, FEC decomposition using cluster models of bare  $\text{Li}_x\text{Si}_y$  structures.** EC and FEC reaction on  $\text{LiSi}_{15}\text{H}_{16}$  clusters representing Si (001) surfaces were used for studying reduction on surfaces with a much lower degree of lithiation, compared to  $\text{LiSi}_4$  discussed in (a). For FEC, bond dissociation *via* 1 and 2  $\text{e}^-$  transfers was found plausible *via* CO bond breaking (carbonyl  $\text{C}_c$  or ethereal  $\text{C}_E$  may be involved) and in some cases simultaneous breaking of two CO bonds was found.  $\text{C}_E\text{-O}$  bond-breakings were thermodynamically favorable for the  $1\text{ e}^-$  mechanism, but kinetically unfavorable due to a high energy barrier (1.14 to 1.57 eV). The lowest energy barrier (0.43 eV) was found for the  $\text{C}_c\text{-O}$  cleavage. The intermediates had more binding site(s) on the Si surface *via* O and  $\text{C}_E$  atoms.  $\text{C}_c\text{-O}$  bond breakings *via* the  $2\text{ e}^-$  mechanism were found both thermodynamically and kinetically favorable in agreement with AIMD simulations. For EC, the barrier for ring opening of the  $1^{\text{st}}$   $\text{e}^-$  transfer was significantly lower suggesting that this may be the preferred mechanism in very low lithiation stages.

**Task 6.5 - PI, INSTITUTION:** Xingcheng Xiao (General Motors) and Yue Qi (Michigan State University)

**TASK TITLE:** Modeling — A Combined Experimental and Modeling Approach for the Design of High Current Efficiency Si Electrodes

**BASELINE SYSTEM:** Conoco Philips CPG-8 Graphite/1 M LiPF<sub>6</sub>+EC:DEC (1:2)/Toda High-energy layered (NMC)

**BARRIERS:** Low calendar and cycle life; low current efficiency, high cost

**OBJECTIVE:** Combine modeling and experimental approaches to understand, design, and make stabilized nanostructured Si anode with high capacity and high coulombic efficiency.

**GENERAL APPROACH:** In this project, four coherent steps will be taken: a) Develop a multi-scale model to predict the stress/strain in the SEI layer (including artificial SEI) on Si and establish a correlation between the capacity loss (or current efficiency) and mechanical degradation of SEI on Si; b) Use atomic simulations combined with experiments to provide critical material properties used in the continuum modeling; c) Investigate the impact of the SEI formation on the stress/strain evolution, combined with modeling to quantify the current efficiency related to a variety artificial SEI layers using *in situ* electrochemical experiments; d) Use the validated model to guide surface-coating design and Si size/geometry optimizations that mitigate mechanical degradation to both SEI and Si.

**STATUS OCT. 1, 2012:** This is a new project initiated on May 1, 2013. Collaboration between all CoPIs: Yue Qi (GM), Xingcheng Xiao (GM), Huajian Gao, (Brown U), Brian W. Sheldon (Brown U), and Yang-Tse Cheng (U. of Kentucky) has been established.

**STATUS SEP. 30, 2013:** In phase one of this project some key mechanical and electrochemical properties of non-coated and coated Si thin-film electrode will be determined.

**RELEVANT USABC GOALS:** 200 Wh/kg (EV requirement); 96 Wh/kg, 316 W/kg, 3000 cycles (PHEV 40 mile requirement). Calendar life: 15 years. Improved abuse tolerance.

**MILESTONES:**

- (a) Determine the elastic properties of artificial SEI on Si (including Li<sub>x</sub>CO<sub>3</sub>, AlO<sub>x</sub>, SiO<sub>x</sub>) *via* both atomic modeling and laser acoustic wave measurements. (May 13) **Complete**
- (b) Correlate the interfacial charge-transfer kinetics and coating thickness on Si film electrode. (Jun. 13) **Complete**
- (c) Evaluate the chemical composition of the initial SEI formed on uncoated Si thin-film electrodes. (Aug. 13) **Complete**
- (d) Evaluate the evolution of stress and surface roughness of the Si electrode during SEI formation and growth in *in situ* cells to inform the continuum stress model. (Sep 13) **Ongoing, due Mar. 14**
- (e) Formulate a theoretical framework to connect mechanical degradation and columbic efficiency. (Sep. 13) **Complete**

## PROGRESS TOWARD MILESTONES

The project was awarded under the 2012 RFP and officially started in May 2013. All milestones are on schedule. The main achievements during this quarter are:

1) **Correlate the interfacial charge-transfer kinetics and coating thickness.** (Accomplished in July). The kinetics of Si thin-film electrodes coated with  $\text{Al}_2\text{O}_3$  by ALD was studied using a model thin-film system that provides the intrinsic properties of electrodes. Using a modified PITT measurement, the overall interfacial resistance of ALD- $\text{Al}_2\text{O}_3$ -coated Si electrodes was quantified by means of a fit exchange-current-density. Three physicochemical parameters were extracted, including the Li diffusion coefficient within Si, the interfacial exchange current density, and the reaction rate constant.

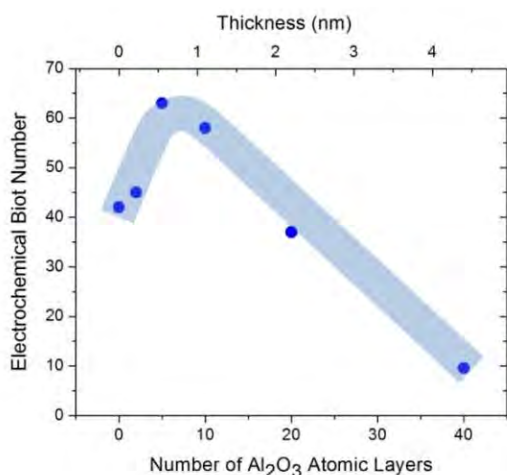


**Figure 1.** Electrochemical Biot number  $B$  obtained from PITT measurement. The light blue curve is provided to portray the trend in the data. The data shows the optimum surface coating thickness was identified as *ca.* 0.7nm. Thus, with five to ten atomic layers of an alumina ALD coating, the silicon electrode can deliver 2600 mAh  $\text{g}^{-1}$  capacity within 3 seconds.

2) **Correlated the Young's modulus (E) of amorphous  $\text{Al}_2\text{O}_3$  coatings with its density (which can be controlled by ALD deposition conditions and cycles), using molecular dynamics (MD) and ReaxFF.** (Initial results, more in progress). To capture the main character of the ALD- $\text{Al}_2\text{O}_3$  coating, the atomic structures were designed to be disordered within the film in the in-plane directions but to have an average layer distance of 1.1Å along the film growth direction. The predicted Young's modulus compared well with limited experimental measurements.<sup>[1]</sup> Since the optimized film thickness is less than 1 nm, laser acoustic wave measurement of its modulus became extremely difficult. Thus, MD simulations will be performed on a range of film thickness to bridge the experimental gap and extrapolate the modulus to ALD coatings with a few atomic layers.

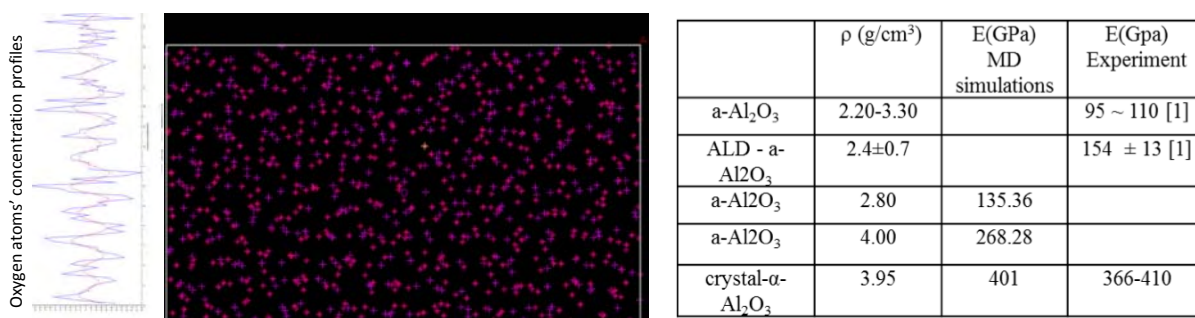


**Figure 2.** The atomic structure of amorphous ALD- $\text{Al}_2\text{O}_3$ , the concentration profile of O atoms shows 1.1Å periodicity, and the computed modulus scales with film density.

**Reference:** [1] Wang, L., et al., *Nano Lett.*, **12**, 3706, (2012).

**Task 6.6 - PI, INSTITUTION:** Dean Wheeler and Brian Mazzeo, Brigham Young University

**TASK TITLE:** Modeling — Predicting Microstructure and Performance for Optimal Cell Fabrication

**BASELINE SYSTEM:** Conoco Philips CPG-8 Graphite/1 M LiPF<sub>6</sub>+EC:DEC (1:2)/Toda High-energy layered (NMC)

**BARRIERS:** Cell performance, life, cost

**OBJECTIVES:** Develop rapid, reliable, and standardized methods for measuring electronic and ionic conductivities in porous electrodes. Determine and predict microstructures for porous electrodes. Understand tradeoffs and relationships between fabrication parameters and electrode performance.

**GENERAL APPROACH:** Use particle-based microstructural modeling, coupled with extensive experimental validation and diagnostics, to understand relationships between fabrication processes, microstructure, and corresponding electron and ion transport in composite electrodes. Assess electronic and ionic conductivities of porous electrodes attached to current collectors, including local heterogeneities and anisotropic effects, through the use of newly-designed instrumentation. Validate and parameterize the particle model using experimental microstructural and macroscopic properties. Use modeling and diagnostic tools to suggest processing conditions that will improve cell performance.

**STATUS OCT 1, 2012:** This is a new project initiated on April 1, 2013. Plans to accomplish the above objectives over a 4-year period are in place.

**STATUS SEP. 30, 2013:** Micro-four-line probe will have been fabricated and the utility of the measurement technique will have been demonstrated on laboratory-prepared and commercial films.

**RELEVANT USABC GOALS:** 200 Wh/kg (EV requirement); 96 Wh/kg, 316 W/kg, 3000 cycles (PHEV 40 mile requirement). Calendar life: 15 years.

**MILESTONES:**

- (a) Fabricate first-generation micro-four-line probe to determine bulk electronic conductivity in non-delaminated battery films. (Sep. 13) **Complete**
- (b) Develop mathematical-model inversion technique to determine current collector contact resistance from film measurements. (Sep.13) **Complete**

## PROGRESS TOWARD MILESTONES

### Milestone (a)

The completed micro four-line probe (Fig. 1) is a means of measuring the effective electronic conductivity of intact battery electrodes. The probe was designed and fabricated using standard microfabrication techniques, such as photolithography, supplemented by electrodeposition steps. Device dimensions and materials were chosen to ensure sufficient passage of current through the device. Protocols for pressure control, relaxation time, and supply voltage have been established and yielded repeatable conductivity data. The data have shown that the measurement variability inherent in the probe is less than the spatial variability of the effective conductivity of intact battery electrodes.

### Milestone (b)

A numerical finite-element model (using COMSOL Multiphysics) of probe electrodes and cathode structure was developed. The model allows one to decouple or invert nearly orthogonal electrical measurements to obtain bulk effective electronic conductivity of the film as well as contact resistance between the electrode film and the current collector for intact electrodes (Fig. 2). Shape factors were determined for multiple electrodes using the model.

### Comments on Expected Status for Sep. 30, 2013

This was the first (partial) year of a new contract and so the above completed milestones are the only ones for FY2013. The expected status was realized. Micro-four-line probes were successfully fabricated and the utility of the measurement technique was demonstrated on laboratory-prepared and commercial films, including those obtained from ANL and A123. Multiple iterations of the probe device and associated computer model took place during the year. Each iteration led to improvement in the robustness and utility of the design.

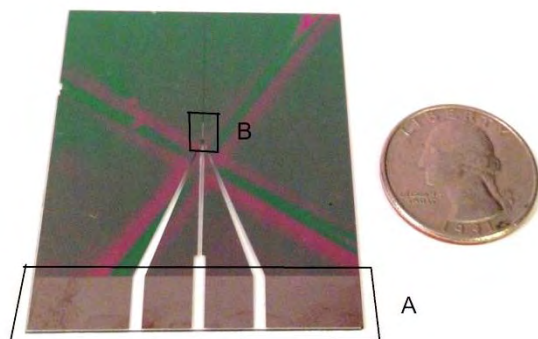


**Figure 1.** Completed micro-four-line-probe showing: (A) exposed connection pads, and (B) window for exposing the four contact lines

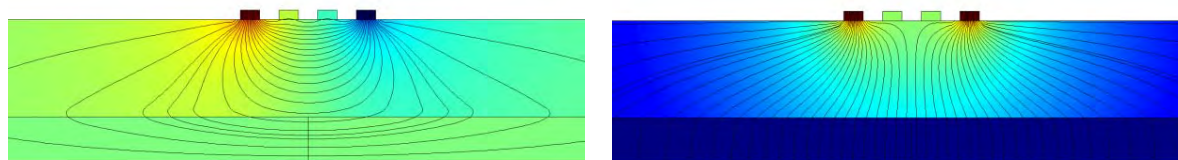


**Figure 2.** Model results (current lines and potential map) for two orthogonal electrical measurements of an intact electrode using the four-line probe.